

A survey on the dynamics of bacterioplankton assemblages associated with an estuarine system and the stomodeum of *Mnemiopsis leidyi* and their functional potential

by

Richard M. Mariita

A dissertation submitted to the Graduate Faculty of
Auburn University
in partial fulfillment of the
requirements for the Degree of
Doctor of Philosophy

Auburn, Alabama
December 10, 2016

Keywords: antibiotic resistance, ctenophore, genomics, metagenomics, chemotaxonomy

Copyright 2016 by Richard M. Mariita

Approved by

Anthony G. Moss, Chair, Associate Professor of Biological Sciences

Mark R. Liles, Professor of Biological Sciences

Nanette Chadwick, Associate Professor of Biological Sciences

Yucheng Feng, Professor of Crop, Soil and Environmental Sciences

Abstract

Estuaries are among the most biologically productive ecosystems. Eighty percent of our sea food is harvested from estuaries, which are popular recreation areas, yet vital to marine transportation. Unfortunately, estuaries also act as sinks for anthropogenic and natural pollutants. From the viewpoint of ecosystem health, it is important to monitor estuarine ecosystems and their resident organisms, especially those with invasive potential. Chapter 1 provides an introduction to estuarine ecosystems and discusses the major pollutants that affect the dynamics of bacterial assemblages and their functional potential. The impacts of anthropogenic and natural perturbations such as atmospheric deposition of gaseous pollutants, acidification, nutrient loads, bacteria and antibiotic resistance genes and invasive species and their effects are covered. The chapter concludes with an exploration of how to mitigate the impacts of pollution in estuarine ecosystems. Chapter 2 correlates changes in the abiotic, physicochemical parameters of Mobile Bay and changes in dominant bacterial assemblages between wet, cold (January and March) and dry, warm (August and September) months. The study also investigates the differences in the taxonomic, phylogenetic and functional potential of the bacterial assemblages between the two sampling periods, using a metagenomic approach. The study also performs a comparative analysis between Mobile Bay and four other coastal ecosystems. Chapter 3 provides a survey of bacterial assemblages in the stomodeum of the *Mnemiopsis leidyi* and predicts their functional potential. A comparative analysis between *M. leidyi* bacterial assemblages and those associated with hosts belonging to two sister phyla (a poriferan and a cnidarian). Chapter 4 examines

previously uncharacterized bacterial isolates from the ctenophore *M. leidy* that display antibiotic resistance, using genomic, chemotaxonomic and classical microbiology techniques. A new species, *Staphylococcus mnemiopsis* nov., isolated from the *M. leidy* stomodeum, displays antibiotic resistance against the penicillins (Penicillin and Ampicillin), fluoroquinolones (Ciprofloxacin, Nalidixic acid), a polypeptide (Bacitracin) and an aminoglycoside (Kanamycin). The present study reveals aspects of the dynamics of bacterial assemblages in Mobile Bay, and the potential for the ctenophore *M. leidy* to harbor bacteria with antibiotic resistance genes. This study could form the basis for future examination of the link between watershed management, estuarine systems and ecosystem health.

Dedication

This work is dedicated to my late mother, Nyanchama Mariita, who was the most committed person towards my progress. She taught me that no matter how many punches life throws at me, I must never quit. Her value for education was unmatched, such that regardless of her painful circumstances on her deathbed, she made me promise that I will stay in school and make the best out of my life. Without her, it is hard to imagine what I will have become. I also dedicate this to those who have supported me in the past and present, my elementary school head teacher, Chris Mabuta, who ensured that I stayed in school and my High School Principal, Mr. Fred Sunda, and his deputy, Mr. Casper Maina, I am extremely thankful for the bursaries they provided. To my mentor, role model and longtime friend, Prof. Paul Okemo, who has always stood by me since I was a sophomore in his laboratory through my master's degree. He did not just teach me to work hard, but made me realize that the harder I work, the luckier I will get. And I have been so lucky. I say thank you. To Dr. John Maingi (Chair of Microbiology Dept., Kenyatta University) and Prof. Callistus Ogot (African Union) for always being there for me. Also, to all my family members, including Naliya Mariita for being the motivator in-chief and Courtney Mariita, my dear wife, for her patience during my intermittent vulgar moods. Her patience and support is a testament of unwavering devotion and enduring love. For that, I am forever grateful.

Acknowledgments

Many thanks to my major professor, Anthony G. Moss, for support, encouragement, and the immense understanding over the course of my education at Auburn University. I thank my dissertation committee Prof. Mark Liles, Prof. Nanette Chadwick and Prof. Yucheng Feng for their input in this work, and for their encouragement, criticism and advice. I am also grateful to Prof. Aharon Oren (The Hebrew University, Israel and IJSEM chief editor), Dr. Lee Zhang, Dr. Scott Miller, Dr. Stephen Kempf, Dr. Alice Ortmann (Bedford Institute of Oceanography, Canada), Mr. Grant Lockridge (DISL), Dr. Lei Hu (DISL), Dr. Jeffrey Krause (DISL), Dr. Mohammad Hossain (Johns Hopkins University) and Srijak Bhatnagar (UCDavis) for their helpful discussions and technical help. I am indebted to my fellow students at Auburn University (Makau Musila, Jessica Gilpin, Susan Rashid, Gen Dong, Ronny Yampolsky, Carlye Ann, Elizabeth McElwee, Rebecca Riggs and Abdul Sajib), and the many friends I made during my stay at the MBL in Woods Hole, MA, and elsewhere (Kessina Lee, Jodi Gronborg, Asha Nelly, Emma Kristine, Taity Changa, Andy Gibbs, Noelle Al-Musaifry, Jess Millar, Jake Cohen, Tino Carr, Britany Waites Josh and Ben Roller) for being supportive. Also to Bonface Nyaribo, Christine Huckle, Michael Huckle, Julie Hobbs-Huckle, Naomi Musila, Loett and Jack Pifher, Irene Momanyi, Judith and George Mason (UK), Murat Sirinoglu (Turkey), Hyrine Munga (Auckland, NZ) for their kind help and encouraging conversations. I acknowledge the Mobile Bay National Estuary Program and NASA's Giovanni Time Series version 4 mission scientists

and associated NASA, personnel for the production of the physicochemical data that I used as part of this research effort. This work was supported in part by an NSF/EPSCoR PhD fellowship (NSF EPS-115886) and AU-Cell & Molecular Biosciences (CMB) Doctoral Graduate Research Fellowship. The study was also partly funded by USDA-Hatch 370225-310100 (AGM, MRL) and NSF-MCB 0348327 (AGM) grants.

Table of Contents

Abstract	ii
Dedication	iv
Acknowledgments.....	v
List of Tables	xii
List of Figures.....	xiv
List of Abbreviations	xx
Chapter 1: Sources of pollution in estuarine ecosystems, their impacts on the dynamics of bacterial assemblages, and mitigation strategies	1
Abstract.....	1
Introduction.....	2
What are estuaries?	2
Types of estuaries	2
Role of estuaries.....	3
Nutrients and other chemical pollutants	5
Sediment and heavy metals.....	7
Oil spills and related waste chemicals	9
Gaseous pollutants	10
Acidification	11

Invasive species	12
Microorganisms and antibiotic resistance genes.....	13
Assessment and pollution control in estuarine ecosystems	16
Conclusion	21
References.....	26
Chapter 2: A survey on the dynamics and diversity of bacterioplankton assemblages and antibiotic resistance determinants of an estuarine system	39
Abstract.....	39
Introduction.....	40
Methods.....	42
Sample collection and processing.....	42
DNA extraction.....	43
Library construction and sequencing.....	44
Quality trimming and assembly	44
OTU clustering and diversity analysis	45
Annotation.....	45
Physicochemical (PC) data	46
Comparative metagenomics of Mobile Bay metagenomes with other coastal systems	48
Results.....	49
Composition and phylogeny of bacterial assemblages	49
Dominant bacterial phyla and their relationships with physicochemical parameters.....	50

Functional annotation.....	52
Comparative metagenomics of bacterial populations in other coastal systems.....	53
Discussion.....	54
Conclusion	57
Data availability	58
References.....	90
Chapter 3: Taxonomic, phylogenetic and functional insights into bacterial assemblages associated with the stomodeum of <i>Mnemiopsis leidyi</i>	98
Abstract.....	98
Introduction.....	99
Methods.....	100
Sample collection.....	100
DNA extraction and library preparation	101
Sequencing and quality trimming.....	101
Merging and Assembly of metagenomes.....	102
Phylogenetic inference from <i>M. leidyi</i> stomodeum metagenomic data.....	103
Annotation of <i>M. leidyi</i> assemblies.....	103
Gene prediction and functional annotation.....	104
Comparisons of <i>M. leidyi</i> bacterial assemblages and functional potential were carried out with representatives other sister phyla: <i>Fungia echinata</i> (Cnidaria) (Badhai et al., 2016) and <i>Arenosclera brasiliensis</i> (Porifera) (Trindade-Silva et al., 2012).....	105
Statistical analysis.....	105

Results.....	106
Bacterial assemblages from the gut of the <i>M. leidy</i>	107
Functional analysis based on <i>M. leidy</i> seasonal metagenomes.....	108
Comparative metagenomics with other basal metazoa.....	109
Discussion.....	110
Conclusion	112
Data availability	113
References.....	133
Chapter 4: Isolation and characterization of coagulase-negative, vancomycin, novobiocin and oxacillin susceptible <i>Staphylococcus mnemiopsis</i> sp. nov., isolated from the <i>Mnemiopsis leidy</i> stomodeum.....	140
Abstract.....	140
Introduction.....	141
Methods.....	141
Sample collection.....	141
Enrichment and isolation	142
Phenotype characterization	143
Chemotaxonomy.....	143
Antimicrobial susceptibility.....	144
DNA extraction and touchdown PCR.....	144
Library preparation and sequencing.....	146

Gene prediction and functional analysis	146
Phylogenetic analysis.....	147
Results.....	148
Phenotypic characterization	148
Phylogenetics	149
Genome mining.....	149
Discussion	150
Conclusion	151
Data availability	151
References.....	167
Appendix.....	172

List of Tables

Table 2.1: Mobile Bay mean physicochemical data. Shown are mean values and standard deviations for each parameter from N= 11 days of sampling around each date of microbial assemblage sampling. All PC data are taken from CTD and TES. The data does not include historical nutrient data.....	60
Table 2.2: Correlations among physicochemical values. Historical nutrient data not included...	61
Table 2.3: Correlations between relative abundance of bacterial phyla in water samples from Mobile Bay from all 4 sampling dates and mean physicochemical parameters from 11 sampling dates.....	62
Table 2.4: The Jaccard similarity and Euclidean dissimilarity matrices for calculation of distance based on the bacterial assemblage composition.....	63
Table 2.5: Metagenome properties indicating differences of the assembled metagenome sequences	64
Table 2.6: Functional annotation of the metagenomes based on IMG/ER	65
Table 3.1: Summary on abundance of features used for functional profiles analysis of microbial assemblages in the ctenophore <i>M. leidy</i> from Dauphin Island Marina, Mobile Bay. Gut summer (GSU), fall (GFL) winter (GWI) and spring (GSP) samples were analyzed using CLC Genomics Workbench and IMG/ER pipeline	114
Table 3.2: Mann-Whitney test P value summary of taxonomic abundance among seasonal metagenomes at phyla level based on KEGG organisms using MG-RAST server (Glass et al., 2010)	115

Table 3.3: Mann-Whitney test P value summary of metabolic genes abundance (KEGG Level 2) between metagenomes representing different seasons using MG-RAST server (Glass et al., 2010)	116
Table 3.4: Correlation coefficients in taxonomy (phylum level) and metabolism genes between ctenophore <i>M. leidyi</i> , coral <i>Fungia echinata</i> (Badhai et al., 2016) and sponge <i>Arenosclera brasiliensis</i> (Trindade-Silva et al., 2012).....	117
Table 3.5: Metagenome properties indicating differences of the assembled <i>M. leidyi</i> stomodeum metagenomes based on IMG/ER pipeline annotation(Lin et al., 2009).....	118
Table 3.6: Mann-Whitney test P value summary of metabolic genes abundance (KEGG Level 2) between organisms representing sister phyla (Cnidaria and Porifera representatives) based on MG-RAST pipeline.....	119
Table 4.1: Antibiotic susceptibility: ZOI (Zone of inhibition)of <i>Staphylococcus mnemiopsis</i> AOAB collected and cultured from the stomodeum of <i>M. leidyi</i> , as measured (in mm) from the edge of disc to edge of inhibition zone (Kaushik et al., 2015). Resistant (R) and susceptible (S) assigned based on previously defined breakpoints (Howe and Andrews, 2012). Below the breakpoints, a given isolate is resistant. Antibiotics with unrevised break points are indicated as dash (-). Experiments were performed in triplicates.	152
Table 4.2: Phenotypic characterization of <i>Staphylococcus mnemiopsis</i> AOAB and comparison with two closely related species, <i>S. warneri</i> and <i>S. pasteurii</i>	153
Table 4.3: Pairwise average nucleotide identity (ANI) analysis and DNA-DNA hybridization (DDH) between <i>S. mnemiopsis</i> AOAB (ANI2) and closely related <i>Staphylococcus</i> species	155
Table 4.4: Genome characteristics of <i>S. mnemiopsis</i> AOAB and close relatives within Genus <i>Staphylococcus</i> based on IMG/ER annotation pipeline.....	156
Table 4.5: Antibiotic resistance genes from <i>S. mnemiopsis</i> AOAB (PATRIC Genome ID: 1279.166)	157

List of Figures

Figure 1.1: Possible co-regulation mechanism for antibiotic resistance induced by heavy metal (a) Two-component signal transduction system pathway BaeRS (b) Global regulator SoxR or MarR pathway [Adopted from Chen et al. 2015]	22
Figure 1.2: Types of pollution and processes that impact the coastal ecosystems	23
Figure 1.3: Cluster diagram indicating several sources of microbial contaminants and antibiotic resistant determinant loads in estuarine ecosystems	24
Figure 1.4: Cycle diagram on the ripple effects of impacts of natural and anthropogenic perturbations to estuarine ecosystems	25
Figure 2.1: LANDSAT photograph of Mobile Bay with 9 sampling sites indicated in red dots. Analysis for upper and lower bay (January and August only) microbial assemblages was done using samples from encircled locations.	66
Figure 2.2a: OTU clustering based on GreenGenes database	67
Figure 2.2b: Shannon entropy values for each of 4 sampling dates of microbial assemblages in Mobile Bay, revealing higher OTU diversity in the January and March metagenomes	68
Figure 2.3a: Box and whisker plot indicating the overall composition of Mobile Bay microbial taxa, for all 4 sampling dates combined	69
Figure 2.3b: Pie chart indicating the composition of bacterioplankton by phyla, for all samples grouped from all 4 sampling dates. Analysis and output done using CLC Microbial Genomics Module (www.clcsupport.com/)	70

Figure 2.4a: Relative abundance of microbial taxa in Mobile Bay during wet, cold (1/26/2013 and 3/14/2013) and dry, warm (8/25/2012 and 9/23/2012) months. The graph shows the most dominant phyla for four Mobile Bay metagenomes based on SILVA database at 97% cut-off using CLC Genomics Workbench 9 71

Figure 2.4b: Heatmap derived from best hit classification showing the composition and relative abundance of major bacterial phyla from Mobile Bay metagenomes (MG-RAST database using M5NR annotation with 80% cut-off) during wet, cold (1/26/2013 and 3/14/2013) and dry, warm (8/25/2012 and 9/23/2012) months 72

Figure 2.5a: Mobile Bay microbial beta diversity based on Principal Coordinate Analysis (PCoA) as characterized using the Bray-Curtis dissimilarity index for wet, cold (1/26/2013 and 3/14/2013) and dry, warm (8/25/2012 and 9/23/2012) months. 73

Figure 2.5b: Mobile Bay microbial beta diversity based on Phylogenetic diversity analysis created using Principal Coordinate Analysis (PCoA) as characterized using UniFrac (D_{0.5}) for wet, cold (1/26/2013 and 3/14/2013) and dry, warm (8/25/2012 and 9/23/2012) months 74

Figure 2.6a: Phylogenetic diversity measures of the Mobile Bay microbial taxa for wet, cold (1/26/2013 and 3/14/2013) and dry, warm (8/25/2012 and 9/23/2012) months. The dynamics of the phylogenetic diversity of seasonal metagenomes as generated by weighted UniFrac Distance Analysis using Past3 software 75

Figure 2.6b: Phylogenetic diversity measures of the Mobile Bay microbial taxa for wet, cold (1/26/2013 and 3/14/2013) and dry, warm (8/25/2012 and 9/23/2012) months. Taxonomic similarity between metagenomes using the Euclidean dissimilarity Index based on Ward's Algorithm using Past3 software..... 76

Figure 2.7a: Bar chart on the taxonomic abundance of dominant phyla in the metagenomes of Mobile Bay from the upper and lower bay during the coldest (1/26/2013) and warmest periods (8/25/2012). 77

Figure 2.7b: Bar chart with Standard errors (SE) indicating the relative abundance all microbial phyla combined, in both the lower and upper sample sites of Mobile Bay during coldest (1/26/2013) and warmest (8/25/2012) periods..... 78

Figure 2.8: MLTreeMap (Stark et al. 2010) analyses of contigs using the 16S rRNA gene for maximum likelihood (ML) phylogeny using GEBA phylogeny (after Wu et al. 2009), from wet, cold (1/26/2013 and 3/14/2013) and dry, warm (8/25/2012 and 9/23/2012)

metagenomic data **a.** Jan. **b.** Mar. **c.** Aug. **d.** Sept. The bubble indicates the relative weight of placement. Figures above are so huge that they needed online support for visualization 79

Figure 2.9: Regression analyses on the relationships between the relative abundances of selected bacterial taxa and various physicochemical parameters in Mobile Bay during wet, cold (1/26/2013 and 3/14/2013) and dry, warm (8/25/2012 and 9/23/2012) sampling period **a.** temperature **b.** dissolved oxygen (DO) **c.** ammonium (NH₄⁺) **d.** nitrogen dioxide (NO₂) **e.** pH and **f.** methane (CH₄) **g.** dissolved organic nitrogen (DON)..... 83

Figure 2.10: Bar graph of the functional categories of dominant genes in the metagenomes of Mobile Bay based on KEGG Analysis. The graph was drawn using GraphPad Prism 5 software (see text for details)..... 84

Figure 2.11: Stacked histogram of the relative abundance of antibiotic resistance determinant genes based on SEED subsystems 85

Figure 2.12: The heatmap of relative abundance of dominant microbial assemblages in Mobile Bay compared to other coastal marine systems based on MG-RAST server and M5NR annotation (see data availability section for details)..... 86

Figure 2.13: A non-metric MDS analysis of ARDs explaining variability in taxonomic relative abundance (Phyla level). Mobile Bay was taxonomically closest to the WECTS [English] (R²=0.84, MSE=0.0132) 87

Figure 2.14: Heatmap on the relative abundance of dominant ARD genes in Mobile Bay compared to other coastal marine systems based on MG-RAST server and SEED annotation (see data availability section for details)..... 88

Figure 2.15: A non-metric MDS analysis of antimicrobial resistance determinants (ARDs) explaining their variability in relative abundance between Mobile Bay and other coastal marine systems..... 89

Figure 3.1: Rarefaction curve of phylogenetic diversity in the microbial assemblages in *M. leidyi* stomodeum for GSU (Aug. 25th 2014), GFL (Oct. 10th 2013), GWI (Feb, 15th 2014) and GSP (May 8th 2014) metagenomes from Dauphin Island Marina, Mobile Bay. Analysis was performed using CLC Genomics Workbench 9..... 120

Figure 3.2: Pie charts showing proportion of KEGG organisms (Phylum level, for proteobacteria at class level) based on predicted protein sequences (FragGeneScan) constructed from the

prokaryotic database on GhostKOALA annotation server for *M. leidy* host. **Key:** (a) Gut summer (GSU) (b) gut fall (GFL) (c) gut winter (GWI) (d) gut spring (GSP) metagenomes 122

Figure 3.3: Inference of differences in the bacterial assemblages in *M. leidy* stomodeum using principal coordinates analysis (PCoA) plot of samples based on (a) Bray-Curtis and (b) Jaccard matrices. Parentheses show variance explaining principal coordinates..... 123

Figure 3.4: Heatmap revealing relative abundance of dominant phyla in *M. leidy* stomodeum, computed by MG-RAST generated using STAMP software. Rows correspond to bacterial taxa, and the columns represent the four seasonal *M. leidy* gut metagenomes used in this study. Dendrograms were created using hierarchical clustering. 124

Figure 3.5: Stacked bar graph showing shared scaffolds for bacterial lineages in *M. leidy* stomodeum based on IMG/ER annotation. The χ^2 test revealed possible association (not random observation) of the 10 observed bacterial lineages in the stomodeum of *M. leidy*125

Figure 3.6: MLTreeMap (Stark et al. 2010) analyses of contigs based on the 16S rRNA gene for maximum likelihood (ML) phylogeny using GEBA phylogeny (Wu et al. 2009), (a) GSU (b) GFL (c) GWI (d) GSP. The bubble indicates relative weight of placement. Figures above were too large and needed online support for visualization. 126

Figure 3.7: Pie charts indicating summary of GhostKOALA (<http://www.kegg.jp/blastkoala/>) annotated functional categories involved in central cellular metabolism in the stomodeum of *M. leidy*. Coding sequences were predicted using FragGeneScan prior to functional analysis..... 127

Figure 3.8: Area bar chart on ontology and category assignments for metagenomes for *M. leidy* bacterial assemblages using CLC Microbial Genomics Module. Abbreviations: gut fall (GFL), gut winter (GWI), gut summer (GSU) and gut spring (GSP) sampling dates 128

Figure 3.9: Plots representing CAZy families in the stomodeum of *M. leidy* (a) Bar graph of gene counts of different CAZy families (b) Over-representation of GT48 was identified using non-metric multidimensional scaling (NMDS). **Key:** AA (auxiliary activity), CBM (carbohydrate-binding module), CE (carbohydrate esterase) GH (glycosyl hydrolases), GT (glycosyl transferase) 129

Figure 3.10: Bar graph showing relative abundance of antibiotic resistance genes in *M. leidy* stomodeum using KEGG annotation on GhostKOALA annotation tool (<http://www.kegg.jp/blastkoala/>) 130

Figure 3.11: Bar graph showing relative abundance of shared bacterial assemblages in <i>M. leidy</i> , <i>F. echinata</i> and <i>A. brasiliensis</i> based on M5NR annotation using MG-RAST pipeline	131
Figure 3.12a: Bar graph indicating the relative abundance of KEGG-level-2 metabolism categories for <i>M. leidy</i> and representative of sister phyla, Cnidaria (<i>Fungia echinata</i>) and Porifera (<i>Arenosclera brasiliensis</i>). (b) Box-plot of the KEGG-Level-2 indicating visual variation metabolism genes were generated using Past3	132
Figure 4.1: Growth of yellow pigmented <i>Staphylococcus mnemiopsis</i> AOAB on LB agar after 3 days at 30°C	159
Figure 4.2: Neighbor-joining tree based on SSU-ALIGN for 16S rRNA gene sequences of <i>S. mnemiopsis</i> AOAB with closely related <i>Staphylococcus</i> species. Numbers at nodes indicate the percentage of bootstrap support based on 1000 replications. Rooting was done using <i>Macrococcus caseolyticus</i> for discriminatory purposes	160
Figure 4.3: Unrooted neighbor-joining tree based on ClustalW alignments for 16S rRNA gene sequences of <i>S. mnemiopsis</i> AOAB with closely related <i>Staphylococcus</i> species. Numbers at nodes indicate the percentage of bootstrap support based on 1000 replications.	161
Figure 4.4: Evolutionary history of <i>S. mnemiopsis</i> AOAB inferred by using Maximum Likelihood method based on Jukes-Cantor model. Evolutionary tree was constructed using MEGA7. The tree is drawn to scale. Numbers on the nodes indicate bootstrap values as a percentage based on 1000 replications with branch lengths measured in the number of substitutions per site. The tree was based on concatenated MLSA of, <i>tuf</i> , <i>sodA</i> , <i>dnaJ</i> , <i>hsp60</i> and <i>rpoB</i> gene sequences.	162
Figure 4.5: Cellular fatty acid composition for <i>Staphylococcus mnemiopsis</i> AOAB using gas chromatography (chromatograph was fitted with a 5% phenyl-methyl silicone capillary column). Peak areas (a) and standard deviation (b) on percentage composition identified 17 fatty acids.	163
Figure 4.6: A dendrogram showing GC fatty acid profile similarities with 19 other <i>Staphylococcus</i> species.	164
Figure 4.7: Polar lipids analysis of <i>Staphylococcus mnemiopsis</i> AOAB (= DSMT102048 =NRRL B-65367T) using two-dimensional silica gel TLC (Macherey-Nagel Art. No. 818 135)	165

Figure 4.8: Subsystem category distribution of *S. mnemiopsis* AOAB (Based on RAST annotation server)..... 166

List of Abbreviations

ANI: Average Nucleotide Identity

ANOVA: Analysis of Variance

ARDs: Antibiotic Resistance Determinants

ARGs: Antibiotic Resistance Genes

BLAST: Basic Local alignment Search Tool

CARD: Comprehensive Antibiotic Resistance Database

CAZy: Carbohydrate-Active EnZymes

CH₄: Methane

DIN: Dissolved Inorganic Nitrogen

DISL: Dauphin Island Sea Lab

DO: Dissolved Oxygen

DON: Dissolved Organic Nitrogen

DSi: Dissolved Silicate

GC: Gas Chromatography

KEGG: Kyoto Encyclopedia of Genes and Genomes

ML: Maximum Likelihood

MLSA: Multi-locus Sequence Analysis

NH₄⁺: Ammonium

nMDS: non-Metric Multidimensional Scaling

NO₂: Nitrogen dioxide

OTU: Operational Taxonomic Unit

PCA: Principle Components Analysis

PCoA: Principal Coordinate Analysis

PCR: Polymerase Chain Reaction

PO₄³⁻: Phosphate

RAST: Rapid Annotation using Subsystem Technology

TLC: Thin-Layer Chromatography

USEPA: United States-Environmental Protection Agency

Chapter 1: Sources of pollution in estuarine ecosystems, their impacts on the dynamics of bacterial assemblages, and mitigation strategies

Abstract

Estuaries are among the most biologically productive ecosystems. They are major sources of shellfish and finfish. Estuaries are also essential in larval and juvenile fish recruitment. Eighty percent of seafood harvested in the USA from 2000 to 2004 was from estuarine ecosystems. They are also important destinations for recreational activities, and serve as migratory routes. Estuaries play important roles in the economy as sites for harbors. Estuarine ecosystem functioning is influenced by complex biotic and abiotic processes. These ecosystems face strong and rapid changes, from both anthropogenic activities and natural perturbations. Estuaries unfortunately also act as sinks for heavy metals, sediment, pesticides, antibiotics and antibiotic resistance genes, wet and dry atmospheric gaseous pollutants, and bacteria and nutrient loads from anthropogenic and natural sources. Nutrient loads can induce harmful algal blooms leading to disturbance of the ecosystem dynamics. Estuaries also offer ideal conditions for the mobility and acquisition of antibiotic resistance genes. Antibiotic resistance genes can be incorporated into mobile genetic elements such as plasmids and transposons and spread to resident bacteria. Pathogenic and antibiotic resistant microbes in estuaries pose ecosystem health risks due to their potential to persist and thrive, altering microbial dynamics in the ecosystem. This review chapter explores the major ecological roles of estuaries, as well as major sources of estuarine pollution and their impacts, especially to bacterial assemblages and ends by discussing key pollution management strategies.

Introduction

What are estuaries?

The term 'estuary' is derived from a Latin word, *aestuarium*, which means marsh or channel (Merriam-Webster, 1979). The word *aestuarium*, in itself is derived from *aestus*, meaning tide or billowing movement (Merriam-Webster, 1979). *Estuaries are coastal ecosystems that can be partially enclosed, with either intermittent or permanent openings to the sea, and which receive input from the watershed, thus maintaining typically less salinity than that of the natural sea. However, estuaries also can become hypersaline during dry spells due to evaporation and decreased water input* (Day, 1980; Elliott and McLusky, 2002; Potter et al., 2010; Pritchard, 1967). Like many other ecosystems, estuaries are defined in terms of their chemistry, physics, biology, geographic nature and socio-economic context (Elliott and McLusky, 2002; Pritchard, 1967). Estuaries are dynamic and unique coastal ecosystems, with those in southern Africa and along south-western Australia being characterized by hypersaline conditions during dry periods (Day, 1980; Potter et al., 2010; Pritchard, 1967).

Types of estuaries

Estuaries are classified based on their geological origin (Perillo, 1995) and how saltwater and fresh water mix in them. Estuaries formed by glaciation scouring like Glacier Bay in Alaska or Geiranger in Norway are called fjords. Drowned river valley estuaries like Chesapeake and Narragansett Bays are a result of rise in sea levels (Perillo, 1995). Those that are formed due to the sinking of land caused by earthquakes that leads to the formation of water filled basins like the San Francisco and Monterey Bays in California are called tectonic estuaries (Valle-Levinson, 2011). Mobile Bay in Alabama was formed from the rise of sea level. As a result, incised valleys

were filled with sediment and sea debris, followed by regression of the sea that moved the sand seawards (Kindinger, 1988).

Estuarine water circulation helps to further classify estuaries (Valle-Levinson, 2011). Water circulation is determined by factors such as shape of the basin, tides, wind and river flow. Some estuaries form a salt wedge (e.g. Columbia and Hudson estuaries at their mouths). Some are termed as well-mixed (e.g. Delaware Bay) while others are partially mixed estuaries (e.g. Puget Sound and San Francisco Bay) (Valle-Levinson, 2011). Some estuaries like Mobile Bay are termed bar-built estuaries, formed when sand spits or barrier islands form across an embayment.

Role of estuaries

Estuaries support high rates of metabolism and primary production because of their high diversity of organisms and organic carbon from both land and ocean sources (Cloern et al., 2014). Estuaries are characterized by high densities of microbial assemblages, planktonic organisms, benthic flora and fauna, as well as nekton (Kennish, 2002). Estuaries are sources of shellfish, including shrimp, oyster, and blue crab (Rashleigh et al., 2009; Smith et al., 2010) and many types of finfish (Elliott and Hemingway, 2002). Shrimp fisheries are the most valuable commercial fishery in the USA (Voorhees et al., 2011). From 2000 to 2004, 68% by value of commercial fish in the USA were from estuaries. Similarly, 80% of the fish harvested in the USA were from estuarine ecosystem (Lellis-Dibble et al., 2008).

Estuarine ecosystems serve as spawning and nursery sites, as well as migration routes for birds and other organisms (Elliott and Hemingway, 2002). Migratory routes include those that enable fish that feed in sea (e.g. Pacific lampreys) to migrate to their spawning sites in rivers. It

also permits those that spawn in oceans (e.g. eel species of the genus *Anguilla*) to migrate to freshwater habitats where they will grow (Elliott et al., 2007; McDowall, 1997).

Estuarine ecosystems play important roles in nutrient cycling (Flindt et al., 1999). The seagrass and phytoplankton in estuaries store, modify and reallocate nutrients such as nitrogen and phosphorus. Estuaries help maintain and regulate healthy nutrient dynamics. Estuaries help keep the right balance of below and above-ground nutrient ratios, depending on the amounts and status of nutrients. Estuaries sequester or store carbon, reducing excess CO₂ in the atmosphere, mitigating the effects of climate change.

Estuaries also provide recreational benefits and are common sites of ports (Ridgway and Shimmiel, 2002). Estuaries act as buffer zones as they filter out pollutants such as antibiotics, herbicides, pesticides, sediment and heavy metals before they enter into seas from terrestrial ecosystems (Dyer, 1995; Perillo, 1995). Because of this, there is hardly any estuary that exists in its natural condition, as they are rapidly being altered and degraded (Dyer, 1995).

More than 3 billion people live within 200 km of the coastline, putting it at a high risk of pollution that can alter the dynamics of microbial assemblages (Vignesh et al., 2014). By 2025, the coastal human population is expected to approach 6 billion, further impacting estuarine ecosystems due to habitat loss, declining biodiversity and altered dynamics of microbial processes (Kennish, 2002; Vignesh et al., 2014). Coastal ecosystems, including estuaries are losing approximately 4,740 acres annually, further complicating their ecosystem function potential (Lellis-Dibble et al., 2008).

Like in any ecosystem, the disturbance of estuaries alters their functions and regulations, leading to health complications (Gavrilescu et al., 2015; Hanski et al., 2012; Rook, 2013; Turnbaugh et al., 2009). As a coastal ecosystem, estuaries are among the most heavily impacted

by pollutants of anthropogenic origin (Kennish, 2002; Kennish, 2016). A study examining 138 estuaries in USA determined that 84 of them were highly eutrophic (Bricker et al., 2008). This was attributed to nitrogen and phosphorus loads, accelerated coastal development and increased agricultural activities (Fertig et al., 2014; Howarth et al., 2002). In Florida's Lake Okeechobee, 33 square miles of the lake were covered in algal blooms in the summer of 2016, leading to poor water quality. The algal blooms were also detected in West Florida Shelf using satellite imagery (El-Habashi et al., 2016). Algal blooms were attributed to pollution from phosphorus and nitrogen fertilizers from the farmlands.

Pollutants jeopardize ecosystem health and the vitality of estuaries (Fleming et al., 2014; Mallin et al., 2000). Microbes are major drivers of biogeochemical processes (Sunagawa et al., 2015), and their structure and functional diversity are affected by multiple stressors (Amalfitano et al., 2015; Jokiel, 2015; Mitchell et al., 2015; Reed and Martiny, 2013). These stressors include:

Nutrients and other chemical pollutants

Water-borne pollutants such as fertilizers, pesticides, sewage, antibiotics and manure create associated risks to estuarine systems such as eutrophication, hypoxia or anoxia, and bioaccumulation of toxins. Nutrients and chemical pollutants can also support biofilm-forming pathogens including *Aeromonas hydrophila*, *Salmonella* spp., *Vibrio* spp. and *Listeria monocytogenes* in coastal systems, potentially contaminating seafood, causing disease outbreaks as well as the spread of antibiotic resistance genes (ARGs) (Mizan et al., 2015; Nogales et al., 2011). Bacteria form biofilms that enhance their survival and persistence on biotic and abiotic surfaces (Teschler et al., 2015), such as on mineral particles suspended in the water column in

estuaries. Estuaries are known to contain more than half the total community of particle-attached bacteria that occur in aquatic ecosystems (Simon et al., 2002). Oysters, shrimps and crabs also are commonly contaminated by biofilm-forming pathogens, including *Vibrio parahaemolyticus*, *Vibrio cholerae*, *Salmonella* and *Listeria* strains (Aagesen et al., 2013; Norhana et al., 2010; Reguera and Kolter, 2005; Teschler et al., 2015).

The introduction of nutrients in the form of fertilizers has deleterious effects that include eutrophication, leading to algal blooms that block sunlight from reaching aquatic vegetation, thus causing eventual loss of seagrass habitats as well as decreased coastal biodiversity (Dumont et al., 2005). Algal blooms are due to increased algae biomass as a consequence of their increased growth or physical aggregation, with harmful effects to the ecosystem (Glibert, 2016). Harmful algal blooms (HABs) are detrimental to human and marine health due to paralytic shellfish toxins (Glibert et al., 2008). HABs levels in coastal ecosystems coincide with elevated levels of fertilizer application in agriculture (Glibert et al., 2001; Trainer et al., 2007). The associated hypoxic conditions ($<2 \text{ mg L}^{-1}$ of dissolved oxygen) are registered at the mouths of rivers, implying anthropogenic origin (Van Der Zwaan, 2000; Zhu et al., 2011). Sometimes, eutrophic estuarine ecosystems can enter anoxic conditions, which is further detrimental to ecosystem health.

An anoxic environment contains no to very little free oxygen, as opposed to an anaerobic one which is totally devoid of molecular oxygen. However, anoxic environments can contain atomic oxygen bound in compounds such as nitrate (NO_3), nitrogen dioxide (NO_2), and sulfites (SO_3) (Diaz, 2016; Elgamal, 2016). In the presence of anthropogenic activity, hypoxia or anoxia can lead to dead zones (Diaz, 2016).

Sediment and heavy metals

Estuaries act as sinks for heavy metals and sediment (Chen et al., 2013; Nesme et al., 2014; Ridgway and Shimmiel, 2002) that aid in the co-selection of antibiotic resistance (AR) genes in resident microbial organisms (Baker-Austin et al., 2006; De Souza et al., 2006; Seiler and Berendonk, 2012). For instance, the selective effect of heavy metals on antibiotic resistance has revealed that the presence of heavy metals like arsenate, zinc and copper fortifies resistance against tetracycline (see adopted Fig. 1.1) (Chen et al., 2015). This is due to the shared structural and functional mechanisms (Baker-Austin et al., 2006) involved in both antibiotic resistance and heavy metal resistance. For instance, resistance to Cu^{++} is via reduction in cell membrane permeability, activation of metal efflux pumps, alteration of cellular targets, and sequestration, with determined co-selection and cross-resistance to commonly used antibiotics (Baker-Austin et al., 2006). This could be due antibiotic resistance and heavy metal resistance genes being harbored on same the plasmid, allowing them to undergo combined transmission (Hasman and Aarestrup, 2002). *Enterococcus faecium* isolates that have the *tcrB* gene (which offers copper resistance) have been found to also contain *tetM* (tetracycline) and *erm(B)* (macrolide) antibiotic resistance genes (Amachawadi et al., 2013). Antibiotic resistance increases in bacteria due to the synergistic effects of heavy metals exposure that threatens ecosystem and human health, via horizontal gene transfer (Dröge et al., 1999; Zhou et al., 2015).

There are many sources of heavy metals, including industrial activities like mining, fossil fuel combustion, shipping, groundwater discharges and atmospheric deposition (Baquero et al., 2013; Kennish, 2016). Additionally, analysis of sediment for heavy metal concentrations has revealed a diffusion pattern from land to sea, revealing input from mines, industries and urban

development, further emphasizing anthropogenic contribution (Ip et al., 2007; Morton and Blackmore, 2001).

The input of sediments into estuarine systems is facilitated by human activities along the coastline, and hastened by the removal of vegetation to pave the way for coastal development projects (Kennish, 2002, 2008). In addition, sediments are a richer source of bacteria than water due to aggregation and flocculation, a process influenced by physical, chemical, and biological factors that leads to the formation of larger particles in estuarine ecosystems (Marquez, 2016; Vignesh et al., 2014). Sediment surfaces have bacteria cell densities of about 10^9 cells/g (Parkes et al., 2000; Vignesh et al., 2014). In some cases, bacterial counts are up to ten-fold higher in sediments compared to in the water column (Vignesh et al., 2014). The density of bacteria in the water column varies from 10^4 to 5×10^6 cells mL⁻¹ (Azam et al., 1983).

Heavy metals (e.g. cadmium, lead, copper, mercury and zinc) impact the structure and dynamics of microbial assemblages in estuaries (Baquero et al., 2013; Yang et al., 2015; Zhou et al., 2015). Antibiotic resistant microbes, pathogens and those involved in nitrogen-cycling (thus relieving the nitrogen loads in estuarine systems), are structured by heavy metals (Schets et al., 2011; Yang et al., 2015). Ammonia oxidizers that are key in sediment compositing are also structured by heavy metals (Stephen et al., 1999; Yan et al., 2015). Controlling heavy metal pollution will help curb selection pressure, and minimize the spread of antibiotic resistance determinants (ARDs) due to co-selection and cross-resistance, and avert impacts on nutrient cycling (Baker-Austin et al., 2006; Yang et al., 2015; Zhou et al., 2015).

Oil spills and related waste chemicals

Industrial wastes, such as from coal mines and oil spills, have huge ecological consequences. The Deepwater Horizon (DH) oil spill in the Gulf of Mexico was transported into the shorelines, with profound impacts on the abundance of resident bacterial assemblages (Kostka et al., 2011). Industrial wastes and oil spills also cause carcinogenic and neurotoxic effects on marine life as well as altering microbial dynamics (Chandra et al., 2013). The normal heavy metal constituents of crude oil include nickel, copper, vanadium, cadmium and lead (Osuji and Onojake, 2004; Van Hamme et al., 2003). Hydrocarbon-contaminated environments thus can select for heavy metal resistant bacteria, which due to co-selection and cross-selection, also lead to antibiotic resistance (Baker-Austin et al., 2006; Mathe et al., 2012; Zhou et al., 2015).

Estuarine organisms also are carriers of potentially pathogenic microbes (Snieszko, 1974). These microbes are asymptomatic because of robust host immune systems. The toxic effects of oil and associated stressors like polycyclic aromatic hydrocarbons (PAHs) enable pathogenicity that threatens the survival of immunocompromised hosts (Snieszko, 1974; Whitehead, 2013). Resident species are exposed to sublethal concentrations of oil that can remain/persist in sediment, further increasing their sensitivity to stress and decreasing the recovery rates of resident species to pathogens over a long period of time (Culbertson et al., 2008). Similarly, resident host organisms (such as crabs) in oil-polluted environments have slow growth and feeding rates, leading to small body sizes and short shell sizes in both the short and long term, relative to those in non-polluted areas (Culbertson et al., 2008).

Hydrocarbons elicit physiological responses from resident microbes, and enrich for those that have the catabolic potential to use it as carbon source, thus altering the composition and functional diversity of ecosystems (Van Hamme et al., 2003). Adaptive responses include

mechanisms and surface alterations in the presence of petroleum substrates that select for Gammaproteobacteria and Acinetobacter bacterial strains (Kostka et al., 2011). Enrichment of specific phyla alters the taxonomic and functional diversity of the impacted coastal ecosystem (Kostka et al., 2011; Van Hamme et al., 2003).

Gaseous pollutants

Although mostly neglected in studies, atmospheric nitrogen deposition contributes 20-40% of the total nitrogen flux in coastal ecosystems (Pryor and Sorensen, 2002). Apart from nutrient loading and sedimentation, some pollutants in estuarine systems are gaseous including CO₂, SO₂, CH₄ and NO₂ (Fig. 1.2). A few studies have determined the impact of gaseous pollutants on environments in the Atlantic Ocean, Baltic Sea and Mediterranean Sea, as well as in terrestrial areas, in terms of their contributions of excess nutrients (Adon et al., 2010; Diesch et al., 2012; Paerl, 1997).

Methane (CH₄) production plays a key role in the carbon cycle (Song, 2013). Biologically generated CH₄ acts as a greenhouse gas, twenty-five times more potent than carbon dioxide (CO₂) (Song, 2013). Methane gas concentrations in eutrophic estuarine ecosystems increase in summer (Gelesh et al., 2016). CH₄ leads to increased ocean acidification, causing altered food webs and biodiversity (Biaostoch et al., 2011; Griffin, 2014). Dissolved oxygen, CH₄ and temperature have been found to be strongly associated, and could be used to predict eutrophication levels (Gelesh et al., 2016). As temperature and salinity increase, dissolved oxygen saturation decreases (Deacutis, 2016). In the Gulf of Mexico, for which Mobile Bay is an inlet, CH₄ is strongly correlated (positively) with the relative abundance of cyanobacteria in the water column (Rakowski et al., 2015).

Emphasis needs to be put on investigating gaseous pollutants, because of their continuous increase in the atmosphere, which prompts many questions regarding sources, sinks and consequences (Nisbet et al., 2014). Monitoring these gaseous pollutants and analyzing their impact on coastal ecosystems is now possible via satellite imagery and data extraction techniques, and should be examined in more detail for their long-term impacts on estuarine ecosystem functioning and climate change (Cronin, 2016). Climate change is not influenced by anthropogenic activities alone, but also by glaciation, variation in earth's orbit, volcanism and plate tectonic processes (Cronin, 2016).

Acidification

Acidification is the reduction of the pH of oceans, estuaries and other bodies of water over a long period of time, primarily due to uptake of CO₂ from the atmosphere. Anthropogenic emission of carbon dioxide (CO₂) from industries (Brierley and Kingsford, 2009; Joint et al., 2011) contribute towards global temperature increase, reduced surface seawater pH and changes in weather patterns that lead to rising sea levels, which threaten ecosystem integrity (Brierley and Kingsford, 2009; Maynard et al., 2015) *via* altered dispersal patterns, seawater carbonate chemistry and species interactions (Doney et al., 2012; Joint et al., 2011; Sunagawa et al., 2015). Experiments simulating the effect of increased temperature and acidification reveal that biofilm forming bacteria are more resistant than non-biofilm formers and may lead to control strategies being inefficient (Norhana et al., 2010). There are strong suggestions that climate change can alter environmental conditions and distribute estuarine associated bacteria such as *Vibrios* to higher latitudes, leading to increased water-borne infections as well as disease outbreaks that will affect marine life (Baker-Austin et al., 2013; Maynard et al., 2015). There have been reports

linking increased incidences of human infections from pathogenic *Vibrio* spp. to elevated water temperatures (Schets et al., 2011; Sterk et al., 2015).

Estuarine integrity is influenced by climate change, which in turn influences marine processes like oceanic waves and winds, riverine nutrients, toxins and sedimentation (Malham et al., 2014; Zhang et al., 2015). The rise in sea level and increased salinity leads to saltwater intrusion, causing low species diversity (Junot et al., 2015), indicative of a stressed and unhealthy environment. An unhealthy environment ensues because salinity gradient is a key factor in influencing microbial composition (Reed and Martiny, 2013).

Estuarine health is inextricably entwined with warming oceans, which in turn influence ecosystem health directly or indirectly *via* emerging pathogens and poor quality of sea food (Jutla et al., 2011; Malham et al., 2014; McCartney et al., 2015) (Fig. 1.1). The pleiotropic impacts of a degraded environment will result in degraded human recreational environments as well.

Invasive species

Pollution of estuaries by invasive species is described as the introduction of nuisance plants, fungi, bacteria and animals that are non-native to the ecosystem. In one year alone, 10 billion tons of oceanic water is transferred using ballast water. About 10,000 non-native species are being introduced to new locations *via* ballast water at any given moment (Bax et al., 2003). Most of these organisms thrive in estuaries, altering these ecosystems.

Invasive macroscopic species such as the ctenophore *Mnemiopsis leidyi* devastate invaded ecosystems because they modify native environments by constant eating and spawning coupled with their mobility. The impact of *M. leidyi* as a super-invasive organism has most

notoriously been observed in the Black Sea (1980s) (Zaika and Sergeyeva, 1990) and, Caspian Sea (1999) (Ivanov et al., 2000), and more recently in the Baltic Sea (2006) (Hansson, 2006; Jaspers et al., 2011). *Mnemiopsis* has induced reductions in the available protein to human populations of the Black Sea and Caspian Sea, leading to untold economic damage to the Turkish fisheries industry in excess of 43 billion \$US (Kideys, 2002). *Mnemiopsis*, as a voracious predator further contributed to eutrophication through indirectly increasing the phytoplankton biomass and primary productivity by consuming zooplankton.

The success of many marine invasive species is in part due to their high rates of reproduction and spread (Drake et al., 2007; McCallum et al., 2003). For instance, as a microbial vector, *M. leidyi* is a hermaphrodite with daily egg production of up to 14, 000 eggs combined with fast growth rates (Jaspers et al., 2011; Kremer, 1976), thus potentially spreading associated microbes at rapid rate. Invasive species also impact the structure and functions of coastal ecosystems such as estuaries, by influencing the population structures of native species (Drake et al., 2007; Ojaveer and Kotta).

Microorganisms and antibiotic resistance genes

The United States Environmental Protection Agency (USEPA) has classified microorganisms and ARGs as emerging pollutants, meaning that there is no existing regulatory status for them (Qiu et al., 2016). Estuaries are susceptible to microbial bioinvasions from fecal coliform bacteria, enteric pathogens, enteroviruses and soil bacteria that threaten ecosystem biodiversity, negatively impacting fishing and tourism industries (Anil, 2006; Bax et al., 2003; Drake et al., 2007; Ivanov et al., 2000; Kideys, 2002; Lipp et al., 2001).

Agricultural, chemical and metallic industries are the major industrial contributors to estuarine pollution (Sousa et al., 2008). A study investigating tetracycline resistance reservoirs and resistant bacteria in estuarine ecosystems revealed that resistance could be associated with both anthropogenic and indigenous estuarine bacteria (Dang et al., 2008). Non-native antibiotic resistance bacteria enter estuarine ecosystems from animal and human sources as well as others (Fig. 1.3) and through horizontal gene transfer, where their genes are spread to resident bacteria. Resident bacteria also contain ARGs. An increase in resistant bacterial load also occurs due to introduced antibiotics from industries, farms, manure, and hospitals (Baquero et al., 2008; Yan et al., 2013). The occurrence of pathogens, antibiotic residues, ARDs and other pharmaceuticals in coastal environments is a major concern because of their biological effects on marine animals and as source of recreational infections (Baquero et al., 2008; Hatje, 2016). This is amplified through mobile genetic elements, giving rise to an increase of resistance phenotypes in estuarine ecosystems (Baquero et al., 2013).

Antibiotic resistance genes from the watershed can be inserted into mobile genetic elements such as plasmids, transposons and integrons, and spread to resident bacteria in estuarine ecosystems, turning them into antibiotic resistant strains (Baquero et al., 2008). Integrons are not mobile, and the mobility of the ARGs on them is transmitted using plasmids and transposons (Baquero et al., 2013). Due to selective pressure and genetic adaptation, antibiotics and ARGs shape bacteria assemblages (Schaefer et al., 2009).

More than 90% of bacterial strains isolated from seawater are resistant to more than one antibiotic, with 20% being resistant at least to five antibiotics (Martinez, 2003). Antibiotic-resistant bacteria have been isolated from estuarine sediments, water, fish, Atlantic bottlenose dolphins (*Tursiops truncatus*) that inhabit estuarine ecosystems, and many other organisms

(Aguirre and Lutz, 2004; Dang et al., 2008; Schaefer et al., 2009). The antibiotic resistant bacteria isolated include those belonging to Enterobacteriaceae, Pseudomonadaceae, Vibrionaceae, Halomonadaceae, Pseudoalteromonadaceae, Rhodobacteraceae, and Shewanellaceae bacteria. Some of the isolated *Vibrio* spp. are pathogenic to green turtles. *Staphylococcus aureus* (MRSA), among other antibiotic resistant bacteria species, have been isolated from bottlenose dolphins inhabiting the estuarine waters of Indian River Lagoon, Florida, USA. The key processes of transportation of the pathogenic bacteria from the watershed are not well known (Ferguson et al., 2003), however, the ripple effects are (Fig. 1.4). One of the known processes is via the use of particles to which bacteria become attached (Ferguson et al., 2003). In seafood, persistence of bacterial contaminants is partly due to type I pili, type IV pili and flagellar structures with adhesive properties (Aagesen et al., 2013). Some pili (hair-like structures in bacteria) are toxin co-regulated pili (TCP) and are essential in intestinal colonization (Reguera and Kolter, 2005).

Due to a lack of barriers, bacteria in marine ecosystems also spread rapidly and can survive outside of hosts for long periods during their dispersion (McCallum et al., 2003; Schets et al., 2011). Enteric bacteria in coastal ecosystems become resistant by entering a stationary phase and avoiding the susceptible exponential growth phase (Rozen and Belkin, 2001). Molecular mechanisms that help in the survival of enteric organisms include the mutation of RNA polymerase, sigma S (*rpoS*) which helps in the regulation of stress response genes (Rozen and Belkin, 2001).

Assessment and pollution control in estuarine ecosystems

Estuaries, like other coastal ecosystems, are maintained by the flow of energy through biological networks, where species are linked directly or indirectly and contribute towards ecosystem structure and function (Doney et al., 2012). The health of this ecosystem is vital, as it is source of seafood and recreation, and is key in biogeochemical cycles. Estuarine systems face strong and rapid change, as a result of anthropogenic activities, climate change and natural perturbations, making assessment and pollution control is important in ensuring that ecosystem health is maintained (Bauer et al., 2013; Reed and Martiny, 2013).

Biomarkers or sentinel species can be used for the assessment of pollution impacts in estuarine systems (Aguirre and Lutz, 2004). An example is green turtles (*Chelonia mydas*), from which pathogenic *Vibrio* spp. have been isolated (Arena et al., 2014; Zavala-Norzagaray et al., 2015). Turtles are threatened by anthropogenic stresses and are susceptible to both heavy metal pollution and pathogenic bacteria, which also have the potential to cause human disease (Aguirre and Lutz, 2004; Arena et al., 2014; Kim and Carlson, 2007). Bottlenose dolphins have also been recommended as sentinels, because cultures of methicillin-resistant *Staphylococcus aureus* (MRSA) isolated from them have demonstrated resistance patterns against penicillins, macrolides, phenicol and tetracycline antibiotics (Schaefer et al., 2009).

Other ways of measuring potential pollution include assessment of indicators such as nutrient and sediment loads delivered into the bay, and the status of chemical contaminant effects on living organisms (Hershner et al., 2007). Albeit mostly overlooked, environmental health and integrity is dependent upon the assessment and maintenance of the appropriate diversity of microbial assemblages, and how the microbial assemblages may re-organize themselves in the face of natural and anthropogenic perturbations (Mitchell et al., 2015; Park et al., 2014; Yang et

al., 2015). The measurement of diversity, including microbial diversity, acts as an indicator of the wellbeing of the environment (Stephen et al., 1999). This can be studied on temporal and or spatial scales. It is critical to understand how seasonal changes drive the dynamics of microbial assemblages and how shifts in dynamics impact the overall integrity of coastal environments (Fleming et al., 2014; Mariita et al., 2015). This type of information will provide stakeholders with critical information on the safest use of the coastline and a better understanding of its microbial dynamics.

Another way to protect estuarine ecosystems is by protecting salt marshes and coastal grass species such as *Spartina maritima*. This grass species helps modify nutrients such as phosphorus and nitrates, minimizing their presence in the water column, and thus reducing chances of algal blooms (Sousa et al., 2008). *S. maritima* has been observed to allocate a higher concentration of nitrogen to leaves during photosynthetic activities, because nitrogen supports metabolic processes. This minimizes the presence of nitrogen in the water column, thus reducing eutrophication, which is one of the principal agents of ecosystem change.

One way of monitoring ecosystem health is by the use of high throughput nucleotide sequencing methods, which can detect the taxonomic composition of bacterial assemblages and the types of ARDs present (Port et al., 2012). Source tracking technologies can be applied to detect potential origins of microbial contaminants and their associated ARDs (Koike et al., 2007). Promising methods involving real-time PCR (TaqMan) have been developed for this purpose (Baker-Austin et al., 2010; Ebdon et al., 2004; Koike et al., 2007). Some methods have been optimized to distinguish fecal bacteria according to their host source (Ebdon et al., 2004; Lamendella et al., 2009).

Given the risks associated with pollution of estuarine systems to food security and ecosystem health, it is paramount to control the levels of pollution in these coastal ecosystems to ensure that biogeochemical cycles based on microbial action are maintained (El Bour, 2016). This involves controlling industrial emissions that disturb weather patterns and which subsequently impact marine organisms and coastal systems (Brierley and Kingsford, 2009), as well as inactivation of sediment loads that could introduce pathogens into estuaries (Ferguson et al., 2003). Activities that lead to increased temperatures, acidification, nutrient loads and ecosystem regime changes all need to be mitigated (Brierley and Kingsford, 2009). A reduction of CO₂ and various nitrogen oxide (NO_x) emissions will be important in controlling regime shifts in these vital coastal ecosystems (Brierley and Kingsford, 2009).

The control of pollution has to involve strategies that will help reduce nitrogen and phosphorus loading to coastal ecosystems. Among these strategies is aid and encouragement to farmers and homeowners to practice best nitrogen and phosphorus management practices, which will reduce runoffs and but still yield the best results (Buzicky et al., 1983; Mitsch et al., 2001). There is a positive correlation between the total concentration of antibiotics in water emanating from the watershed, and dissolved organic carbon and nutrients (Yan et al., 2013). High concentrations of antibiotic residues and nutrients pose a threat to organisms in estuaries and alter the dynamics of resident bacterial assemblages. This calls for risk assessment and tracking of major sources of pollution.

Nutrient runoff and antibiotic resistant bacteria mostly affect coastal ecosystems through rivers, so it will be important to have off-site nitrogen sinks and riparian buffers to trap antibiotic resistant bacteria between rivers and agricultural settings, and to control the drainage into coastal ecosystems (Ferguson et al., 2003; Osborne and Kovacic, 1993). Since municipal

wastewater is a primary source of nitrogen, it is recommended to apply tertiary treatment and use marshes that act as sinks to reduce the level of nutrients reaching coastal ecosystems (Guardabassi et al., 2002; Mitsch et al., 2001; Vymazal, 2010). Tertiary treatment will also to reduce antimicrobial resistant bacteria being released into the watershed from industries, farms, hospitals and municipal sewages (Guardabassi et al., 2002). Heavy metal pollution in estuarine ecosystems from industrial waters could also be processed for removal using constructed wetlands that act as sinks (Dunbabin and Bowmer, 1992).

We need to move beyond being concerned only about nutrient enrichment through the waterways that flow into coastal ecosystems, and also to curb the gaseous pollutants that contribute to acidification and eutrophication (Gelesh et al., 2016; Rakowski et al., 2015). Controls on atmospheric NO_x ($\text{NO} + \text{NO}_2$) and SO_x ($\text{SO} + \text{SO}_2$) emissions from automobile and marine vessels is achievable through emission control strategies (Dunbabin and Bowmer, 1992). Among them should be vehicle emission inspection in states like Alabama, which have not incorporated them as part of automobile inspections (Schuster et al., 2004). International treaties with countries like China will also help curb the disturbing trend of acidification in coastal ecosystems due to atmospheric pollutants (Zhao et al., 2013).

Regulation of microbial bioinvasions can be achieved by monitoring bacteria and treatment of ballast water, as well as by reprimanding and banning vessels that break internationally established protocols (Maranda et al., 2013; Tryland et al., 2010). Killing invasive species in ship ballast water using hydroxyl radicals has been recommended. A pilot study revealed that this method kills bacteria, algae and protozoans within 2.67 seconds if the hydrogen radical concentration is 0.63 mL^{-1} (Bai et al., 2005). This method involves processes that produce

hydroxyl radicals and induce a series of reactions that kill the organisms, reducing them to CO₂, water and inorganic salts (Bai et al., 2005).

Co-selection and cross resistance between heavy metals due to shared regulatory responses means that we have to monitor both heavy metal and antibiotic pollution together (Baker-Austin et al., 2006). The abundance and distribution of ARGs can be quantified using LC-MS/MS (Xu et al., 2015), which have been used to monitor levels of pollution in an effluent-receiving river in China, and detected antibiotic pollutants including tetracycline, sulfonamide and quinolone. That study similarly employed quantitative PCR, and detected relatively high concentrations of different types of tetracycline (tetA, tetB, tetW, tetZ, and tetM), sulfonamide (sul1, sul2 and sul3) as well as quinolone (gryA, parC, qnrC and qnrD) genes. Rapid screening of heavy metals and trace elements to detect pollution hotspots is possible using progressive methods including portable X-ray fluorescence spectrometer.

X-ray fluorescence spectrometer can be used for the analysis of heavy metals and trace elements in water (McComb et al., 2014). An X-ray fluorescence spectrometer, which is non-destructive, has been used to study hot spots in 119 estuaries, with limited sample preparation (Butler et al., 2012). Other methods that can be used to assess levels of heavy metal pollution include an inductively coupled plasma optical emission spectrometer (ICP-OES) and inductively coupled plasma mass spectrometry (ICP-MS). The ICP-OES and ICP-MS methods are destructive, as they involve acid-extraction of heavy metals from study samples prior to analysis.

Monitoring of algal blooms is now feasible using satellite-retrieved data for the analysis of the early signs of alga blooms. The technology has been used to assess the extent of algal blooms in the West Florida Shelf (El-Habashi et al., 2016), and employs a Visible Infrared Imaging Radiometer Suite (VIIRS) to detect algal blooms. A Moderate Resolution Imaging

Spectroradiometer Aqua (MODIS-A) satellite has also been previously used to monitor algal blooms. The data from these satellites can be assessed by using among other means, such as the Giovanni tool (disc.sci.gsfc.nasa.gov/giovanni) (Olalekan and Malik, 2015). This tool is cheap and rapid, and has great potential in assessing incidences of algal blooms using high quality data.

Conclusion

Estuarine ecosystems are important for global sustainability because of their high productivity, roles in biogeochemical cycles, and use for recreational and transportation activities. Because of increased population, extreme weather events, climate change and pollution, estuarine ecosystem integrity is under increased threat. Pollution from nutrient loading, organic matter, heavy metals and other chemicals released into estuaries, leads to altered biogeochemical cycles, increased algal biomass, reduced dissolved oxygen and increased marine life mortality rates and unhealthy shifts in microbial assemblages (Álvarez-Vázquez et al., 2016). This compromises the water quality of estuarine systems, especially those in urban areas (Kennish, 2002). Compromised estuarine ecosystems cause harmful effects to both human and marine health. To prevent these deleterious effects, estuaries need to be monitored and pollution minimized through solid land use planning, controlled atmospheric deposition, and waste management. Policies that can prevent the mixing of pathogenic bacteria assemblages from industries, animals, farms with estuarine resident bacteria are encouraged (Baquero et al., 2008). This is achievable by incorporating pathogens into coast water management models.

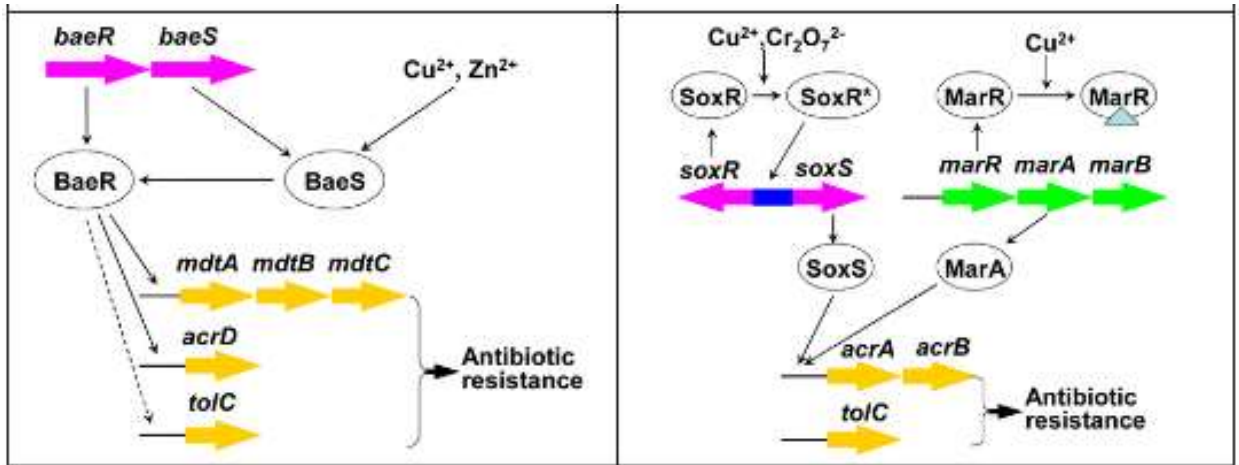


Figure 1.1: Possible co-regulation mechanism for antibiotic resistance induced by heavy metal
 (a) Two-component signal transduction system pathway BaeRS (b) Global regulator SoxR or MarR pathway [Adopted from Chen et al. 2015]

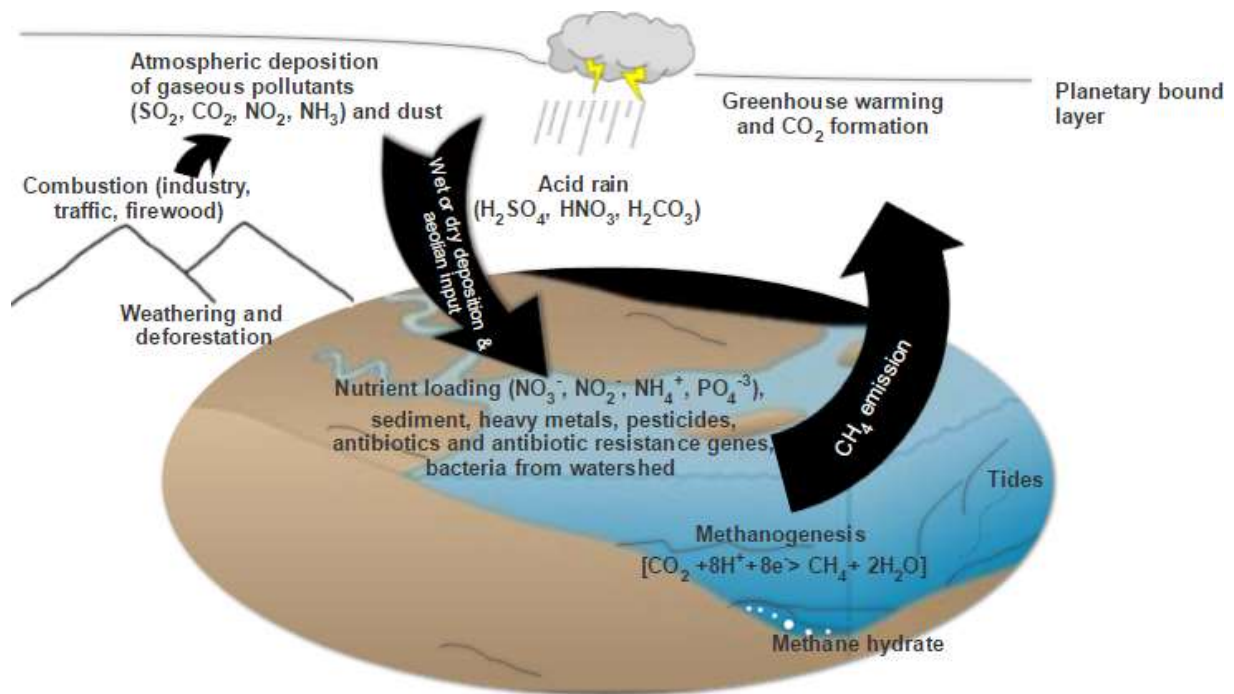


Figure 1.2: Types of pollution and processes that impact the coastal ecosystems [R.M. Mariita, 2016, <https://dx.doi.org/10.6084/m9.figshare.3826638.v7>]

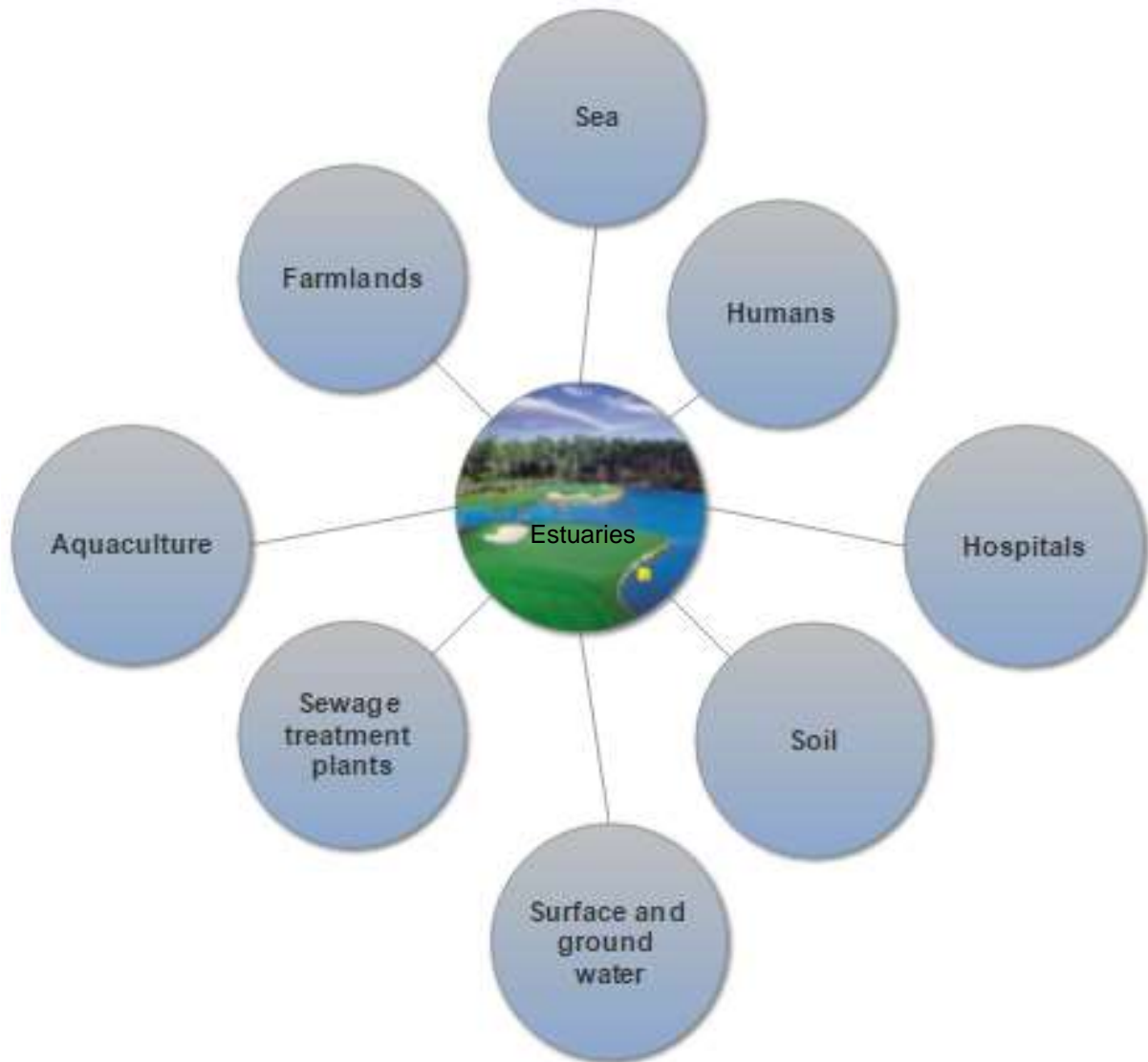


Figure 1.3: Cluster diagram indicating several sources of microbial contaminants and antibiotic resistant determinant loads in estuarine ecosystems

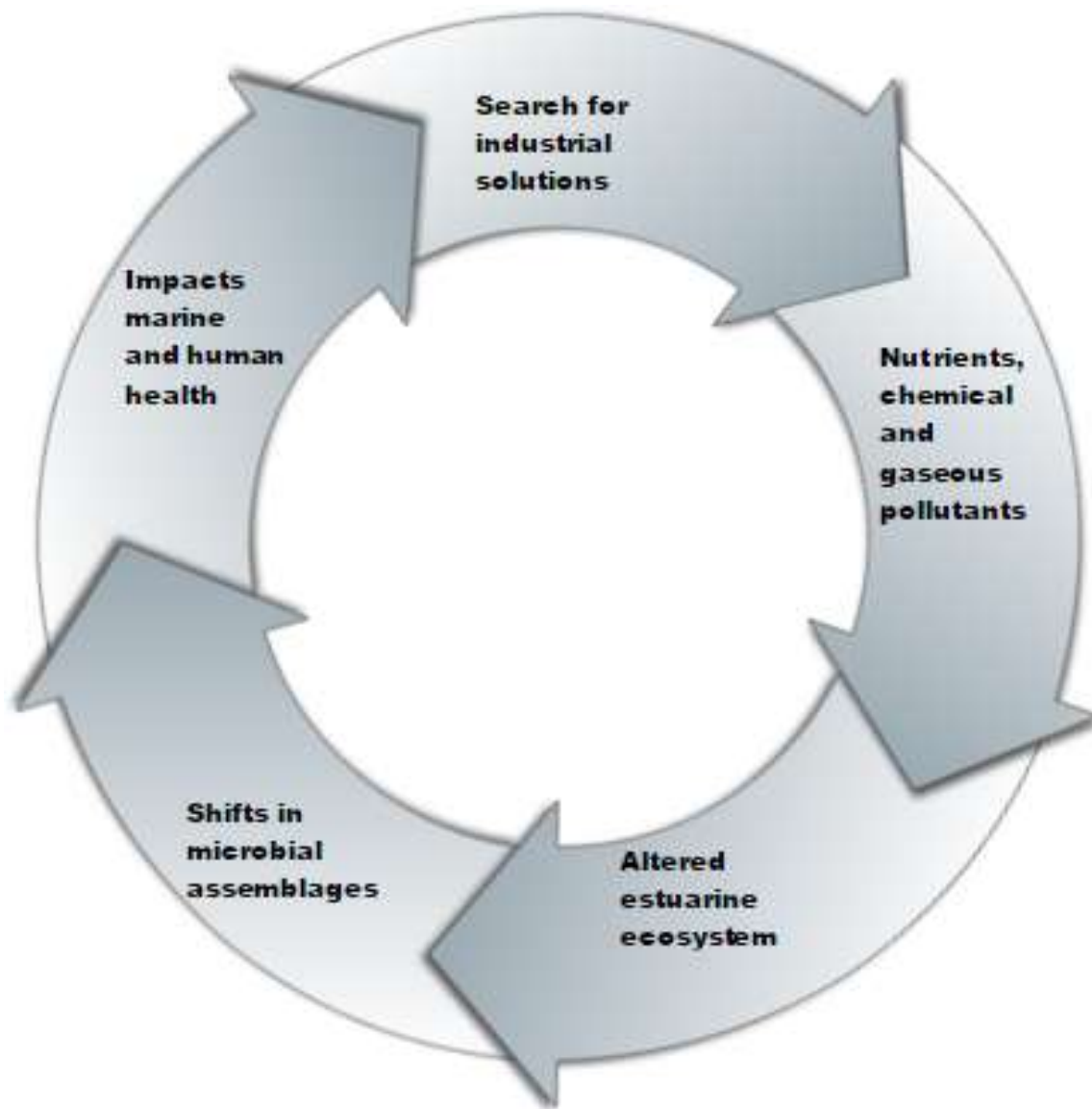


Figure 1.4: Cycle diagram on the ripple effects of impacts of natural and anthropogenic perturbations to estuarine ecosystems

References

- Estuarium Exhibits: Mobile Bay". "Dauphin Island Sea Lab". Retrieved 2014-03-24.
www.disl.org/estuarium/exhibits.htm.
- Adon, M., Galy-Lacaux, C., Yoboué, V., Delon, C., Lacaux, J., Castera, P., Gardrat, E., Pienaar, J., Ourabi, H.A., Laouali, D., 2010. Long term measurements of sulfur dioxide, nitrogen dioxide, ammonia, nitric acid and ozone in Africa using passive samplers. *Atmospheric Chemistry and Physics* 10, 7467-7487.
- Aguirre, A.A., Lutz, P.L., 2004. Marine turtles as sentinels of ecosystem health: is fibropapillomatosis an indicator? *EcoHealth* 1, 275-283.
- Álvarez-Vázquez, M.A., Prego, R., Ospina-Alvarez, N., Caetano, M., Bernárdez, P., Doval, M., Filgueiras, A.V., Vale, C., 2016. Anthropogenic changes in the fluxes to estuaries: Wastewater discharges compared with river loads in small rias. *Estuarine, Coastal and Shelf Science* 179, 112-123.
- Amachawadi, R.G., Scott, H.M., Alvarado, C.A., Mainini, T.R., Vinasco, J., Drouillard, J.S., Nagaraja, T.G., 2013. Occurrence of the Transferable Copper Resistance Gene *tcuB* among Fecal Enterococci of U.S. Feedlot Cattle Fed Copper-Supplemented Diets. *Applied and environmental microbiology* 79, 4369-4375.
- Amalfitano, S., Coci, M., Corno, G., Luna, G.M., 2015. A microbial perspective on biological invasions in aquatic ecosystems. *Hydrobiologia* 746, 13-22.
- Anil, A., 2006. A perspective of marine bioinvasion. 203-213.
<http://drs.nio.org/drs/handle/2264/2200>.
- Arena, P.C., Warwick, C., Steedman, C., 2014. Welfare and environmental implications of farmed sea turtles. *Journal of agricultural and environmental ethics* 27, 309-330.
- Azam, F., Fenchel, T., Field, J.G., Gray, J., Meyer-Reil, L., Thingstad, F., 1983. The ecological role of water-column microbes in the sea. *Estuaries* 50, 257-263.
- Bai, X., Zhang, Z., Bai, M., Yang, B., Bai, M., 2005. Killing of Invasive Species of Ship's Ballast Water in 20t/h System Using Hydroxyl Radicals. *Plasma Chemistry and Plasma Processing* 25, 41-54.
- Baker-Austin, C., Rangdale, R., Lowther, J., Lees, D.N., 2010. Application of mitochondrial DNA analysis for microbial source tracking purposes in shellfish harvesting waters. *Water science and technology : a journal of the International Association on Water Pollution Research* 61, 1-7.

- Baker-Austin, C., Trinanés, J.A., Taylor, N.G.H., Hartnell, R., Siitonen, A., Martínez-Urtaza, J., 2013. Emerging *Vibrio* risk at high latitudes in response to ocean warming. *Nature Climate Change* 3, 73-77.
- Baker-Austin, C., Wright, M.S., Stepanauskas, R., McArthur, J.V., 2006. Co-selection of antibiotic and metal resistance. *Trends in microbiology* 14, 176-182.
- Baquero, F., Martínez, J.-L., Cantón, R., 2008. Antibiotics and antibiotic resistance in water environments. *Current opinion in biotechnology* 19, 260-265.
- Baquero, F., Tedim, A.P., Coque, T.M., 2013. Antibiotic resistance shaping multi-level population biology of bacteria. *Frontiers in microbiology* 4, 1-14.
- Bauer, J.E., Cai, W.J., Raymond, P.A., Bianchi, T.S., Hopkinson, C.S., Regnier, P.A., 2013. The changing carbon cycle of the coastal ocean. *Nature* 504, 61-70.
- Bax, N., Williamson, A., Agüero, M., González, E., Geeves, W., 2003. Marine invasive alien species: a threat to global biodiversity. *Marine Policy* 27, 313-323.
- Biaśtoch, A., Treude, T., Rüpke, L.H., Riebesell, U., Roth, C., Burwicz, E.B., Park, W., Latif, M., Böning, C.W., Madec, G., 2011. Rising Arctic Ocean temperatures cause gas hydrate destabilization and ocean acidification. *Geophysical Research Letters* 38, 1-5.
- Bricker, S.B., Longstaff, B., Dennison, W., Jones, A., Boicourt, K., Wicks, C., Woerner, J., 2008. Effects of nutrient enrichment in the nation's estuaries: a decade of change. *Harmful Algae* 8, 21-32.
- Brierley, A.S., Kingsford, M.J., 2009. Impacts of climate change on marine organisms and ecosystems. *Curr Biol* 19, 602-614.
- Butler, O.T., Cairns, W.R., Cook, J.M., Davidson, C.M., 2012. Atomic spectrometry update. *Environmental analysis. Journal of Analytical Atomic Spectrometry* 27, 187-221.
- Buzicky, G., Randall, G., Hauck, R., Caldwell, A., 1983. Fertilizer N losses from a tile-drained mollisol as influenced by rate and time of 15-N depleted fertilizer application, *Agronomy Abstracts*, p. 213.
- Chandra, S., Sharma, R., Singh, K., Sharma, A., 2013. Application of bioremediation technology in the environment contaminated with petroleum hydrocarbon. *Annals of Microbiology* 63, 417-431.

Chen, B., Yang, Y., Liang, X., Yu, K., Zhang, T., Li, X., 2013. Metagenomic profiles of antibiotic resistance genes (ARGs) between human impacted estuary and deep ocean sediments. *Environmental science & technology* 47, 12753-12760.

Chen, S., Li, X., Sun, G., Zhang, Y., Su, J., Ye, J., 2015. Heavy Metal Induced Antibiotic Resistance in Bacterium LSJC7. *International journal of molecular sciences* 16, 23390-23404.

Cloern, J.E., Foster, S.Q., Kleckner, A.E., 2014. Phytoplankton primary production in the world's estuarine-coastal ecosystems. *Biogeosciences* 11, 2477-2501.

Cronin, T.M., 2016. Climate Change, in: Kennish, M.J. (Ed.), *Encyclopedia of Estuaries*. Springer Netherlands, Dordrecht, pp. 122-128.

Culbertson, J.B., Valiela, I., Olsen, Y.S., Reddy, C.M., 2008. Effect of field exposure to 38-year-old residual petroleum hydrocarbons on growth, condition index, and filtration rate of the ribbed mussel, *Geukensia demissa*. *Environmental Pollution* 154, 312-319.

Dang, H., Ren, J., Song, L., Sun, S., An, L., 2008. Diverse tetracycline resistant bacteria and resistance genes from coastal waters of Jiaozhou Bay. *Microb Ecol* 55, 237-246.

Day, J.H., 1980. What is an estuary? *South African Journal of Science* 76, 198.

De Souza, M.J., Nair, S., Loka Bharathi, P.A., Chandramohan, D., 2006. Metal and antibiotic-resistance in psychrotrophic bacteria from Antarctic Marine waters. *Ecotoxicology* 15, 379-384.

Deacutis, C.F., 2016. Dissolved Oxygen, in: Kennish, M.J. (Ed.), *Encyclopedia of Estuaries*. Springer Netherlands, Dordrecht, pp. 202-203.

Diesch, J.M., Drewnick, F., Zorn, S.R., von der Weiden-Reinmüller, S.L., Martinez, M., Borrmann, S., 2012. Variability of aerosol, gaseous pollutants and meteorological characteristics associated with changes in air mass origin at the SW Atlantic coast of Iberia. *Atmos. Chem. Phys.* 12, 3761-3782.

Doney, S.C., Ruckelshaus, M., Duffy, J.E., Barry, J.P., Chan, F., English, C.A., Galindo, H.M., Grebmeier, J.M., Hollowed, A.B., Knowlton, N., Polovina, J., Rabalais, N.N., Sydeman, W.J., Talley, L.D., 2012. Climate change impacts on marine ecosystems. *Annual review of marine science* 4, 11-37.

Drake, L.A., Doblin, M.A., Dobbs, F.C., 2007. Potential microbial bioinvasions via ships' ballast water, sediment, and biofilm. *Mar Pollut Bull* 55, 333-341.

Dröge, M., Pühler, A., Selbitschka, W., 1999. Horizontal gene transfer among bacteria in terrestrial and aquatic habitats as assessed by microcosm and field studies. *Biology and Fertility of Soils* 29, 221-245.

Dunbabin, J.S., Bowmer, K.H., 1992. Potential use of constructed wetlands for treatment of industrial wastewaters containing metals. *Science of The Total Environment* 111, 151-168.

Dyer, K.R., 1995. Sediment transport processes in estuaries. *Developments in Sedimentology* 53, 423-449.

Ebdon, J.E., Wallis, J.L., Taylor, H.D., 2004. A simplified low-cost approach to antibiotic resistance profiling for faecal source tracking. *Water Science and Technology* 50, 185-191.

El-Habashi, A., Ioannou, I., Tomlinson, M.C., Stumpf, R.P., Ahmed, S., 2016. Satellite Retrievals of *Karenia brevis* Harmful Algal Blooms in the West Florida Shelf Using Neural Networks and Comparisons with Other Techniques. *Remote Sensing* 8, 1-25.

El Bour, M., 2016. Microbial Degradation, in: Kennish, M.J. (Ed.), *Encyclopedia of Estuaries*. Springer Netherlands, Dordrecht, pp. 433-433.

Elliott, M., Hemingway, K., 2002. *Fishes in estuaries*. Blackwell Science, Oxford ; Malden, Mass. Ames, Iowa Iowa State University Press. Chapter 2, pp.1-44.

Elliott, M., McLusky, D.S., 2002. The Need for Definitions in Understanding Estuaries. *Estuarine, Coastal and Shelf Science* 55, 815-827.

Elliott, M., Whitfield, A.K., Potter, I.C., Blaber, S.J., Cyrus, D.P., Nordlie, F.G., Harrison, T.D., 2007. The guild approach to categorizing estuarine fish assemblages: a global review. *Fish and Fisheries* 8, 241-268.

Ferguson, C., Husman, A.M.d.R., Altavilla, N., Deere, D., Ashbolt, N., 2003. Fate and Transport of Surface Water Pathogens in Watersheds. *Critical Reviews in Environmental Science and Technology* 33, 299-361.

Fertig, B., Kennish, M.J., Sakowicz, G.P., Reynolds, L.K., 2014. Mind the data gap: identifying and assessing drivers of changing eutrophication condition. *Estuaries and Coasts* 37, 198-221.

Fleming, L.E., McDonough, N., Austen, M., Mee, L., Moore, M., Hess, P., Depledge, M.H., White, M., Philippart, K., Bradbrook, P., Smalley, A., 2014. Oceans and Human Health: A rising tide of challenges and opportunities for Europe. *Mar Environ Res* 99, 16-19.

Flindt, M.R., Pardal, M.Â., Lillebø, A.I., Martins, I., Marques, J.C., 1999. Nutrient cycling and plant dynamics in estuaries: A brief review. *Acta Oecologica* 20, 237-248.

Gavrilescu, M., Demnerová, K., Aamand, J., Agathos, S., Fava, F., 2015. Emerging pollutants in the environment: present and future challenges in biomonitoring, ecological risks and bioremediation. *New Biotechnology* 32, 147-156.

Gelesh, L., Marshall, K., Boicourt, W., Lapham, L., 2016. Methane concentrations increase in bottom waters during summertime anoxia in the highly eutrophic estuary, Chesapeake Bay, U.S.A. *Limnology and Oceanography* 10, 1002-1027.

Griffin, J., 2014. Ocean Acidification and Methane Hydrates
http://www.climateemergencyinstitute.com/uploads/Ocean_Acidification_Methane.pdf. pp.1-10.

Guardabassi, L., Lo Fo Wong, D.M.A., Dalsgaard, A., 2002. The effects of tertiary wastewater treatment on the prevalence of antimicrobial resistant bacteria. *Water Research* 36, 1955-1964.

Hanski, I., von Hertzen, L., Fyhrquist, N., Koskinen, K., Torppa, K., Laatikainen, T., Karisola, P., Auvinen, P., Paulin, L., Makela, M.J., Vartiainen, E., Kosunen, T.U., Alenius, H., Haahtela, T., 2012. Environmental biodiversity, human microbiota, and allergy are interrelated. *Proceedings of the National Academy of Sciences of the United States of America* 109, 8334-8339.

Hansson, H.G., 2006. Ctenophores of the Baltic and adjacent Seas-the invader *Mnemiopsis* is here! *Aquatic Invasions* 1, 295-298

Hasman, H., Aarestrup, F.M., 2002. *tcxB*, a gene conferring transferable copper resistance in *Enterococcus faecium*: occurrence, transferability, and linkage to macrolide and glycopeptide resistance. *Antimicrobial agents and chemotherapy* 46, 1410-1416.

Hatje, V., 2016. Pharmaceuticals, in: Kennish, M.J. (Ed.), *Encyclopedia of Estuaries*. Springer Netherlands, Dordrecht, pp. 481-483.

Hershner, C., Havens, K., Bilkovic, D., Wardrop, D., 2007. Assessment of Chesapeake Bay Program Selection and Use of Indicators. *EcoHealth* 4, 187-193.

Howarth, R.W., Sharpley, A., Walker, D., 2002. Sources of nutrient pollution to coastal waters in the United States: Implications for achieving coastal water quality goals. *Estuaries* 25, 656-676.

Ip, C.C., Li, X.D., Zhang, G., Wai, O.W., Li, Y.S., 2007. Trace metal distribution in sediments of the Pearl River Estuary and the surrounding coastal area, South China. *Environ Pollut* 147, 311-323.

Ivanov, V., Kamakin, A., Ushivtzev, V., Shiganova, T., Zhukova, O., Aladin, N., Wilson, S., Harbison, G.R., Dumont, H., 2000. Invasion of the Caspian Sea by the Comb Jellyfish *Mnemiopsis leidyi* (Ctenophora). *Biological Invasions* 2, 255-258.

Jaspers, C., Moller, L.F., Kiorboe, T., 2011. Salinity gradient of the Baltic Sea limits the reproduction and population expansion of the newly invaded comb jelly *Mnemiopsis leidyi*. *PLoS one* 6, 809-812.

Joint, I., Doney, S.C., Karl, D.M., 2011. Will ocean acidification affect marine microbes? *The ISME journal* 5, 1-7.

Jokiel, P.L., 2015. Predicting the impact of ocean acidification on coral reefs: evaluating the assumptions involved. *ICES Journal of Marine Science: Journal du Conseil* 4, 2-8.

Junot, J.A., Poirrier, M.A., Soniat, T.M., 2015. Effects of saltwater intrusion from the Inner Harbor Navigation Canal on the benthos of Lake Pontchartrain, Louisiana. *Gulf and Caribbean Research* 7, 247-254.

Jutla, A.S., Akanda, A.S., Griffiths, J.K., Colwell, R., Islam, S., 2011. Warming Oceans, Phytoplankton, and River Discharge: Implications for Cholera Outbreaks. *American Journal of Tropical Medicine and Hygiene* 85, 303-308.

Kennish, M.J., 2002. Environmental threats and environmental future of estuaries. *Environmental conservation* 29, 78-107.

Kennish, M.J., 2008. Environmental future of estuaries. *Aquatic Ecosystems: Trends and global prospects* 8, 188-208.

Kennish, M.J., 2016. Anthropogenic Impacts, in: Kennish, M.J. (Ed.), *Encyclopedia of Estuaries*. Springer Netherlands, Dordrecht, pp. 29-35.

Kideys, A.E., 2002. Ecology. Fall and rise of the Black Sea ecosystem. *Science* 297, 1482-1484.

Kim, S.C., Carlson, K., 2007. Quantification of human and veterinary antibiotics in water and sediment using SPE/LC/MS/MS. *Anal Bioanal Chem* 387, 1301-1315.

Kindinger, J.L., 1988. Seismic stratigraphy of the Mississippi-Alabama shelf and upper continental slope. *Marine Geology* 83, 79-94.

Koike, S., Krapac, I.G., Oliver, H.D., Yannarell, A.C., Chee-Sanford, J.C., Aminov, R.I., Mackie, R.I., 2007. Monitoring and source tracking of tetracycline resistance genes in lagoons and groundwater adjacent to swine production facilities over a 3-year period. *Applied and environmental microbiology* 73, 4813-4823.

Kostka, J.E., Prakash, O., Overholt, W.A., Green, S.J., Freyer, G., Canion, A., Delgardio, J., Norton, N., Hazen, T.C., Huettel, M., 2011. Hydrocarbon-degrading bacteria and the bacterial

community response in gulf of Mexico beach sands impacted by the deepwater horizon oil spill. *Applied and environmental microbiology* 77, 7962-7974.

Kremer, P., 1976. Population dynamics and ecological energetics of a pulsed zooplankton predator, the ctenophore *Mnemiopsis leidyi*. Academic Press pp.197-215.

Lamendella, R., Santo Domingo, J.W., Yannarell, A.C., Ghosh, S., Di Giovanni, G., Mackie, R.I., Oerther, D.B., 2009. Evaluation of swine-specific PCR assays used for fecal source tracking and analysis of molecular diversity of swine-specific "Bacteroidales" populations. *Applied and environmental microbiology* 75, 5787-5996.

Lellis-Dibble, K.A., McGlynn, K.E., Bigford, T.E., 2008. Estuarine Fish and Shellfish Species in U.S. Commercial and Recreational Fisheries: Economic Value as an Incentive to Protect and Restore Estuarine Habitat. NOAA Technical Memorandum NMFS-F/SPO-90.
http://www.habitat.noaa.gov/pdf/publications_general_estuarinefishshellfish.pdf

Lipp, E.K., Farrah, S.A., Rose, J.B., 2001. Assessment and impact of microbial fecal pollution and human enteric pathogens in a coastal community. *Marine pollution bulletin* 42, 286-293.

Malham, S.K., Rajko-Nenow, P., Howlett, E., Tuson, K.E., Perkins, T.L., Pallett, D.W., Wang, H., Jago, C.F., Jones, D.L., McDonald, J.E., 2014. The interaction of human microbial pathogens, particulate material and nutrients in estuarine environments and their impacts on recreational and shellfish waters. *Environ Sci Process Impacts* 16, 2145-2155.

Mallin, M.A., Williams, K.E., Esham, E.C., Lowe, R.P., 2000. Effect of human development on bacteriological water quality in coastal watersheds. *Ecological applications* 10, 1047-1056.

Maranda, L., Cox, A.M., Campbell, R.G., Smith, D.C., 2013. Chlorine dioxide as a treatment for ballast water to control invasive species: shipboard testing. *Marine pollution bulletin* 75, 76-89.

Mariita, R.M., Hossain, M.J., Liles, M.R., Moss, A.G., 2015. Seasonal Variability in the Diversity of Microbial Assemblages and Antibiotic Resistance Determinants of an Estuary System. <http://ir-library.ku.ac.ke/handle/123456789/12418>

Marquez, D.J.D., 2016. Estuarine Flocculation, in: Kennish, M.J. (Ed.), *Encyclopedia of Estuaries*. Springer Netherlands, Dordrecht, pp. 272-273.

Martinez, J., 2003. Recent Advances in Marine Biotechnology. *Molecular Genetics of Marine Organisms*. Recent advances on antibiotic resistance genes. Cal West Med Fingerman N, editor.10, 13-32.

Mathe, I., Benedek, T., Tancsics, A., Palatinszky, M., Lanyi, S., Marialigeti, K., 2012. Diversity, activity, antibiotic and heavy metal resistance of bacteria from petroleum hydrocarbon

contaminated soils located in Harghita County (Romania). *International Biodeterioration & Biodegradation* 73, 41-49.

Maynard, J., van Hooijdonk, R., Eakin, C.M., Puotinen, M., Garren, M., Williams, G., Heron, S.F., Lamb, J., Weil, E., Willis, B., Harvell, C.D., 2015. Projections of climate conditions that increase coral disease susceptibility and pathogen abundance and virulence. *Nature Clim. Change* 5, 688-694.

McCallum, H., Harvell, D., Dobson, A., 2003. Rates of spread of marine pathogens. *Ecology letters* 6, 1062-1067.

McCartney, M.P., Rebelo, L.-M., Sellamuttu, S.S., 2015. Wetlands, Livelihoods and Human Health, *Wetlands and Human Health*. Springer, pp. 123-148.

McComb, J.Q., Rogers, C., Han, F.X., Tchounwou, P.B., 2014. Rapid screening of heavy metals and trace elements in environmental samples using portable X-ray fluorescence spectrometer, A comparative study. *Water, Air, & Soil Pollution* 225, 1-10.

McDowall, R.M., 1997. The evolution of diadromy in fishes (revisited) and its place in phylogenetic analysis. *Reviews in Fish Biology and Fisheries* 7, 443-462.

Merriam-Webster, 1979. *Webster's New Collegiate Dictionary*, G and C Merriam Co., . Springfield, MA.

Mitchell, S.B., Jennerjahn, T.C., Vizzini, S., Zhang, W.G., 2015. Changes to processes in estuaries and coastal waters due to intense multiple pressures: An introduction and synthesis. *Estuarine Coastal and Shelf Science* 156, 1-6.

Mitsch, W.J., Day, J.W., Gilliam, J.W., Groffman, P.M., Hey, D.L., Randall, G.W., Wang, N., 2001. Reducing Nitrogen Loading to the Gulf of Mexico from the Mississippi River Basin: Strategies to Counter a Persistent Ecological Problem: Ecotechnology-the use of natural ecosystems to solve environmental problems-should be a part of efforts to shrink the zone of hypoxia in the Gulf of Mexico. *BioScience* 51, 373-388.

Morton, B., Blackmore, G., 2001. South China Sea. *Mar Pollut Bull* 42, 1236-1263.

Nesme, J., Cecillon, S., Delmont, T.O., Monier, J.M., Vogel, T.M., Simonet, P., 2014. Large-scale metagenomic-based study of antibiotic resistance in the environment. *Curr Biol* 24, 1096-1100.

Nisbet, E.G., Dlugokencky, E.J., Bousquet, P., 2014. Atmospheric science. Methane on the rise-again. *Science* 343, 493-495.

- Norhana, M.N.W., Poole, S.E., Deeth, H.C., Dykes, G.A., 2010. The effects of temperature, chlorine and acids on the survival of *Listeria* and *Salmonella* strains associated with uncooked shrimp carapace and cooked shrimp flesh. *Food microbiology* 27, 250-256.
- Ojaveer, H., Kotta, J., Ecosystem impacts of the widespread non-indigenous species in the Baltic Sea: literature survey evidences major limitations in knowledge. *Hydrobiologia* 750, 171-185.
- Olalekan, A.A., Malik, K., 2015. Application of Giovanni for rapid assessment of harmful algal blooms in the Arabian Gulf. *Arabian Journal of Geosciences* 8, 8767-8775.
- Osborne, L.L., Kovacic, D.A., 1993. Riparian vegetated buffer strips in water quality restoration and stream management. *Freshwater biology* 29, 243-258.
- Osuji, L.C., Onojake, C.M., 2004. Trace heavy metals associated with crude oil: a case study of Ebocha-8 oil-spill-polluted site in Niger Delta, Nigeria. *Chemistry & biodiversity* 1, 1708-1715.
- Paerl, H.W., 1997. Coastal eutrophication and harmful algal blooms: Importance of atmospheric deposition and groundwater as “new” nitrogen and other nutrient sources. *Limnology and Oceanography* 42, 1154-1165.
- Park, K., Powers, S.P., Bosarge, G.S., Jung, H.S., 2014. Plugging the leak: barrier island restoration following Hurricane Katrina enhances larval retention and improves salinity regime for oysters in Mobile Bay, Alabama. *Mar Environ Res* 94, 48-55.
- Parkes, R.J., Cragg, B.A., Wellsbury, P., 2000. Recent studies on bacterial populations and processes in subseafloor sediments: A review. *Hydrogeology Journal* 8, 11-28.
- Perillo, G.M., 1995. *Geomorphology and sedimentology of estuaries*. Elsevier 53, 179-205.
- Port, J.A., Wallace, J.C., Griffith, W.C., Faustman, E.M., 2012. Metagenomic profiling of microbial composition and antibiotic resistance determinants in Puget Sound. *PloS one* 7, 1-14.
- Potter, I.C., Chuwen, B.M., Hoeksema, S.D., Elliott, M., 2010. The concept of an estuary: A definition that incorporates systems which can become closed to the ocean and hypersaline. *Estuarine, Coastal and Shelf Science* 87, 497-500.
- Pritchard, D.W., 1967. What is an estuary: physical viewpoint. *American Association for the Advancement of Science*, 83, 3-5.
- Pryor, S.C., Sorensen, L.L., 2002. Dry deposition of reactive nitrogen to marine environments: recent advances and remaining uncertainties. *Mar Pollut Bull* 44, 1336-1340.

Qiu, L., Dong, Z., Sun, H., Li, H., Chang, C.C., 2016. Emerging Pollutants - Part I: Occurrence, Fate and Transport. Water environment research : a research publication of the Water Environment Federation 88, 1855-1875.

Rakowski, C., Magen, C., Bosman, S., Gillies, L., Rogers, K., Chanton, J., Mason, O., 2015. Methane and microbial dynamics in the Gulf of Mexico water column. *Frontiers in Marine Science* 2, 1-10.

Rashleigh, B., Cyterski, M., Smith, L.M., Nestlerode, J.A., 2009. Relation of fish and shellfish distributions to habitat and water quality in the Mobile Bay estuary, USA. *Environmental monitoring and assessment* 150, 181-192.

Reed, H.E., Martiny, J.B.H., 2013. Microbial composition affects the functioning of estuarine sediments. *Isme Journal* 7, 868-879.

Ridgway, J., Shimmield, G., 2002. Estuaries as repositories of historical contamination and their impact on shelf seas. *Estuarine Coastal and Shelf Science* 55, 903-928.

Rook, G.A., 2013. Regulation of the immune system by biodiversity from the natural environment: An ecosystem service essential to health. *Proceedings of the National Academy of Sciences of the United States of America* 110, 18360-18367.

Rozen, Y., Belkin, S., 2001. Survival of enteric bacteria in seawater. *FEMS Microbiol Rev* 25, 513-529.

Schaefer, A.M., Goldstein, J.D., Reif, J.S., Fair, P.A., Bossart, G.D., 2009. Antibiotic-Resistant Organisms Cultured from Atlantic Bottlenose Dolphins (*Tursiops truncatus*) Inhabiting Estuarine Waters of Charleston, SC and Indian River Lagoon, FL. *EcoHealth* 6, 33-41.

Schets, F.M., van den Berg, H.H., Marchese, A., Garbom, S., de Roda Husman, A.M., 2011. Potentially human pathogenic vibrios in marine and fresh bathing waters related to environmental conditions and disease outcome. *International journal of hygiene and environmental health* 214, 399-406.

Schuster, T.D., Schuster, M., Banerjee, A., Shankar, A., Byrne, J., Glover, D.L., Assembly, D.G., 2004. Transportation strategies to improve air quality. http://ceep.udel.edu/wp-content/uploads/2013/08/2004_transport_strategies2.pdf. 11-61.

Seiler, C., Berendonk, T.U., 2012. Heavy metal driven co-selection of antibiotic resistance in soil and water bodies impacted by agriculture and aquaculture. *Frontiers in microbiology* 3, 1-10.

Smith, L.M., Nestlerode, J.A., Harwell, L.C., Bourgeois, P., 2010. The areal extent of brown shrimp habitat suitability in Mobile Bay, Alabama, USA: targeting vegetated habitat restoration. *Environmental monitoring and assessment* 171, 611-620.

Snieszko, S., 1974. The effects of environmental stress on outbreaks of infectious diseases of fishes. *Journal of Fish Biology* 6, 197-208.

Song, Y.C., 2013. Exploring microbial controls on methane cycling using MLTreeMap. Master of Science. University of British Columbia. Vancouver. pp 21-28.

Sousa, A.I., Lillebø, A.I., Caçador, I., Pardal, M.A., 2008. Contribution of *Spartina maritima* to the reduction of eutrophication in estuarine systems. *Environmental Pollution* 156, 628-635.

Stephen, J.R., Chang, Y.-J., Macnaughton, S.J., Kowalchuk, G.A., Leung, K.T., Flemming, C.A., White, D.C., 1999. Effect of toxic metals on indigenous soil β -subgroup proteobacterium ammonia oxidizer community structure and protection against toxicity by inoculated metal-resistant bacteria. *Applied and environmental microbiology* 65, 95-101.

Sterk, A., Schets, F.M., de Roda Husman, A.M., de Nijs, T., Schijven, J.F., 2015. Effect of Climate Change on the Concentration and Associated Risks of *Vibrio* Spp. in Dutch Recreational Waters. *Risk analysis : an official publication of the Society for Risk Analysis* 35, 1717-1729.

Sunagawa, S., Coelho, L.P., Chaffron, S., Kultima, J.R., Labadie, K., Salazar, G., Djahanschiri, B., Zeller, G., Mende, D.R., Alberti, A., 2015. Structure and function of the global ocean microbiome. *Science* 348, 1261359.

Tryland, I., Fykse, E.-M., Bomo, A.-M., Jantsch, T.G., Nielsen, A.D., Liltved, H., 2010. Monitoring of bacteria in ballast water. *Emerging Ballast Water Management Systems* 26, 219-230.

Turnbaugh, P.J., Hamady, M., Yatsunencko, T., Cantarel, B.L., Duncan, A., Ley, R.E., Sogin, M.L., Jones, W.J., Roe, B.A., Affourtit, J.P., Egholm, M., Henrissat, B., Heath, A.C., Knight, R., Gordon, J.I., 2009. A core gut microbiome in obese and lean twins. *Nature* 457, 480-U487.

Valle-Levinson, A., 2011. Classification of Estuarine Circulation. www.essie.ufl.edu/

Van Hamme, J.D., Singh, A., Ward, O.P., 2003. Recent advances in petroleum microbiology. *Microbiology and molecular biology reviews : MMBR* 67, 503-549.

Vignesh, S., Dahms, H.-U., Emmanuel, K., Gokul, M., Muthukumar, K., Kim, B.-R., James, R., 2014. Physicochemical parameters aid microbial community? A case study from marine recreational beaches, Southern India. *Environmental monitoring and assessment* 186, 1875-1887.

Voorhees, D.V., Lowther, A., Spring, S., 2011. Fisheries of the United States. National Marine Fisheries Service Office of Science and Technology. Current Fishery Statistics No. 2011, pp.23-46.

Vymazal, J., 2010. Constructed wetlands for wastewater treatment. *Water* 2, 530-549.

Whitehead, A., 2013. Interactions between oil-spill pollutants and natural stressors can compound ecotoxicological effects. *Integrative and comparative biology* 53, 635-647.

Xu, J., Xu, Y., Wang, H., Guo, C., Qiu, H., He, Y., Zhang, Y., Li, X., Meng, W., 2015. Occurrence of antibiotics and antibiotic resistance genes in a sewage treatment plant and its effluent-receiving river. *Chemosphere* 119, 1379-1385.

Yan, C., Yang, Y., Zhou, J., Liu, M., Nie, M., Shi, H., Gu, L., 2013. Antibiotics in the surface water of the Yangtze Estuary: occurrence, distribution and risk assessment. *Environ Pollut* 175, 22-29.

Yan, L., Li, Z., Bao, J., Wang, G., Wang, C., Wang, W., 2015. Diversity of ammonia-oxidizing bacteria and ammonia-oxidizing archaea during composting of municipal sludge. *Annals of Microbiology* 65, 1729-1739.

Yang, A., Zhang, X., Agogué, H., Dupuy, C., Gong, J., 2015. Contrasting spatiotemporal patterns and environmental drivers of diversity and community structure of ammonia oxidizers, denitrifiers, and anammox bacteria in sediments of estuarine tidal flats. *Annals of Microbiology* 65, 879-890.

Zaika, V.Y., Sergeyeva, N.G., 1990. Morphology and development of *Mnemiopsis mccradyi* (Ctenophora, Lobata) in the Black Sea. *Zoologicheskiy Zhurnal* 69, 5-11.

Zavala-Norzagaray, A.A., Aguirre, A.A., Velazquez-Roman, J., Flores-Villasenor, H., Leon-Sicairos, N., Ley-Quinonez, C.P., Hernandez-Diaz Lde, J., Canizalez-Roman, A., 2015. Isolation, characterization, and antibiotic resistance of *Vibrio* spp. in sea turtles from Northwestern Mexico. *Frontiers in microbiology* 6, 1-10.

Zhang, L., Wu, B.F., Yin, K., Li, X.S., Kia, K., Zhu, L., 2015. Impacts of human activities on the evolution of estuarine wetland in the Yangtze Delta from 2000 to 2010. *Environmental Earth Sciences* 73, 435-447.

Zhao, Y., Zhang, J., Nielsen, C., 2013. The effects of recent control policies on trends in emissions of anthropogenic atmospheric pollutants and CO₂ in China. *Atmospheric Chemistry and Physics* 13, 487-508.

Zhou, Y., Xu, Y.B., Xu, J.X., Zhang, X.H., Xu, S.H., Du, Q.P., 2015. Combined toxic effects of heavy metals and antibiotics on a *Pseudomonas fluorescens* strain ZY2 isolated from swine wastewater. International journal of molecular sciences 16, 2839-2850.

Chapter 2: A survey on the dynamics and diversity of bacterioplankton assemblages and antibiotic resistance determinants of an estuarine system

Abstract

Estuaries are economically important ecosystems as they are sources of shellfish and finfish and are popular destinations for recreational activities. Unfortunately, estuaries also act as sinks for heavy metals and antibiotics from natural and anthropogenic sources. From the viewpoint of ecosystem health, it is vital to monitor the dynamics of the bacterial assemblages and antibiotic resistance determinants (ARDs) in estuaries, particularly the ones heavily used by the public. The bacterial assemblage of Mobile Bay, Alabama, USA was investigated using shotgun metagenomics. The objective of this study was to compare bacterioplankton assemblages and ARDs in Mobile Bay between the wet, cold and dry, warm periods of the year. DNA samples were pooled from January and March collections, representing a wet, cold period with high riverine discharge and separately from August and September, which represented a dry, warm period with low river discharge into the bay. The results revealed high taxonomic and phylogenetic diversity of the bacterial assemblage during the wet, cold months, in which the assemblage was dominated by Proteobacteria, Actinobacteria and Bacteroidetes. In contrast, the dry, warm period exhibited a less diverse assemblage dominated by Cyanobacteria and Verrucomicrobia. Analyses of correlations in bacterial abundance with temporal variation in physicochemical parameters in Mobile Bay revealed that the abundances of Cyanobacteria, Verrucomicrobia, Gemmatimonadetes and Proteobacteria correlated with levels of nitrogen dioxide, ammonium, and temperature. This is possibly due to strong influence from the environmental parameters. The wet, cold period also exhibited a relatively high abundance in the microbial assemblage of antibiotic resistance determinants (ARDs), including genes for phages

and prophages, pathogenicity islands, fluoroquinolone resistance, multidrug resistance (MDR) efflux pumps, heavy metal (arsenic and cobalt-zinc-cadmium) resistance genes. This is possibly due to selective pressure from pollutants from the watershed coupled with changes in physicochemical parameters. The present study extends our knowledge base about microbial assemblages in Mobile Bay, and enhances our understanding of the link between microbial dynamics and underlying ecosystem health based on the corresponding changes in their predicted functional potential.

Introduction

Estuaries are important ecological interfaces between terrestrial and marine environments (Sun et al., 2014). As one of the most biologically productive ecosystems (Whittaker and Likens, 1975), they are important sources of seafood (Mitra and Zaman, 2016), including shellfish such as shrimp, oyster, and blue crab (Rashleigh et al., 2009; Smith et al., 2010) as well as many types of finfish (Elliott and Hemingway, 2002). Estuaries are also critical for nutrient cycling (Cai, 2011) while also providing ideal destinations for recreational activities (Mitra and Zaman, 2016).

Mobile Bay has the 6th largest watershed and represents the 4th largest freshwater drainage in the United States (Huhtanen et al., 2014) (Fig. 1). On average, Mobile Bay is 3 meters deep and receives annually 4,500 million kg of suspended sediment and 56.8 km³ of water from a 107,000 km² drainage basin leading into the Mobile-Tensaw River Delta (Curtis et al., 1973; Smith et al., 2013). The Mobile-Tensaw River Delta is the largest inland delta in the U.S., at 656 km², with a catchment area of 43, 662 square miles (Howe et al., 1999; Stout et al., 1998). Tourism and fishing that depend upon Mobile Bay are important to Alabama's economy, with about \$3

billion of Alabama's \$9 billion travel industry coming from Baldwin and Mobile counties alone (Swann, 2014).

Mobile bay receives an average $2,246 \text{ m}^3 \text{ s}^{-1}$ of water input from the watershed (Pennock et al., 1998) and is vulnerable to erosion and flooding during extreme weather events which occur between June and November each year (Zhao and Chen, 2008). Eutrophication arising from anthropogenic sources of pollution, in contrast, tends to be concentrated during the drier half of the year, from the months of June to November (Conner et al., 1989; Rabalais, 2011; Wetz and Yoskowitz, 2013), due to hurricanes and associated nutrients and sediment input that leads to short-term increased productivity (Conner et al., 1989). In addition, Mobile Bay receives over 42,000 tons of total nitrogen each year, mostly due to land-use practices which promotes eutrophication and reduction of dissolved oxygen (Rashleigh et al., 2009). Pollutants and altered physicochemical (PC) parameters can affect the integrity of estuarine systems, leading to shifts in microbial assemblage structures and function (Pinckney et al., 1995). Because bacterial assemblages are major drivers of estuarine processes, monitoring their taxonomic composition and predicting their functional capacities is of great importance for understanding estuarine ecosystem health, especially since estuaries tend to be very urbanized coastal ecosystems (Line and White, 2007). Some estuarine pollutants are gases, including CO_2 , SO_2 and NO_2 . Although many studies neglect the contribution of atmospheric nitrogen to the total nitrogen flux in coastal ecosystems, it can constitute as much as 20 to 40% of total nitrogen flux (Pryor and Sorensen, 2002). Methane (CH_4) leads to increased ocean acidification via bacteria driven-oxidation, resulting in increased carbon dioxide, and is also a sign of hypoxia or anoxic conditions in coastal ecosystems (Biajstoch et al., 2011; Gelesh et al., 2016). Carbon dioxide together with methane loads can cause altered food webs and biodiversity (Biajstoch et al., 2011; Griffin,

2014). Satellite data can be used to monitor gaseous pollutants and their impacts on aquatic ecosystems.

The overarching aim of this study was to assess the diversity of bacterial assemblages and antibiotic resistance determinant (ARD) genes during wet, cold (January/March, with high riverine discharge) and dry, warm (August/September, with low riverine discharge) months, and to explore the potential for Mobile Bay to act as a reservoir of antibiotic resistance. The study also sought to test if the observed shifts in bacterial assemblages correlated with physicochemical variables [temperature, salinity, conductivity, pH, dissolved oxygen (DO), ammonium (NH_4^+), nitrogen dioxide (NO_2) and methane (CH_4)] in Mobile Bay. The study specifically targeted the taxonomic composition of microbes, and correlated those results with PC parameters from wet and dry months. Using publically available metagenomic data, we further sought to compare the taxonomic and functional potential of Mobile Bay with four other marine systems (Monterey, Guanabara and Botany Bays and the Western English Channel Time Series [WECTS]). This study adds to the knowledge of variation in the bacterial taxonomic composition of Mobile Bay between wet, cold and dry, warm months and is, to the best of our knowledge, the first to investigate its potential to harbor ARDs. Our efforts also provide insight into methods for monitoring this important ecosystem.

Methods

Sample collection and processing

Surface water samples from nine collection sites (Fig. 2.1) were collected using sterile containers. Five hundred milliliters (0.5 liters) of raw seawater were collected at each of 9 sites during each of 4 sample periods, by dipping at the surface and immediately placed on ice.

Sampling for a wet, cold (1/26/2013 and 3/14/2013) and a dry, warm (8/25/2012 and 9/23/2012)

period (N=4 periods) was done at N=9 sites along the bay (coordinates 30°34'59.5"N 88°02'13.3"W, 30°29'55.5"N 88°04'05.0"W, 30°29'43.4"N 88°03'16.7"W, 30°28'22.1"N 88°01'25.7"W, 30°25'15.7"N 88°00'33.4"W, 30°21'31.8"N 88°00'34.8"W, 30°16'32.3"N 88°03'21.2"W, 30°17'00.7"N 88°01'20.7"W and 30°15'16.2"N 88°03'02.6"W, Fig. 2.1). The sampling periods were chosen depending on travel logistics and weather patterns in the bay. The water from all 9 sites then was pooled to obtain enough microbial DNA for analysis. Then pooled water samples (i.e. from the whole bay) on each date was additionally pooled for the 2 dates in the warm, dry period and the 2 dates in the wet, cold period, resulting in 2 pooled samples for the warm dry period, and 2 pooled samples for the wet cold period.

To assess the differences in the dynamics of microbial assemblages between upper bay and lower bay areas during wet, cold and dry warm periods, additional samples for one dated in January (1/26/2013) (N=3 sites) and one dated in August (8/25/2012) (N=3 sites) were collected (coordinates 30°29'55.5"N 88°04'05.0"W, 30°29'43.4"N 88°03'16.7"W and 30°28'22.1"N 88°01'25.7"W for upper bay and 30°16'32.3"N 88°03'21.2"W, 30°17'00.7"N 88°01'20.7"W and 30°15'16.2"N 88°03'02.6"W for lower bay). Again, these samples were pooled among the 3 sites per bay region, for a total of 1 upper and 1 lower bay sample during each of the 2 dates.

Upon arrival at the Auburn campus (usually not more than six hours later), the raw seawater was resuspended by swirling and then subjected to two-stage vacuum filtration, first through a 7 µm glass microfiber filter and then through a 0.2 µm polyamide filter. Both filters were stored at -80°C in sterile bags until DNA extraction.

DNA extraction

DNA was extracted from the 0.2 µm filters using the CTAB method (Dempster et al., 1999). DNA quality was assessed using a NanoDrop ND-1000 Spectrophotometer (NanoDrop

Technologies Inc.). DNA was specifically quantified by use of a Qubit 2.0 fluorometer (Invitrogen, Carlsbad, CA, USA). As described above, prior to library preparation, equal quantities of DNA from the 9 sites were added together to make one pooled sample for each of the seasonal periods (2 wet vs. 2 dry months' samples). For the upper and lower bay, samples were also pooled together to make two sets of pooled sample for wet cold upper and lower, and dry, warm upper and lower.

Library construction and sequencing

DNA was size fractionated and quantified using Agilent 2100 BioAnalyzer (Agilent Technologies, USA). It was then fragmented and libraries prepared using a Nextera XT 2 x 250 sequencing kit (Illumina, San Diego, CA) according to the manufacturer's protocol.

Quantification of the final library was performed using a Kapa quantification kit (RT-PCR) (Kapa Biosystems, Wilmington, MA) before loading on a MiSeq (Illumina) sequencer. For the upper and lower bay samples (for January and August), FC-402-4001 TruSeq® Rapid SBS Kit (200 cycle) and PE-402-4001 TruSeq® Rapid PE Cluster Kit were used.

Quality trimming and assembly

Imported sequence reads were quality trimmed using CLC Genomics Workbench 9 (CLC Bio Aarhus, Denmark) (Kim et al., 2013). Trimming was done to remove barcode and adapter sequences. Reads were then assembled using default settings. Reads for OTU clustering were merged prior to analysis using the Microbial Genomics Module on CLC Genomics Workbench 9.

OTU clustering and diversity analysis

Sequences were clustered into OTUs and used to estimate alpha and beta diversities in metagenomes using CLC Microbial Genomics Module. For alpha diversity, taxonomic classification of the representative sequence for each OTU was performed against the Greengenes 16S rRNA database (greengenes.lbl.gov) with 97% identity cutoff (Albanese et al., 2015). Rarefaction curves were used to represent the taxonomic relationship between the number of sequenced reads and the number of OTUs (Fig. 2.2a). The Shannon entropy (Shannon, 2001) was also calculated to confirm variation in taxonomic diversities between wet, cold and dry, warm months' metagenomes. The Shannon entropy results are represented using rarefaction curves in Figure 2.2b. For beta diversity analysis, principal coordinates analysis (PCoA) was used to explain variance (%) based on the Bray-Curtis Dissimilarity Index (Bray and Curtis, 1957). To gain insight into phylogenetic and relative relatedness of the bacterial assemblages, weighted UniFrac (D_{0.5}) was used as recommended by Lozupone et al., (Lozupone et al., 2007b).

Annotation

For taxonomic analysis and investigation of functional characteristics within the metagenomes, assembled reads were uploaded to the IMG/ER (Lin et al., 2009) and MG-RAST (Meyer et al., 2008) pipelines for annotation. The identification of taxonomic affiliation of functional genes was achieved by applying the best hit classification algorithm of the MG-RAST pipeline using annotations from the M5NR database (Wilke et al., 2012), using 80% identity and a maximum E-value cutoff of 1×10^{-5} . The taxonomic analysis of bacterial assemblages from lower and upper part of Mobile Bay during the coldest (January upper and lower) and warmest (August upper and lower) periods was analyzed using same settings. Phylogenetic inference

from the wet, cold and dry, warm months' metagenomic data was used to gain insight into the phylogenetic diversity of the microbial assemblages. This was achieved by performing a maximum likelihood (ML) analysis of assembled DNA sequences using MLTreeMap (Stark et al., 2010) based on the Genomic Encyclopedia of Bacteria and Archaea (GEBA) phylogeny (Wu et al., 2009). The phylogenetic relationships within the metagenomes were inferred by alignment of query sequences against reference sequences.

Results were placed into the RaxML tool following ML model parameters (Stamatakis, 2014). For KEGG taxonomic and functional analysis, GhostKOALA (Kanehisa et al., 2016), a database with non-redundant sets of genes, was used to annotate amino acid sequences which had been predicted from assembled reads using FragGeneScan software (Rho et al., 2010). Functional annotation of the assembled reads was achieved by first identifying protein coding sequences (CDS) in the contiguous consensus sequences (contigs) using the MetaGeneMark tool (Besemer et al., 2001; Borodovsky and Lomsadze, 2014) in CLC Genomics 9.0 Workbench. CDS were then annotated with Pfam domains (pfam.xfam.org/) (Finn et al., 2016) and gene ontology (GO) terms (release/2016-05-18) (Consortium, 2015). CLC Genomics Workbench has been reported to perform the best functional annotations (Li et al., 2015), thus its use alongside common pipelines.

Physicochemical (PC) data

The PC parameters, including water surface (~ 20-30 cm deep) salinity, conductivity, temperature, pH and DO, CH₄, NH₄⁺ and total surface nitrogen dioxide (NO₂) were extracted from publicly-available databases (Table 2.1). Data were extracted for the day of microbial assemblage sampling, and for a period 5 days before and after the sampling day, so each datum includes information from a total of 11 days of PC data, which were averaged to obtain mean

value around the microbial sampling date. The sampling was done over 11 days to capture short-term nutrient behavior, processing and potential regulation of dynamics of the microbial assemblages (Pennock et al., 1998) The data were extracted from <http://www.mymobilebay.com/>, which is curated by the Dauphin Island Sea Lab (DISL) and The Mobile Bay National Estuary Program, for temperature, salinity, pH, conductivity and DO, which were measured using a Seabird 911 conductivity, temperature and depth (CTD). The data for NO₂ and CH₄ were extracted from the NASA Giovanni Time Series version 4 (<http://giovanni.gsfc.nasa.gov/giovanni>) (Acker and Leptoukh, 2007), monitored using the Tropospheric Emission Spectrometer (TES). TES uses infrared high resolution Fourier Transform Spectrometer for high spectral resolution. Historical data were used to assess seasonal variation in the levels of some nutrients (nitrogen, phosphate, silicate) because they were not available for the period during which microbial samples were taken. Data from 2010 and 2011 from Mid Bay (MB) and Dauphin Island (DI) site (Table S2.1 in the appendix) were averaged to determine their seasonal relationships with the other physiochemical parameters and bacterial assemblages. For the historical samples, surface water samples were collected for nutrient analysis from the two sites, MB (n = 12), DI (n = 12) and processed by filtering through a 0.7 µm glass-fiber filter before analyzing the filtrate using a Skalar SAN⁺ autoanalyzer (Whitledge et al., 1981). These historical nutrient data included seasonal levels of dissolved inorganic nitrogen [DIN], phosphate [PO₄³⁻], dissolved organic nitrogen [DON (DON= total N-DIN)] and dissolved silicate [DSi]. The historical data were from monthly mean for January, March, July and September for 2010 and 2011. This was the only historical data collected in 2010 and 2011.

The physicochemical data were used for linear regression and Pearson correlation analyses with aspects of the microbial assemblages. Two-way ANOVA was used to analyze the contribution of PC parameters to the observed variability of bacterial assemblages, using GraphPad Prism 5 (GraphPad Software, Inc.). Differences between bacterial assemblages were confirmed using Jaccard similarity and Euclidean dissimilarity matrices. Dissimilarity indices were generated by calculating distances between bacterial assemblages combined with their environmental characteristics.

Comparative metagenomics of Mobile Bay metagenomes with other coastal systems

Four additional publicly available metagenomes of microbial assemblages for Monterey, Botany and Guanabara Bays as well as the Western English Channel Time Series (WECTS) were selected for comparison against Mobile Bay metagenomes. Metagenomes were compared as groups for both taxonomic and functional differences. The data from each metagenome were first annotated with M5NR (for taxonomic analysis) and SEED subsystems (for functional analysis) using a maximum e-value of 1×10^{-5} , a minimum identity of 80 %, and a minimum alignment length of 15 amino acids for both protein and base pairs for RNA databases. The data were normalized to values between 0 and 1 before the comparative analysis using Past3 (Hammer et al., 2001) and GraphPad Prism 5. Comparative analyses were displayed using heatmaps and dissimilarity determined by nonmetric multidimensional scaling plots based on the Bray-Curtis dissimilarity index.

Results

Composition and phylogeny of bacterial assemblages

The total filtered reads from Mobile Bay estuarine metagenomes were assigned into 42,633 OTUs belonging to 12 bacterial Phyla, 21 Classes and 53 Genera, as revealed by comparison with the Greengenes database. Sequence reads, clustered at 97% similarity to avoid overestimation of diversity and possible sequencing errors (Huse et al., 2007), revealed that the January and March (wet, cold) metagenomes had a higher number of unique resolved OTUs when compared to the August and September (dry, warm) metagenomes (Fig. 2.2A). Calculation of the Shannon entropy revealed a higher alpha diversity in the wet, cold months compared to dry, warm months (Fig. 2.2B).

In totality, Mobile Bay metagenomes were dominated by Proteobacteria, Cyanobacteria, Bacteroidetes, Firmicutes, Actinobacteria and other unclassified bacteria (Fig. 2.3A). Beta and gamma-Proteobacteria Classes dominated microbes in the Phylum Proteobacteria, Class Synechococcus dominated Phylum Cyanobacteria, Class Flavobacteriia dominated Phylum Bacteroidetes, Class Actinobacteria dominated Phylum Actinobacteria, and Class Clostridia dominated Phylum Firmicutes, while Class ZB2 dominated the Candidate Phylum OD1 (Fig. 2.3B).

Specifically, OTU-based taxonomic profiling indicated that Phylum Proteobacteria dominated during both wet, cold and dry, warm months (> 30% of observed taxa), but was particularly numerous in the wet months (Fig. 2.4A). Based on the best hit classification using MG-RAST, the wet, cold and dry, warm month metagenomes combined were composed of Acidobacteria, Actinobacteria, Bacteroidetes, Chlamydiae, Chlorobi, Chloflexi, Cyanobacteria, Deferribacteres,

Deinococcus-Thermus, Firmicutes, Fusobacteria, Gemmatimonadetes, Nitrospirae, Planctomycetes, Proteobacteria, Spirochaetes, Tenericutes, Verrucomicrobia and unclassified bacteria with varying relative abundances (Fig 2.4B).

A multivariate analysis employing the Bray-Curtis Dissimilarity Index revealed that based on relative abundance, the bacterial assemblages clustered separately, although those representing the wet, cold months and those from dry, warm months clustered, respectively, closer to each other (Fig. 2.5A). PCoA based on weighted UniFrac (D_{0.5}), which utilizes both taxonomic and phylogenetic information, revealed a similar trend (Fig. 2.5B). The phylogenetic diversity was again higher in wet, cold months compared to dry, warm months (Fig. 2.6A). The bacterial assemblages in wet, cold months were more similar to each other (i.e., less intermonth variability) compared to dry, warm months (Fig. 2.6B). The upper and lower parts of the Mobile Bay were dominated by a microbial assemblage belonging mainly to the Phyla Proteobacteria and Actinobacteria during the coldest period (Jan.) compared to the warmest period (Aug.) (Fig. 2.7a and 2.7b). The quantitative phylogenetic analysis using MLTreeMap revealed that altogether, wet, cold months had higher total diversity of different bacterial lineages relative to dry, warm months (Fig. 2.8a., b., c. and d.).

Dominant bacterial phyla and their relationships with physicochemical parameters

As expected, some PC parameters demonstrated strong autocorrelation (Table 2.2). NO₂ was strongly correlated with temperature and NH₄⁺ possibly because tightly coupled relationships of biogeochemical processes and its role in ozone formation (Fisher and Oppenheimer, 1991; Scharko et al., 2014; Tzortziou et al., 2015).

Linear regression analyses revealed the abundance of microbes in that Phyla Cyanobacteria and Proteobacteria was strongly associated with four PC parameters

(Temperature, DO, NH_4^+ , NO_2 and CH_4), while Phylum Cyanobacteria, Gemmatimonadetes and Proteobacteria also varied with four parameters: temperature (Fig. 2.9A), DO (Fig. 2.9B), NH_4^+ (Fig. 2.9C) and NO_2 (Fig. 2.9D). Phylum Actinobacteria abundance varied only with pH (Fig. 2.9E). The strongest observed relationship was between Phylum Cyanobacteria and CH_4 ($R^2=0.9997$, $p=0.0001$) (Fig. 2.9F).

Pearson correlation analyses revealed that physicochemical parameters ($n=8$) exhibited a strong relationship with shifts in the bacterial assemblages between the wet and dry months (Table 2.3). Apart from Phylum Proteobacteria (the most dominant) which had a strong negative correlation with temperature, NH_4^+ , NO_2 , and CH_4 , all other phyla exhibited strong positive correlations with 8 parameters (Table 2.3). Class Alphaproteobacteria had strong negative correlation with salinity ($r=0.976$, $p=0.024$) and conductivity ($r=-0.973$, $p=0.027$), but strong positive correlation with DO ($r=0.984$, $p=0.016$). Betaproteobacteria were strongly negatively correlated with CH_4 ($r=-0.999$, $p=0.0006$), NO_2 ($r=-0.988$, $p=0.0115$), NH_4^+ ($r=-0.985$, $p=0.0150$), and temperature ($r=0.998$, $p=0.0016$), but positively correlated with DO ($r=0.968$, $P=0.0319$). Gammaproteobacteria had strong negative correlations with CH_4 ($r=-0.968$, $p=0.032$), NO_2 ($r=-0.980$, $p=0.032$), NH_4^+ ($r=-0.987$, $p=0.013$), temperature ($r=0.964$, $p=0.036$), and conductivity ($r=0.958$, $p=0.042$), but a positive correlation with DO ($r=0.965$, $p=0.035$).

The relative abundance of members of the Phylum Verrucomicrobia positively correlated with temperature, NH_4^+ ($r=0.978$, $p<0.05$), CH_4 ($r=0.978$, $p<0.05$) and NO_2 ($r=0.987$, $p<0.05$) Although the relative abundance of 12 other microbial taxa (Acidobacteria, Chlamydiae, Chlorobi, Plancomycetes, Chloflexi, Deffribacteria, Deinococcus-Thermus, Firmicutes, Fusobacteria, Nitrospirae, Spirochaetes and Tenericutes) did not exhibit any significant shifts across any of the physicochemical parameters, their abundances exhibited high correlations in

some cases. The salinity gradient, which is known to be a key factor in influencing microbial composition and structure in other environments (Lozupone and Knight, 2005; Reed and Martiny, 2013), was, surprisingly, not significantly associated with changes in the abundance of any bacterial phyla in Mobile Bay (Table 2.3). The nature of the relationships between PC parameters and all dominant phyla is shown in detail in Table 2.3.

The interaction between PC parameters and bacterial assemblages at the Phylum level accounted for 99.71 % ($p < 0.0001$, 2-way ANOVA) of the total variance observed. The chance of observing the observed variation in bacterial assemblages randomly was 0.01%. Sampling dates alone accounted for < 0.1 % ($p < 0.05$) of the total variance, which was insignificant. Both the Jaccard similarity and Euclidean Dissimilarity Indices revealed relatively closer distances between the two wet, cold months when combined with their environmental variables (Table 2.4). A similar observation was made with the two dry, warm months.

The wet, cold months were associated with historically high levels of most of the nutrient parameters (DIN, DON and DSi, whereas the dry, warm periods were associated with high levels of PO_4^{-3} . Historical DON had the most association with the levels of other physicochemical parameters (Table S2.2 in appendix). DIN had a significant correlation with Bacteroidetes, whereas DON had a significant relationship with Bacteroidetes, Proteobacteria, and Cyanobacteria (Table S2.3 in appendix, Fig. 2.9g).

Functional annotation

Analysis of the results obtained from the IMG/ER analysis showed that bacterial populations during the wet months carried more functional properties than those from the dry months (Table 2.5). The wet, cold pool had almost twice as many total rRNA genes (2118) compared to dry, warm (1207). The same pattern was true for functional properties including protein coding

genes, genes with COG, Pfam and KO (KEGG Orthology). GhostKOALA CDS functional annotation revealed a high relative abundance of genes for cellular metabolism and processes, as well as environmental information processing during the wet, cold months as opposed to dry, warm months (Fig. 2.10). Also, functional annotation of CDS (predicted using MetaGeneMark) with Gene Ontology (GO) with Pfam domains on CLC Microbial Genomics Module further demonstrated that GO functional categories with Pfam domains were abundant during wet months compared to dry months (Table 2.6). An overview of the GO functions confirmed high abundance of those involved in metabolic, cellular and catalytic activities.

Analysis for ARDs based on SEED subsystems also revealed a similar pattern to that displayed by genes for metabolism and cellular processes (Fig. 2.11). The most prevalent ARD genes included those for cobalt-zinc-cadmium resistance, resistance to fluoroquinolones, pathogenicity islands, phages and prophages.

Comparative metagenomics of bacterial populations in other coastal systems

All the coastal ecosystems used for comparative metagenomics (Monterey, Guanabara and Botany Bays and the WECTS) had a high relative abundance of Phylum Proteobacteria (Fig. 2.12). Compared to the bays, the WECTS had a high relative abundance of bacteria representing Phylum Bacteroidetes and Cyanobacteria. This could reflect the profoundly different oceanographic characteristics of this location when compared to the other four marine ecosystems. These findings support the suggestion that bacterial assemblages could be structured not just by physical-chemical factors but by input sources (e.g. Bays' input into the English Channel) into the system (Falcón et al., 2008; Gilbert et al., 2012). The English Channel also has 3.5 million people along its busy coastline (Millward et al., 2015), compared to Mobile's population of slightly over 400,000 people (Tinnon, 2010). Unlike the other four estuaries,

Mobile Bay metagenomes distinctively contained the unique bacterial Phylum Deferribacteres, which can respire anaerobically and utilize iron (II) as a terminal electron acceptor (Garrity et al., 2001). Considering the iron-rich clays of the Southeastern US and variable oxygen availability in the Bay, this may not be surprising. The Mobile Bay metagenomes were taxonomically most similar to the WECTS ($R^2=0.84$, $MSE=0.0132$) (Fig. 2.13).

All of the compared marine ecosystems had a high relative abundance of phages and prophages as well as fluoroquinolone resistance genes (Fig. 2.14). Interestingly, Botany Bay had the highest relative abundance of arsenic resistance and copper homeostasis genes. Mobile Bay also had two unique functional features; MexA-MexB-OprM Multidrug Efflux System a tripartite multidrug efflux system (Daury et al., 2016) and teicoplanin-resistant *Staphylococcus*. Teicoplanin-resistance is thought to be associated with both domesticated and non-domesticated animals as it is used to treat infections caused by Gram-positive bacteria, including those caused by *Staphylococcus* (Ghoshal et al., 2015; Li and Zhang, 2015; Trueba et al., 2006). Based on overall functional capabilities, the relative abundance of ARD genes in Mobile Bay was closest to that of Monterey Bay ($R^2=0.5186$, $MSE=0.0612$) (Fig. 2.15). Mobile Bay had the greatest diversity of ARDs ($n=18$), followed by the WECTS ($n=16$).

Discussion

The high bacterial diversity and domination of the microbial assemblage by Proteobacteria, Bacteroidetes and Actinobacteria during the wet, cold months could be largely due to the low temperature during the sampling periods (Fig. 2.7a, b). (Ladau et al., 2013). This pattern may represent the influence of coupled PC parameters that offer ideal conditions for abundant microbial growth during the cold, wet periods in Mobile Bay. Our study emphasizes that physicochemical factors could define the observed bacterial assemblage dynamics. Low oxygen

levels in the warm, dry months, coupled with restricted water circulation in Mobile Bay (May, 1973; Kyeong Park et al., 2007; Schroeder & Wiseman, 1988) could partly explain the observed taxonomic and functional shifts of the bacterial assemblages, because this would be expected to have significant impacts on methane generation. For instance, in the Chesapeake Bay, DO, CH₄ and temperature have been found to have a strong association with each other, with CH₄ concentrations increasing during anoxic conditions and reducing with the return of oxygenated conditions (Gelesh et al., 2016). In agreement with the current study, CH₄ has also been strongly correlated with the relative abundance of cyanobacteria (Rakowski et al., 2015). Actinobacteria relative abundance increased with increasing pH, which in turn increased in Mobile Bay during the wet, cold months. This observation could reflect low rates of grazing and relatively high productivity rates, conditions which are typically associated with the colder months (NOAA, 2008). Increased alkalinity has recently been found to be a key driver of the growth of members of Phylum Actinobacteria in Antarctic soils (Tytgat et al., 2016). NO₂ has also been found to be an acidifying and eutrophying agent in aquatic ecosystems (Jickells, 2006).

Our study surprisingly showed no strong relationship with salinity or conductivity at the Phylum level. This is unlike the situation in the Delaware estuary where the microbial structure were observed to have a strong relationship with salinity (Campbell and Kirchman, 2013). This could be because the transects for sampling in this study were from within Mobile Bay itself, whereas in the Delaware Bay study samples included those from a wider salinity gradient, all the way from freshwater to the open ocean. High historical levels of nutrients (DIN, DON and DSi) were associated with the wet, cold months, possibly due to increased riverine input, which is highest in winter, and lowest in summer (McManus et al., 2004).

Temperature has previously been determined to be an important regulator of bacterioplankton production in Mobile Bay (McManus et al., 2004). Our study reveals that in addition to temperature, the dynamics of bacterial assemblages is influenced strongly by DO, NH_4^+ , NO_2 and DON. Based on our study, Proteobacteria and Bacteroidetes are r-selected, based on their significant association with nutrients (Table S2.3 in appendix). The lack of statistical differences between upper and lower bay within January samples as well as August samples could be due to estuarine water circulation cause by currents and tidal motion (Walters et al., 1985). The dominance of Phylum Proteobacteria in the four bays as well as in the WECTS is consistent with several previous studies carried out in different environments (Jung et al., 2016; Liu et al., 2015; Pucciarelli et al., 2015; Xia et al., 2016; Zhu et al., 2015). Although the Mobile Bay metagenomes revealed *taxonomic* similarity with the WECTS, the metagenomes were *functionally* close to those from Monterey Bay. The differences could be explained by environmental variables, and geographical distance (Lozupone et al., 2007a), type of coastlines and their usage and adjacent landmasses. The English Channel is among the busiest seaways in Europe, with about 400 ships and 100 ferries running per day (Glegg et al., 2015). The high bacterial diversity in the WECTS metagenome could be attributed to input from Bays alongside it (Cawsand, Lyme and Pegwell Bays), ports, marinas and increased density of industries (Glegg et al., 2015). Mobile Bay has more than 400 point source dischargers consisting of toxic chemicals, metals and organics, perhaps explaining the high diversity of ARDs (ADEM, 1996). Most of these chemicals could stay in the bay for long because of Mobile Bay's partially enclosed geomorphology. With an average depth of only 3 m, the water input could contribute to the distribution of pollutants and interaction of the abiotic and biotic factors, thus impacting the functional potential (Pennock et al., 1998).

The taxonomic and functional dissimilarity between Mobile Bay metagenomes and Guanabara Bay could be due to the high mean salinity of the latter (13-36 salinity units in Guanabara Bay compared to 8-23 in Mobile Bay). Moreover, there are distinct differences in the rainy periods (October to April in Guanabara Bay, which is in the southern hemisphere), and high temperature and human habitation (Fistarol et al., 2015; Mayr et al., 1989). Botany Bay was the most dissimilar compared to all the other coastal systems used in this study, both taxonomically and functionally. This could be due to it being an ocean embayment served by a small catchment area of 1165 km². Botany bay also had the highest relative abundance of arsenic resistance and copper homeostasis genes, possibly, a result of evolution due to proximity to intense industrialization and urbanization of the western shore, and the locating of a marine shipping container port and the Sydney airport that results in routine flyover of passenger and cargo jets (Knott et al., 2009; Spooner et al., 2003). It also has high pH and salinity, among other factors including an almost circular shape and extensive human modification (Burke et al., 2011; Knott et al., 2009; Roy et al., 2001), could account for the differences compared to Mobile Bay.

Validation of this type of study would have improved by designing primers targeting conserved regions of marker genes for qPCR analysis, as well as sampling and processing samples from the coastal ecosystems used to comparative analysis to ensure that they are processed together to minimize errors.

Conclusion

Mobile Bay has considerable economic, environmental and recreational importance for Alabama and adjacent states. Our study reveals that microbial taxonomic, functional, and AR gene diversity is highest during wet, cold months, possibly because of expanded riverine input during the rainy periods. A previous study has determined that the riverine input in Mobile bay has

strong influence on the microbial loop in surface waters (Ortell and Ortmann, 2014).

Temperature is an important regulator of bacterioplankton production in Mobile Bay (McManus et al., 2004). Our study reveals that in addition to temperature, the dynamics of bacterial assemblages was strongly associated DO, NH_4^+ , NO_2 and DON. The study reveals that PC parameters under investigation could explain shifts in some bacterial assemblages more strongly than periods of sample collection alone. Also, high relative abundance of diverse ARD genes occurred in wet, cold months. Potential biases in the study include those arising from filtration for removal of eukaryotic organisms, since some of them have microbial symbionts. Other potential biases include those arising from sample processing techniques, sequencing technology, and bioinformatic tools used for downstream analysis. Collectively, the study effort offers the first insights into the diversity and composition, and associated ARD functional potential of bacterial assemblages of Mobile Bay, and forms a basis for future examination of the link between watershed management, estuarine systems and ecosystem health. Future efforts need to include investigating the influence of tidal action in nutrient loads in Mobile Bay and if possible, include specific measurements for nutrient and ARD loads from the watershed and the sea.

Data availability

The metagenomic data have been submitted to NCBI under SRA: fall/September (SRS1544005), winter/January (SRS1544008), spring/March (SRS1544010) and summer/August (SRS1544012).

Gut metagenome samples have been deposited in MG-RAST Web server

(<http://metagenomics.anl.gov>) under projects 4579797.3 (fall/September), 4579800.3

(winter/January), 4579799.3 (spring/March) and 4579798.3 (summer/August) . The MG-RAST

metadata includes geographical coordinates, sequence counts and country. The metagenome

browser for the study includes overviews containing analysis flowcharts, taxonomic and

functional category distribution. On IMG Genome portal (<https://img.jgi.doe.gov>) under IMG Genome ID 3300003520 (winter), 3300003519 (fall) 3300003515 (summer) and 3300003522 (spring). The winter upper and lower metagenomes (Jan.) are deposited in MG-RAST under project 4701114.3 and 4701116.3 respectively. The summer upper and lower metagenomes (Aug.) are deposited under project 4701113.3 and 4701117.3 respectively.

Table 2.1: Mobile Bay mean physicochemical data. Shown are mean values and standard deviations for each parameter from N= 11 days of sampling around each date of microbial assemblage sampling. All PC data are taken from CTD and TES. The data does not include historical nutrient data.

Date of microbial sampling		Tem p. (°C)	Salinity (psu)	DO (mg. L ⁻¹)	conductivity (mS.cm ⁻¹)	NO ₂ (1.cm ⁻² x 10 ¹⁵)	pH	NH ₄ ⁺ (mg. L ⁻¹ x 10 ⁻²)	CH ₄ (mol.cm ⁻² x 10 ¹⁹)
Aug. 25 th 2012	Mean	28.09	23.62	6.341	37.28	3.49	7.138	6.996	3.73
	SD	0.8433	5.382	1.092	7.669	9.16e+14	1.099	0.03480	1.98e+18
	SE	0.0367	0.2342	0.0475	0.3337	ND	0.0337	0.0071	ND
Sept. 23 rd 2012	Mean	26.72	18.24	7.273	29.52	3.52	6.919	7.046	3.73
	SD	0.8535	2.979	0.9626	29.52	8.52e+14	0.1744	0.0651	2.08e+18
	SE	0.0373	0.1303	0.0420	0.1908	ND	0.0053	0.0133	ND
Jan. 26 th 2013	Mean	13.97	8.059	9.594	13.62	3.12	8.108	5.839	3.70
	SD	1.475	5.112	1.161	13.62	8.49e+14	0.3456	0.06015	2.13e+18
	SE	0.0641	0.2225	0.0368	0.2524	ND	0.0106	0.0125	ND
Mar. 14 th 2013	Mean	15.65	11.17	9.632	18.55	3.19	7.407	6.108	3.70
	SD	1.366	5.740	1.183	18.55	7.14e+14	0.3846	0.03283	2.10e+18
	SE	0.0594	0.2498	0.0514	0.3813	ND	0.0118	0.0067	ND

ND: Not done for the two types of satellite data (NO₂ and CH₄). Satellite data were also an average from 11 days.

Table 2.2: Correlations among physicochemical values. Historical nutrient data not included.

	CH ₄	pH	NO ₂	NH ₄ ⁺	Temp	Salinity	DO	Conductivity
CH ₄		-0.81	0.989*	0.983*	0.998*	0.842	-0.960*	0.859
pH			-0.893	-0.906	-0.785	-0.811	0.739	-0.866
NO ₂				0.999*	0.979*	0.857	-0.934	0.885
NH ₄ ⁺					0.974*	0.877	-0.937	0.905
Temp.						0.849	-0.972*	0.860
Salinity							-0.925	0.995*
DO								-0.917
Conductivity								

Note: *Correlation is significant at 0.05 level (one-tailed)

Table 2.3: Correlations between relative abundance of bacterial phyla in water samples from Mobile Bay from all 4 sampling dates and mean physicochemical parameters from 11 sampling dates

Phyla	Temp. (°C)	Salinity (psu)	DO (mg. L ⁻¹)	Cond (mS.cm ⁻¹)	pH	NH ₄ ⁺ (mg. L ⁻¹)	NO ₂ (1.cm ⁻²)	CH ₄ (mol.cm ⁻²)
Acidobacteria	0.473	0.041	-0.254	0.119	-0.496	0.511	0.541	0.513
Actinobacteria	-0.834	-0.781	0.763	-0.838	0.990*	-0.935	-0.929	-0.863
Bacteroidetes	-0.928	-0.843	0.971*	-0.816	0.559	-0.840	-0.842	-0.904
Chlamydiae	0.524	0.683	-0.694	0.607	-0.133	0.404	0.391	0.474
Chlorobi	0.618	0.819	-0.782	0.757	-0.329	0.541	0.522	0.577
Chloroflexi	-0.195	-0.041	0.014	-0.142	0.618	-0.364	-0.369	-0.254
Cyanobacteria	0.999*	0.850	-0.965*	0.866	-0.814	0.984*	0.988*	1.000*
Deffribacteria	0.535	0.153	-0.326	0.234	-0.612	0.595	0.620	0.577
Deinococcus-Thermus	0.618	0.819	-0.782	0.757	-0.329	0.541	0.522	0.577
Firmicutes	-0.225	-0.677	0.348	-0.686	0.609	-0.375	-0.331	-0.235
Fusobacteria	-0.159	-0.610	0.268	-0.627	0.597	-0.326	-0.282	-0.174
Gemmatimonadetes	0.998*	0.842	-0.960*	0.859	-0.814	0.983*	0.988*	1.000
Nitrospirae	-0.604	-0.197	0.547	-0.169	0.018	-0.422	-0.457	-0.577
Plancomycetes	0.473	0.018	-0.392	-0.006	0.106	0.287	0.327	0.449
Proteobacteria	-0.993*	-0.905	0.984*	-0.915	0.825	-0.983*	-0.982*	-0.991*
Spirochaetes	0.771	0.327	-0.611	0.367	-0.523	0.723	0.755	0.785
Tenericutes	-0.740	-0.919	0.877	-0.875	0.516	-0.693	-0.674	-0.709
Verrumicrobia	0.990*	0.790	-0.927	0.815	-0.817	0.978*	0.987*	0.995*
"unclassified bacteria"	-0.936	-0.911	0.990*	-0.888	0.642	-0.876	-0.873	-0.916

Note: *Correlation is significant at 0.05 level (one-tailed)

Table 2.4: The Jaccard similarity and Euclidean dissimilarity matrices for calculation of distance based on the bacterial assemblage composition.

Jaccard	Sept.	Aug	Mar.	Jan.
Sept.	1	0.89182305	0.79521252	0.64061458
Aug.		1	0.7032626	0.55398113
Mar.			1	0.81399252
Jan				1
Euclidean	Sept.	Aug	Mar.	Jan.
Sept.	0	11.491498	15.947444	24.111788
Aug.		0	24.258165	34.550252
Mar.			0	12.478794
Jan				0

Table 2.5: Metagenome properties indicating differences of the assembled metagenome sequences

Attribute	Jan.	Mar.	Aug.	Sept.
IMG Genome ID	3300003520	3300003522	3300003515	3300003519
Assembled genome size (bp)	63,011,793	95,325,398	34,841,000	50,479,201
Number of sequences	352,866	509,940	188,524	273,571
CRISPR Count	19	30	13	27
rRNA	721	1397	493	714
tRNA genes	973	1630	472	627
Protein coding genes	338,805	493557	180,896	260,998
with Product Name	79,205	125,815	41,361	57337
with COG	119,427	186,109	60,046	84,005
with Pfam	87,322	139,611	46,858	64,827
with KO	77,904	122,136	38,387	53,655
with Enzyme	77,904	122,136	38,387	53,655
with MetaCyc	53,675	85,154	26,538	37,186
with KEGG	62,703	98,725	30,959	43,343
COG Clusters	3,478	3,645	3,249	3,416
Pfam Clusters	3,910	4,135	3,762	4,191

Table 2.6: Functional annotation of the metagenomes based on IMG/ER

Month	Pfam profiles		GO profiles	
	Number of features	Total abundance	Number of features	Total abundance
Jan.	2,318	70,959	1,718	963,049
Mar.	2,513	148,183	1,685	1,768,710
Aug.	1,524	25,833	1,488	368,252
Sept.	1,566	21,018	1,415	29,6848



Figure 2.1: LANDSAT photograph of Mobile Bay with 9 sampling sites indicated in red dots. Analysis for upper and lower bay (January and August only) microbial assemblages was done using samples from encircled locations.

2.2a.

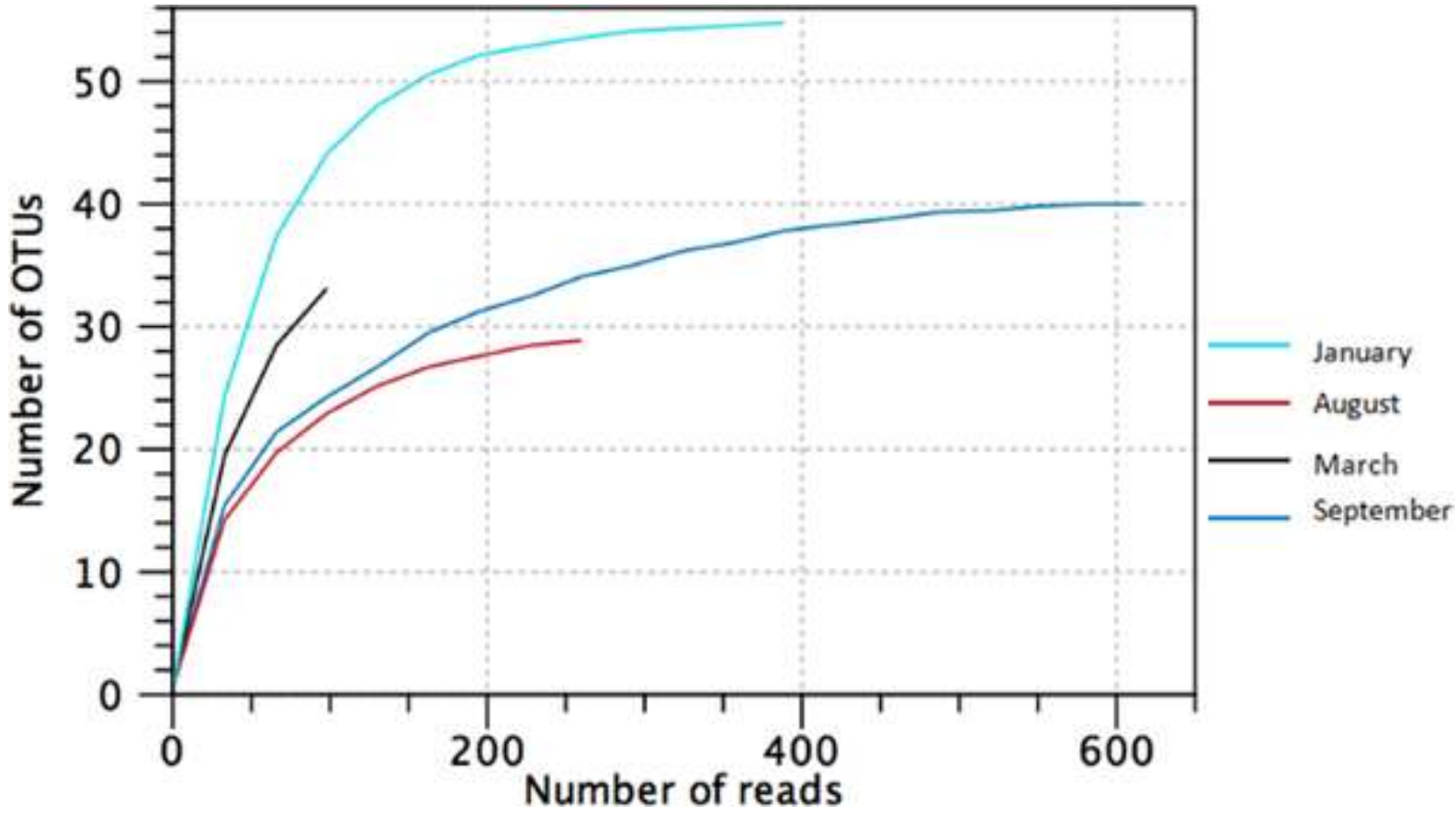


Figure 2.2a: OTU clustering based on GreenGenes database

2.2b.

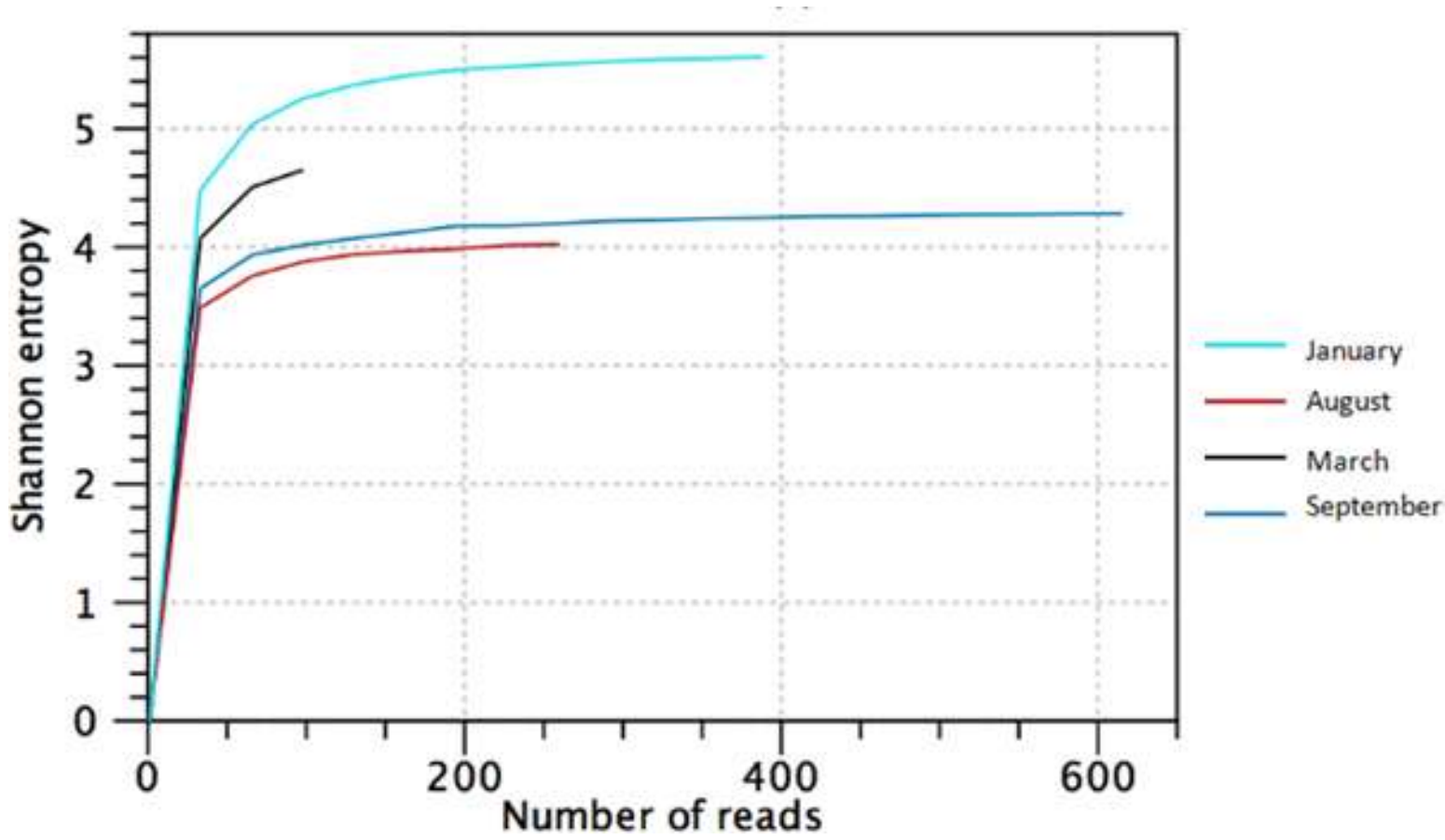


Figure 2.2b: Shannon entropy values for each of 4 sampling dates of microbial assemblages in Mobile Bay, revealing higher OTU diversity in the January and March metagenomes

2.3a.

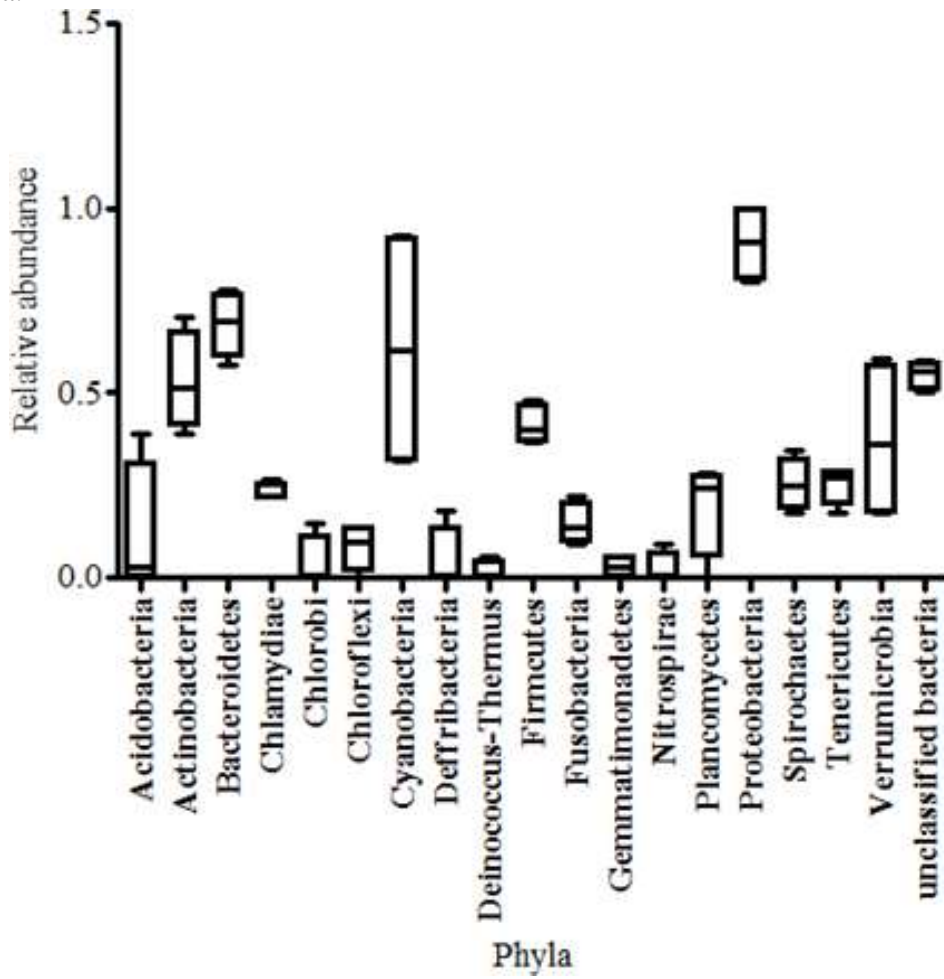


Figure 2.3a: Box and whisker plot indicating the overall composition of Mobile Bay microbial taxa, for all 4 sampling dates combined

2.3b.

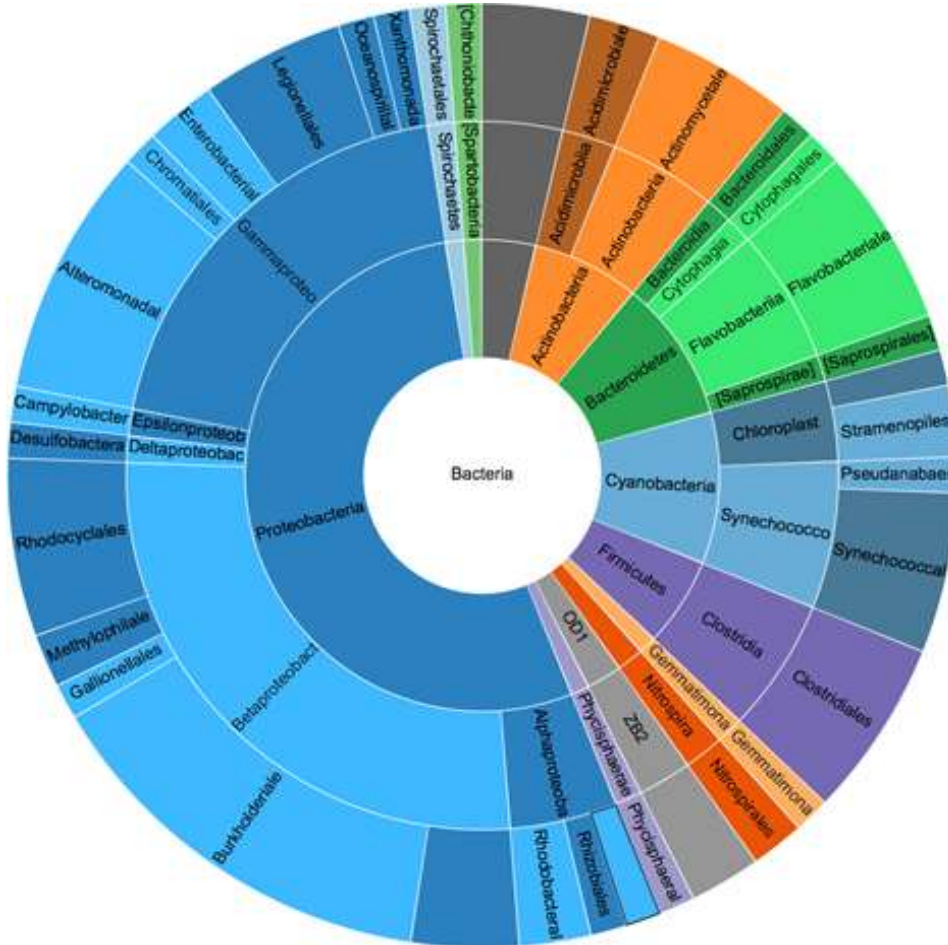


Figure 2.3b: Pie chart indicating the composition of bacterioplankton by phyla, for all samples grouped from all 4 sampling dates. Analysis and output done using CLC Microbial Genomics Module (www.clcsupport.com/)

2.4a.

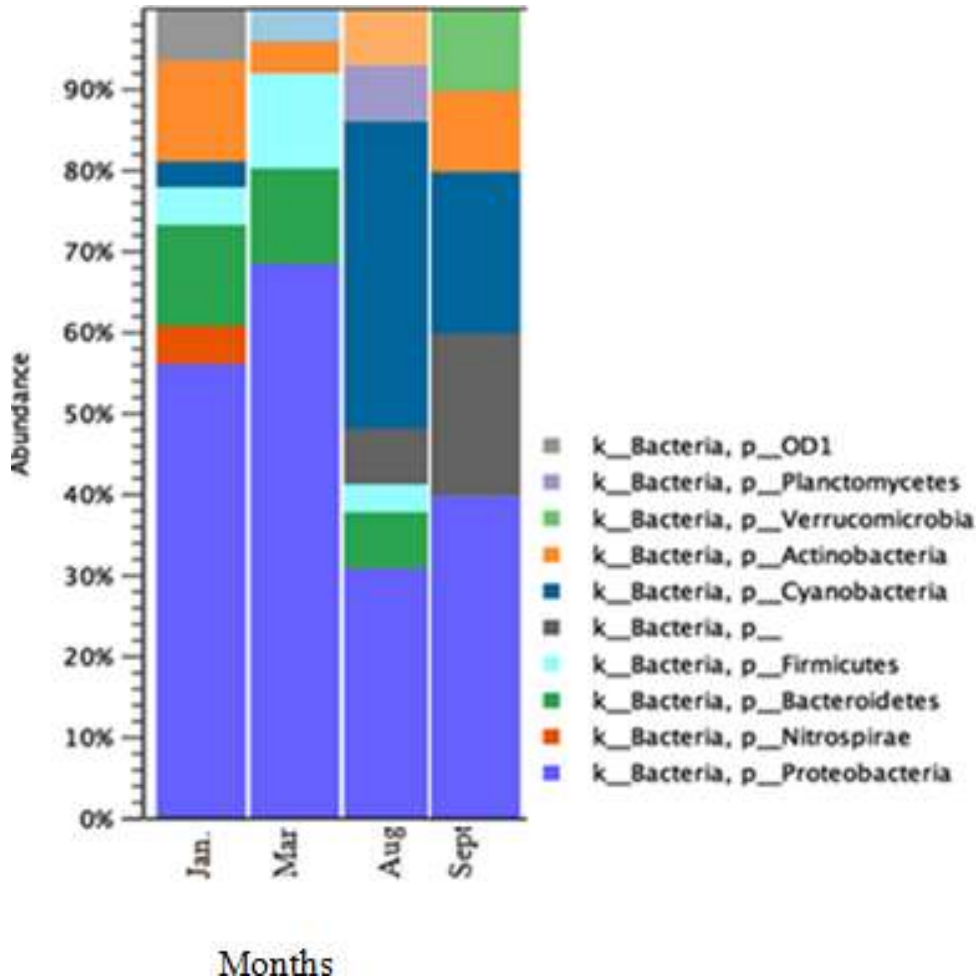


Figure 2.4a: Relative abundance of microbial taxa in Mobile Bay during wet, cold (1/26/2013 and 3/14/2013) and dry, warm (8/25/2012 and 9/23/2012) months. The graph shows the most dominant phyla for four Mobile Bay metagenomes based on SILVA database at 97% cut-off using CLC Genomics Workbench 9

2.4b.

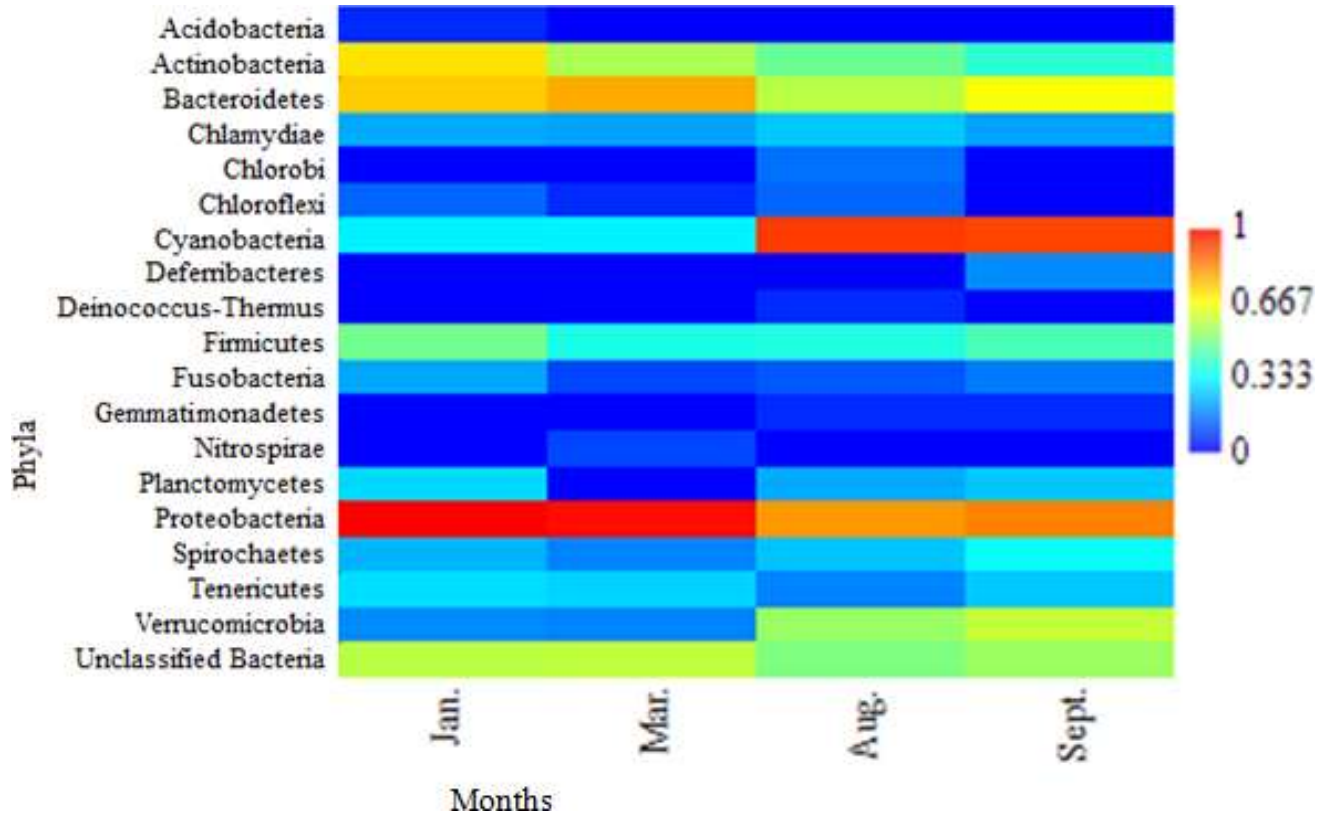


Figure 2.4b: Heatmap derived from best hit classification showing the composition and relative abundance of major bacterial phyla from Mobile Bay metagenomes (MG-RAST database using M5NR annotation with 80% cut-off) during wet, cold (1/26/2013 and 3/14/2013) and dry, warm (8/25/2012 and 9/23/2012) months

2.5a.

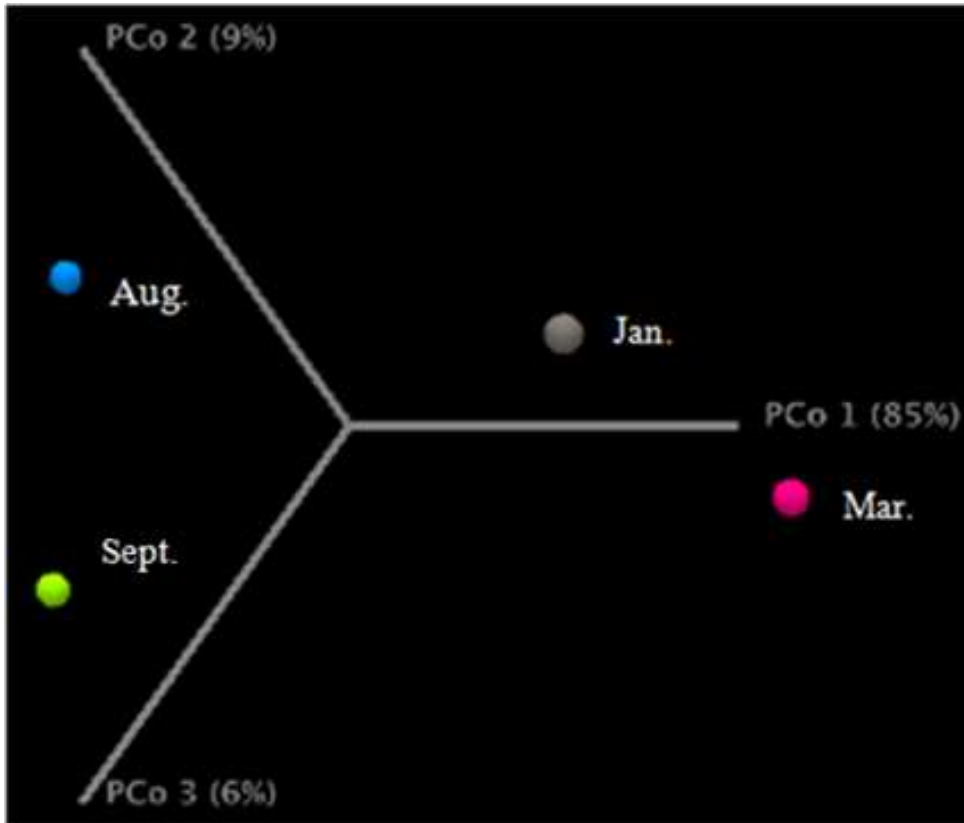


Figure 2.5a: Mobile Bay microbial beta diversity based on Principal Coordinate Analysis (PCoA) as characterized using the Bray-Curtis dissimilarity index for wet, cold (1/26/2013 and 3/14/2013) and dry, warm (8/25/2012 and 9/23/2012) months.

2.5b.



Figure 2.5b: Mobile Bay microbial beta diversity based on Phylogenetic diversity analysis created using Principal Coordinate Analysis (PCoA) as characterized using UniFrac (D_{0.5}) for wet, cold (1/26/2013 and 3/14/2013) and dry, warm (8/25/2012 and 9/23/2012) months

2.6a.

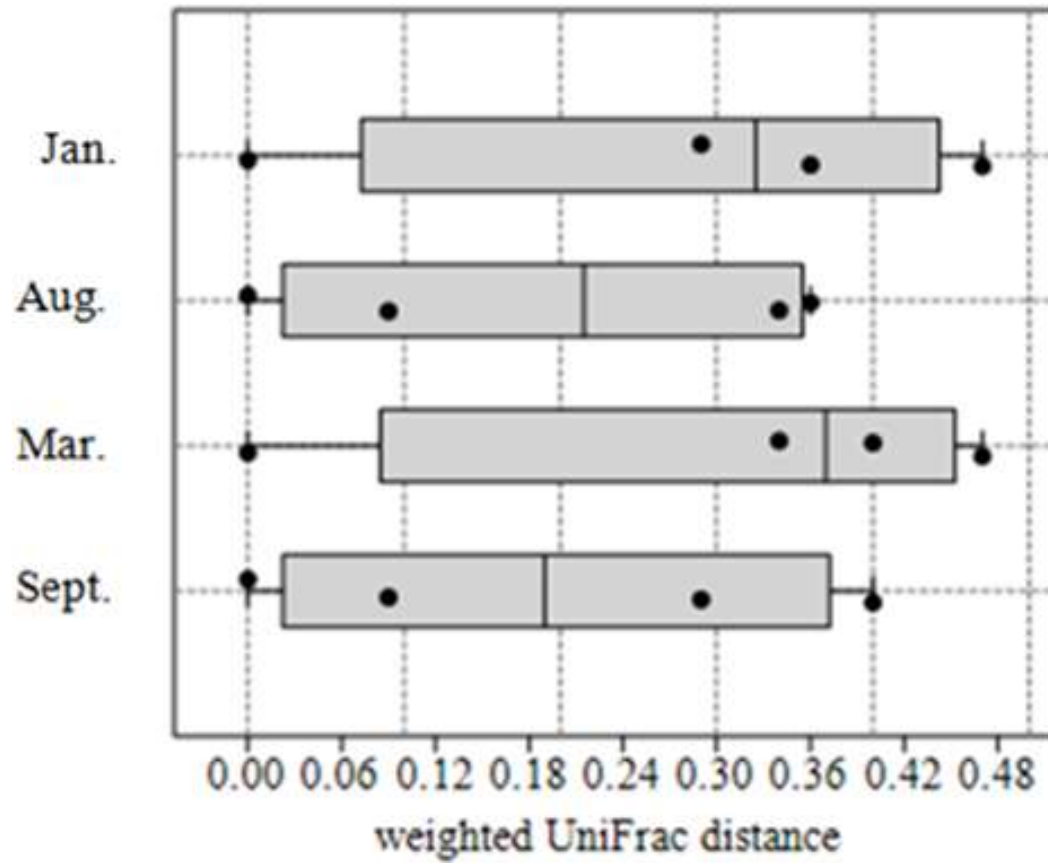


Figure 2.6a: Phylogenetic diversity measures of the Mobile Bay microbial taxa for wet, cold (1/26/2013 and 3/14/2013) and dry, warm (8/25/2012 and 9/23/2012) months. The dynamics of the phylogenetic diversity of seasonal metagenomes as generated by weighted UniFrac Distance Analysis using Past3 software

2.6b.

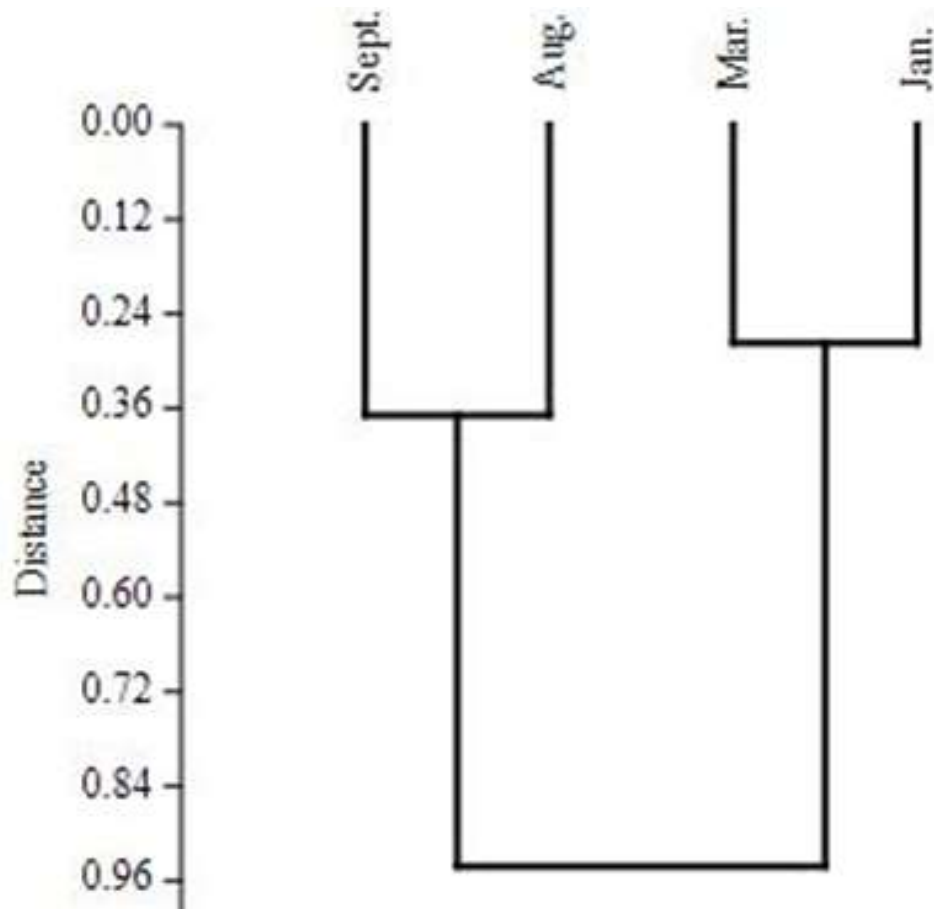


Figure 2.6b: Phylogenetic diversity measures of the Mobile Bay microbial taxa for wet, cold (1/26/2013 and 3/14/2013) and dry, warm (8/25/2012 and 9/23/2012) months. Taxonomic similarity between metagenomes using the Euclidean dissimilarity Index based on Ward's Algorithm using Past3 software

2.7a.

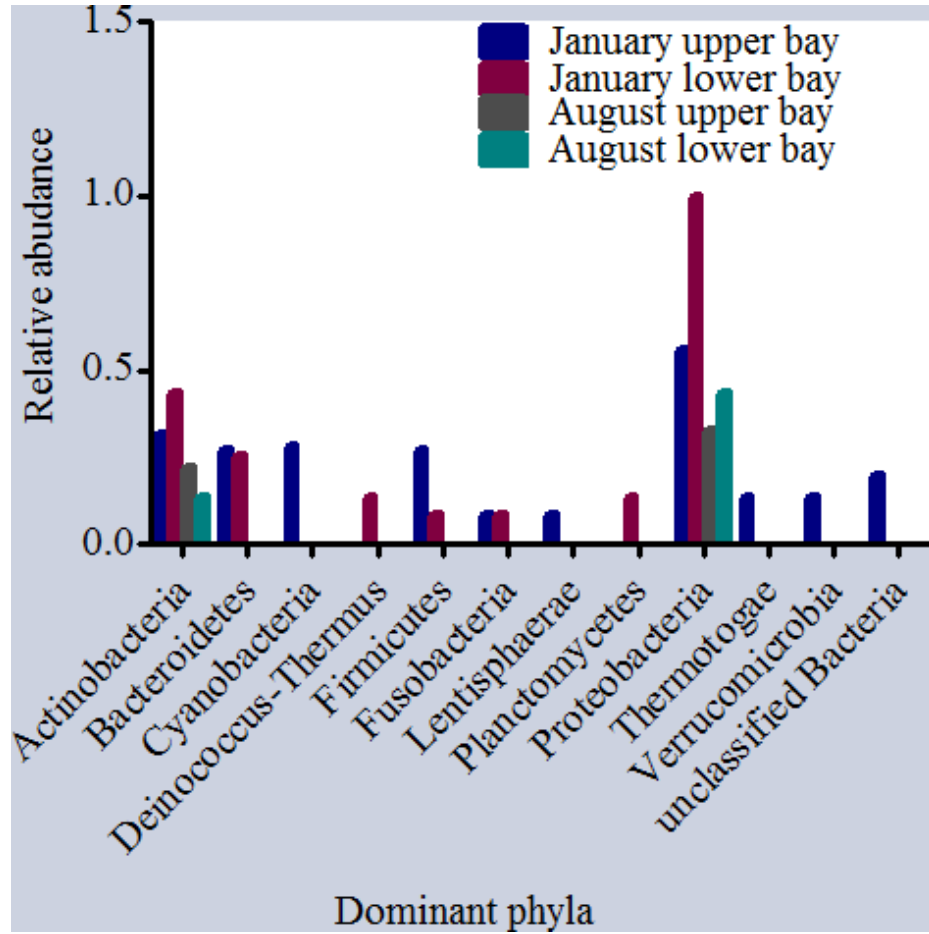


Figure 2.7a: Bar chart on the taxonomic abundance of dominant phyla in the metagenomes of Mobile Bay from the upper and lower bay during the coldest (1/26/2013) and warmest periods (8/25/2012).

2.7b.

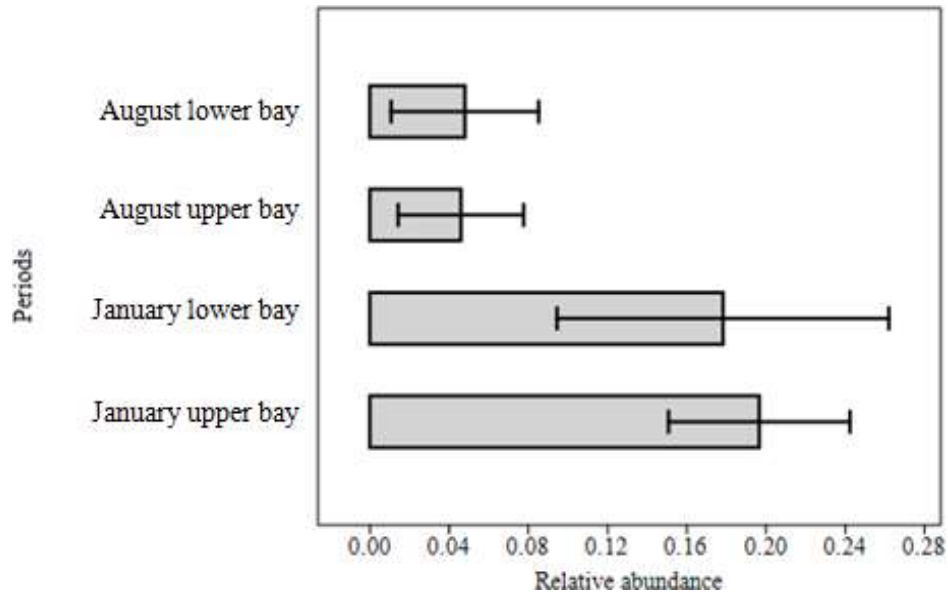


Figure 2.7b: Bar chart with Standard errors (SE) indicating the relative abundance all microbial phyla combined, in both the lower and upper sample sites of Mobile Bay during coldest (1/26/2013) and warmest (8/25/2012) periods

Online support for figure 2.8 (a): <https://figshare.com/s/60e6b5fc0009aa0a94d4> (DOI 10.6084/m9.figshare.3806292)

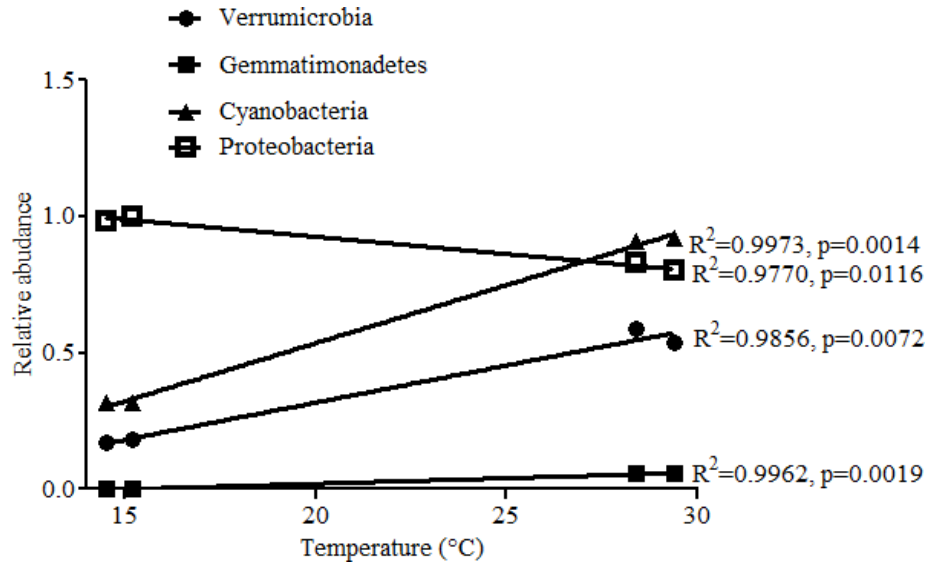
Online support for figure 2.8 (b): <https://figshare.com/s/3b76cc3f015c57997cd1> (DOI 10.6084/m9.figshare.3806295)

Online support for figure 2.8 (c): <https://figshare.com/s/cdfa5fee849310113eef> (DOI 10.6084/m9.figshare.3806298)

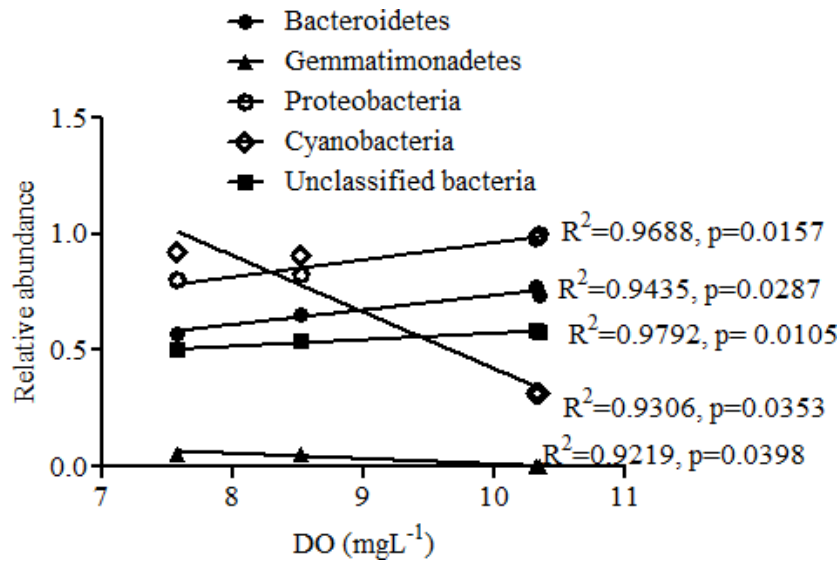
Online support for figure 2.8 (d): <https://figshare.com/s/e9c895467d28c90e71b0> (DOI 10.6084/m9.figshare.3806328)

Figure 2.8: MLTreeMap (Stark et al. 2010) analyses of contigs using the 16S rRNA gene for maximum likelihood (ML) phylogeny using GEBA phylogeny (after Wu et al. 2009), from wet, cold (1/26/2013 and 3/14/2013) and dry, warm (8/25/2012 and 9/23/2012) metagenomic data **a.** Jan. **b.** Mar. **c.** Aug. **d.** Sept. The bubble indicates the relative weight of placement. Figures above are so huge that they needed online support for visualization

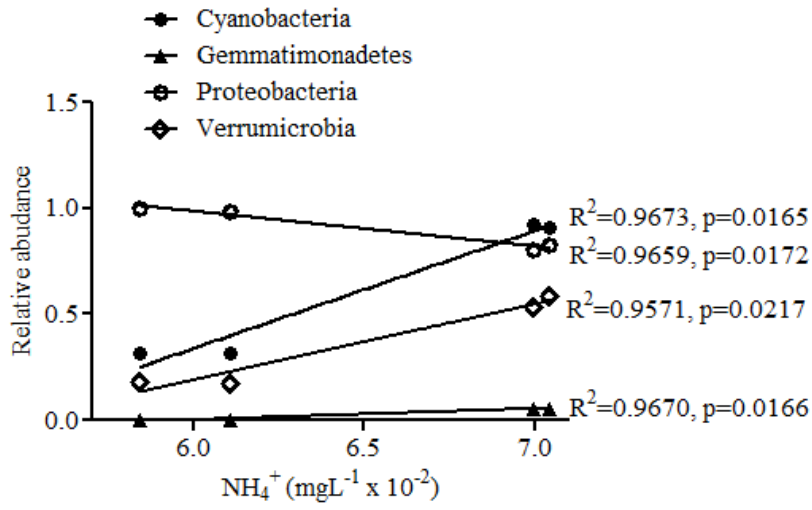
2.9a



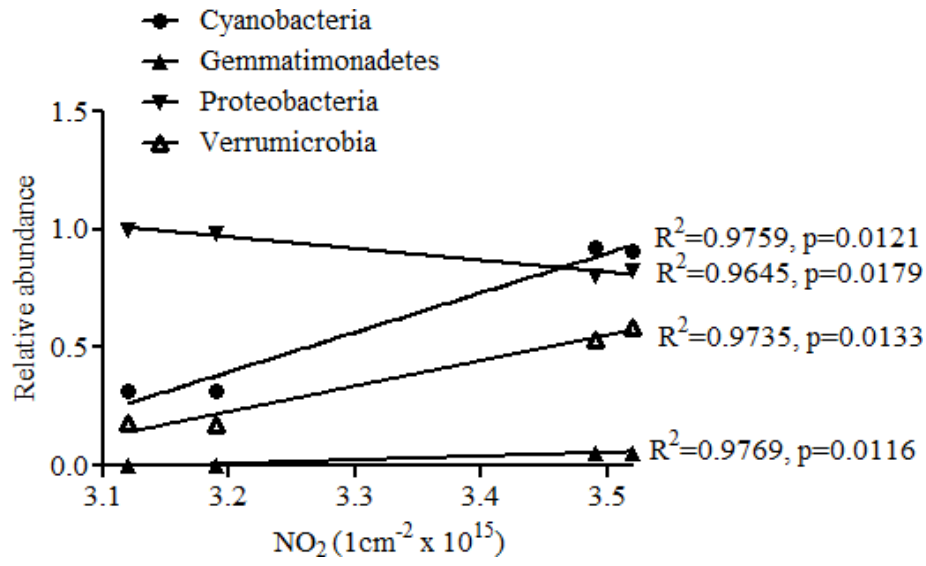
2.9b



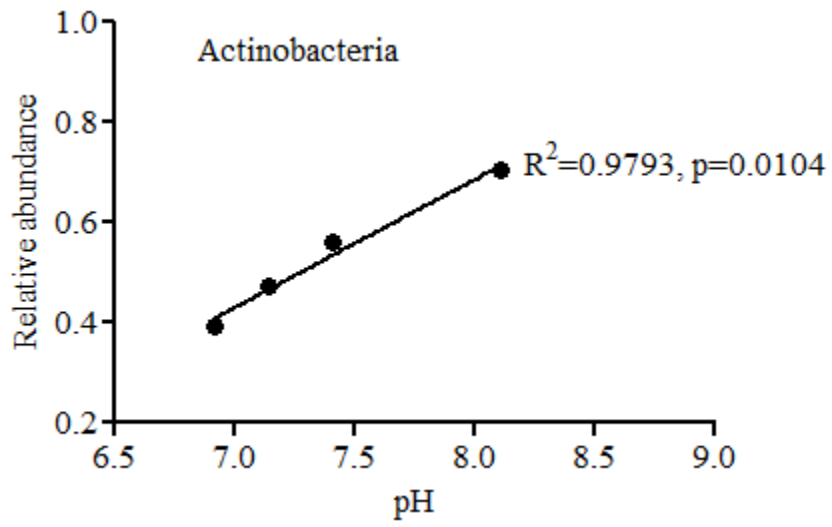
2.9c



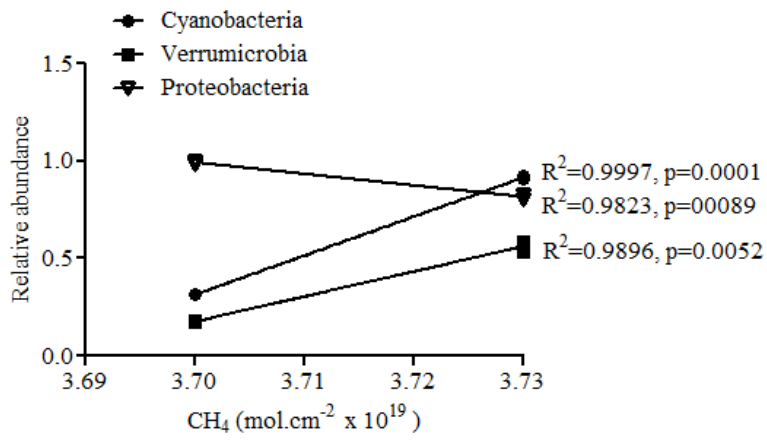
2.9d



2.9e



2.9f



2.9g

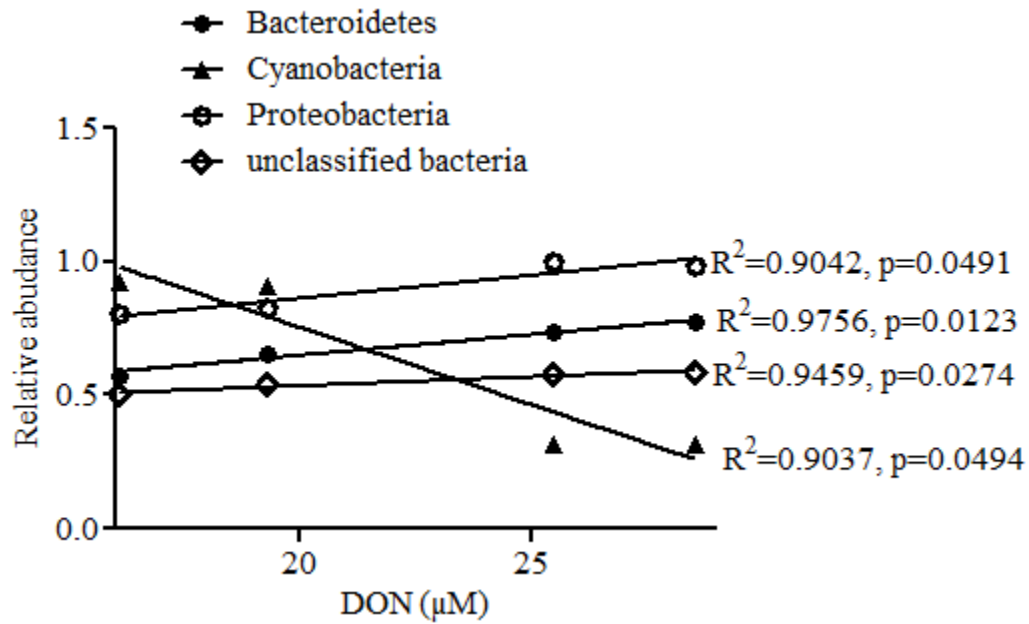


Figure 2.9: Regression analyses on the relationships between the relative abundances of selected bacterial taxa and various physicochemical parameters in Mobile Bay during wet, cold (1/26/2013 and 3/14/2013) and dry, warm (8/25/2012 and 9/23/2012) sampling period **a.** temperature **b.** dissolved oxygen (DO) **c.** ammonium (NH_4^+) **d.** nitrogen dioxide (NO_2) **e.** pH and **f.** methane (CH_4) **g.** dissolved organic nitrogen (DON)

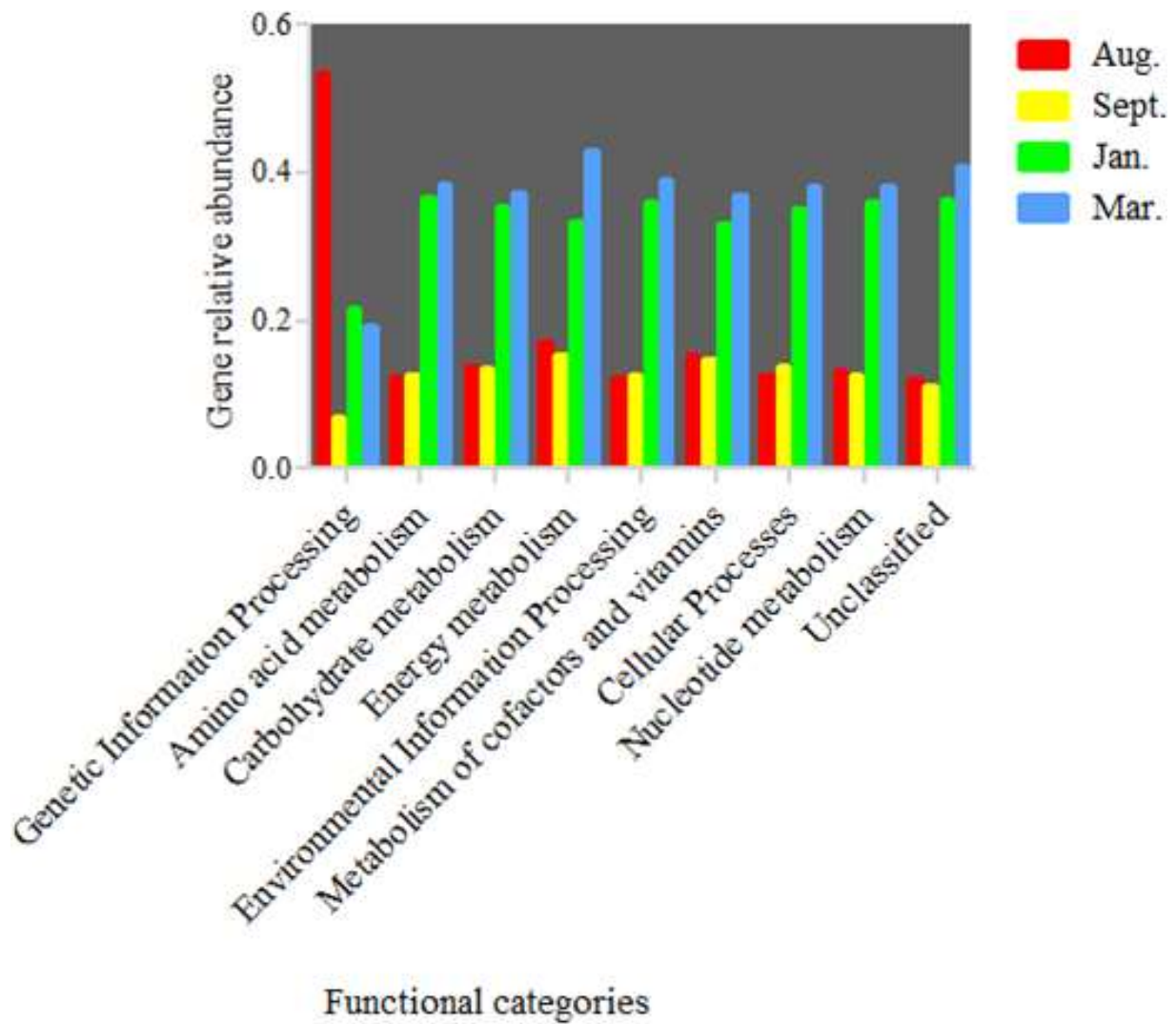


Figure 2.10: Bar graph of the functional categories of dominant genes in the metagenomes of Mobile Bay based on KEGG Analysis. The graph was drawn using GraphPad Prism 5 software (see text for details)

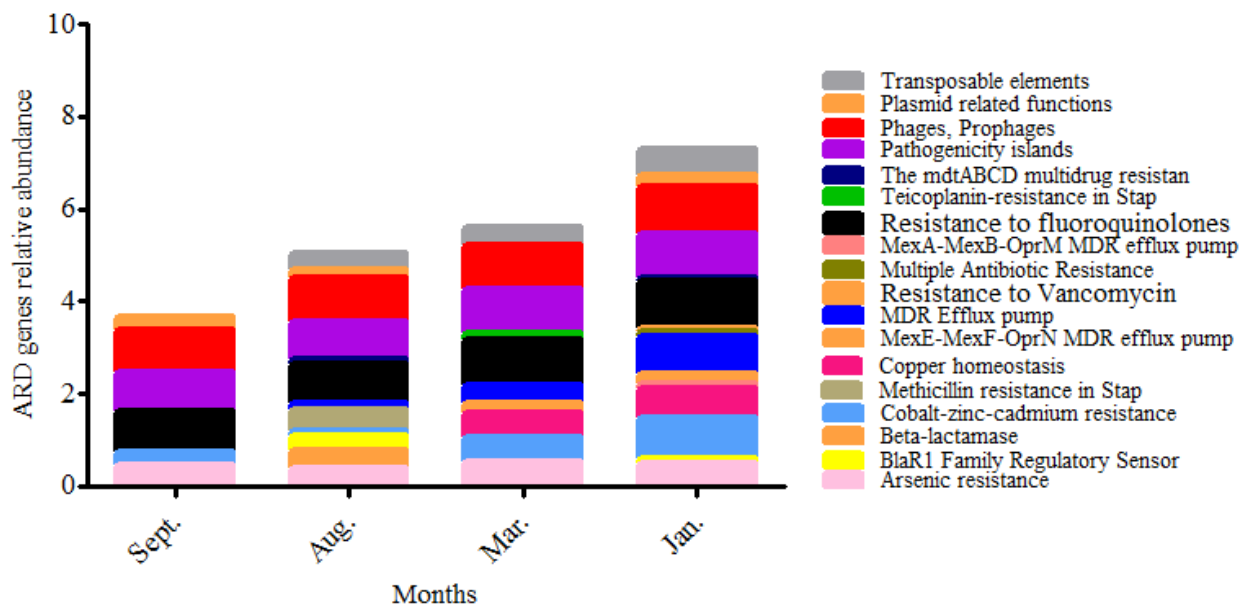


Figure 2.11: Stacked histogram of the relative abundance of antibiotic resistance determinant genes based on SEED subsystems

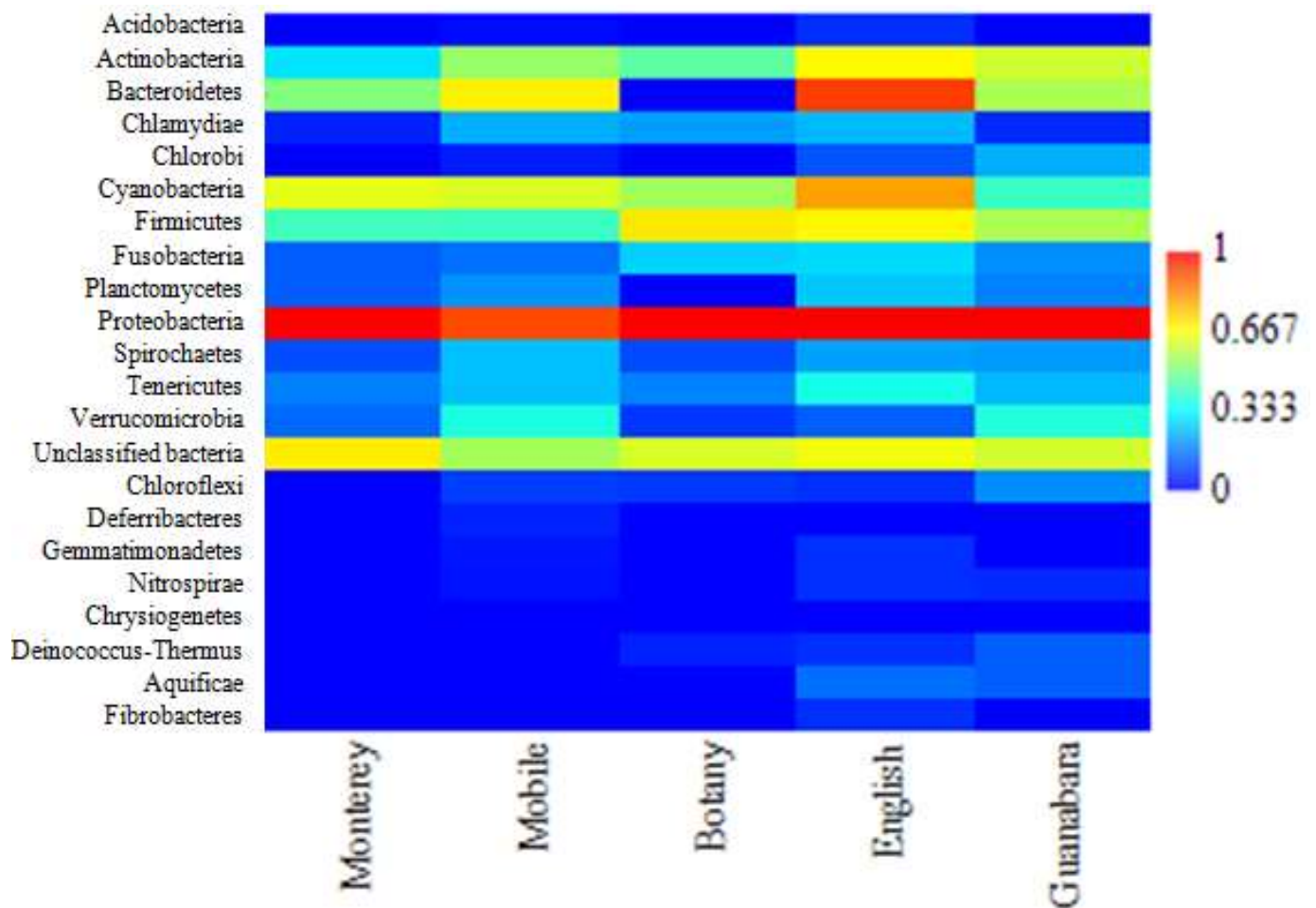


Figure 2.12: The heatmap of relative abundance of dominant microbial assemblages in Mobile Bay compared to other coastal marine systems based on MG-RAST server and M5NR annotation (see data availability section for details).

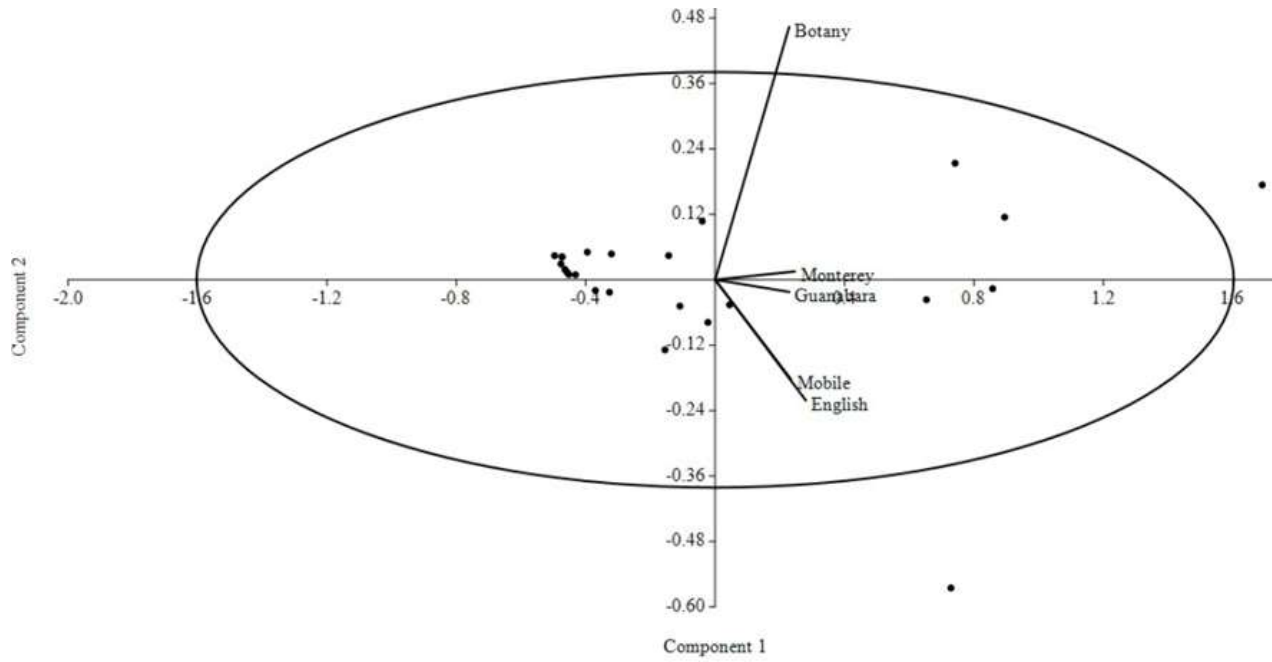


Figure 2.13: A non-metric MDS analysis of ARDs explaining variability in taxonomic relative abundance (Phyla level). Mobile Bay was taxonomically closest to the WECTS [English] ($R^2=0.84$, $MSE=0.0132$)

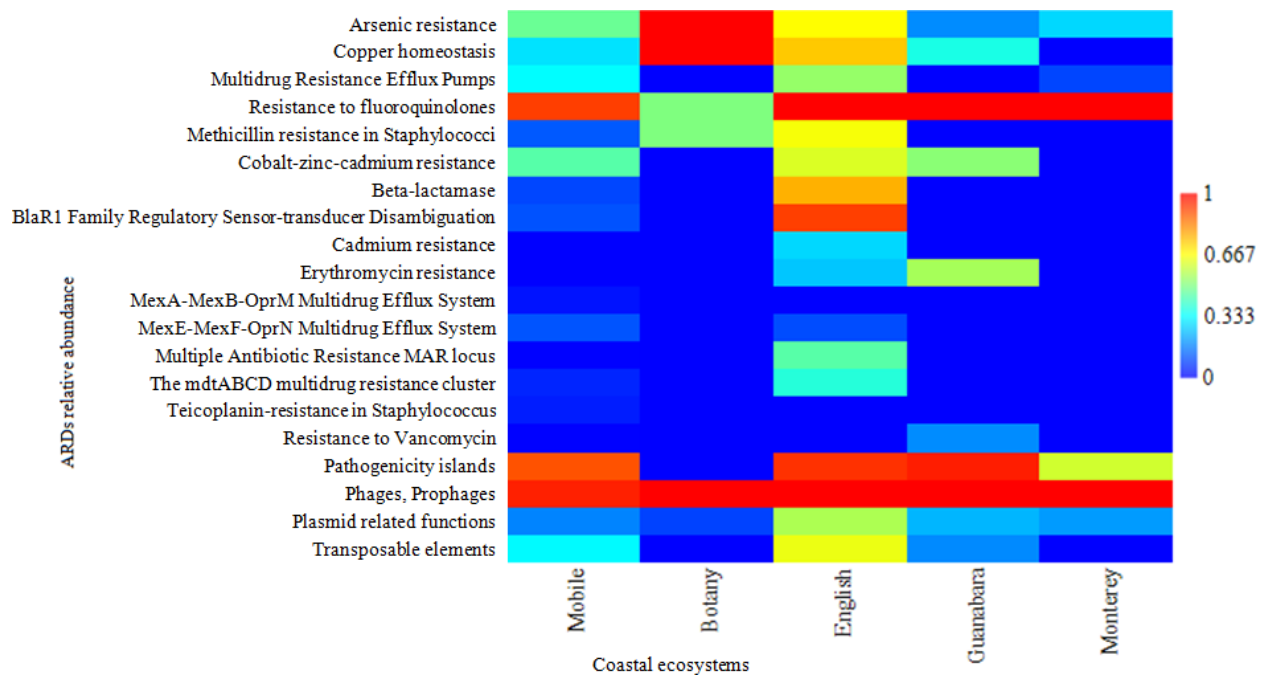


Figure 2.14: Heatmap on the relative abundance of dominant ARD genes in Mobile Bay compared to other coastal marine systems based on MG-RAST sever and SEED annotation (see data availability section for details).

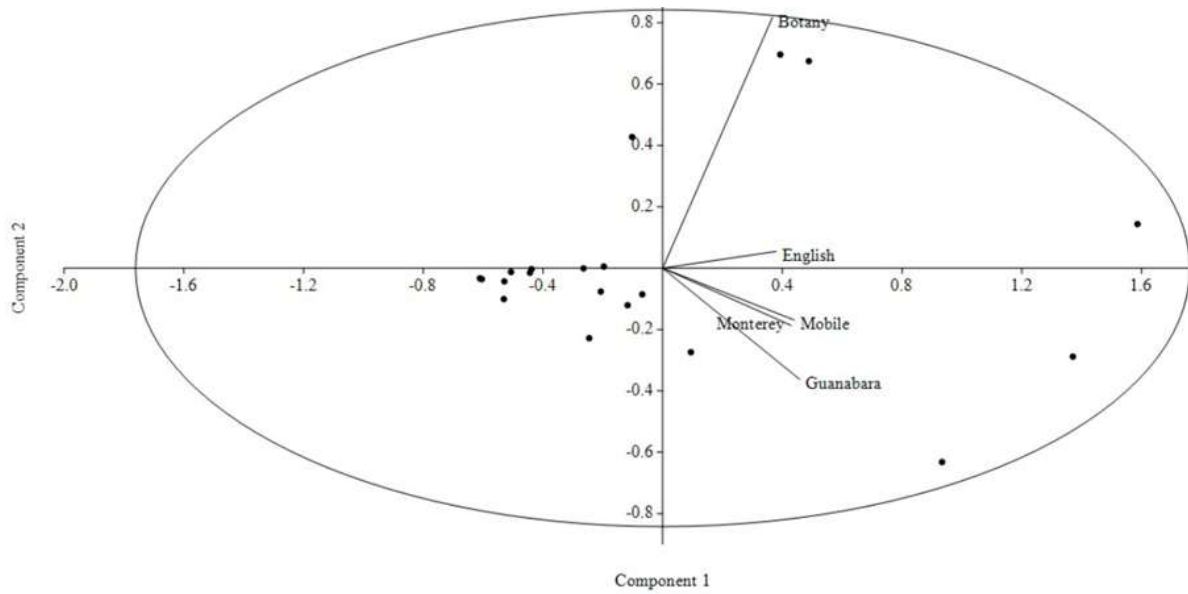


Figure 2.15: A non-metric MDS analysis of antimicrobial resistance determinants (ARDs) explaining their variability in relative abundance between Mobile Bay and other coastal marine systems

References

- Acker, J.G., Leptoukh, G., 2007. Online analysis enhances use of NASA earth science data. *Eos, Transactions American Geophysical Union* 88, 14-17.
- ADEM, 1996. (Alabama Department of Environmental Management), 1996. Water quality report to congress-“305b” Report. Alabama Department of Environmental Management, Montgomery, Alabama.
<http://www.adem.state.al.us/programs/water/wqsurvey/1997AssessStrategy.pdf>.
- Albanese, D., Fontana, P., De Filippo, C., Cavalieri, D., Donati, C., 2015. MICCA: a complete and accurate software for taxonomic profiling of metagenomic data. *Scientific reports* 5, 9743.
- Besemer, J., Lomsadze, A., Borodovsky, M., 2001. GeneMarkS: a self-training method for prediction of gene starts in microbial genomes. Implications for finding sequence motifs in regulatory regions. *Nucleic acids research* 29, 2607-2618.
- Biaostoch, A., Treude, T., Rüpke, L.H., Riebesell, U., Roth, C., Burwicz, E.B., Park, W., Latif, M., Böning, C.W., Madec, G., 2011. Rising Arctic Ocean temperatures cause gas hydrate destabilization and ocean acidification. *Geophysical Research Letters* 38, 1-5.
- Borodovsky, M., Lomsadze, A., 2014. Gene identification in prokaryotic genomes, phages, metagenomes, and EST sequences with GeneMarkS suite. *Current protocols in microbiology* 32, Unit 1E 7. <http://www.currentprotocols.com/protocol/mc01e07>.
- Bray, J.R., Curtis, J.T., 1957. An ordination of the upland forest communities of southern Wisconsin. *Ecological monographs* 27, 325-349.
- Burke, C., Steinberg, P., Rusch, D., Kjelleberg, S., Thomas, T., 2011. Bacterial community assembly based on functional genes rather than species. *Proceedings of the National Academy of Sciences* 108, 14288-14293.
- Cai, W.-J., 2011. Estuarine and Coastal Ocean Carbon Paradox: CO₂ Sinks or Sites of Terrestrial Carbon Incineration? *Annual review of marine science* 3, 123-145.
- Campbell, B.J., Kirchman, D.L., 2013. Bacterial diversity, community structure and potential growth rates along an estuarine salinity gradient. *The ISME journal* 7, 210-220.
- Conner, W., Day, J., Jr., Baumann, R., Randall, J., 1989. Influence of hurricanes on coastal ecosystems along the northern Gulf of Mexico. *Wetlands Ecology and Management* 1, 45-56.
- Consortium, T.G.O., 2015. Gene Ontology Consortium: going forward. *Nucleic acids research* 43, D1049-1056.

Curtis, W.F., Culbertson, J.J., Chase, E.B., 1973. Fluvial-sediment discharge to the oceans from the conterminous United States. US Geological Survey. <https://pubs.er.usgs.gov/publication/cir670> pp.1-24.

Daury, L., Orange, F., Taveau, J.-C., Verchere, A., Monlezun, L., Gounou, C., Marreddy, R.K.R., Picard, M., Broutin, I., Pos, K.M., Lambert, O., 2016. Tripartite assembly of RND multidrug efflux pumps. *Nat Commun* 7, 1-8.

Dempster, E., Pryor, K., Francis, D., Young, J., Rogers, H., 1999. Rapid DNA extraction from ferns for PCR-based analyses. *Biotechniques* 27, 66.

Elliott, M., Hemingway, K., 2002. Fishes in estuaries. Blackwell Science, Oxford ; Malden, Mass. Ames, Iowa Iowa State University Press. Chapter 2, pp.1-44.

Falcón, L.I., Noguez, A.M., Espinosa-Asuar, L., Eguiarte, L.E., Souza, V., 2008. Evidence of biogeography in surface ocean bacterioplankton assemblages. *Marine Genomics* 1, 55-61.

Finn, R.D., Coghill, P., Eberhardt, R.Y., Eddy, S.R., Mistry, J., Mitchell, A.L., Potter, S.C., Punta, M., Qureshi, M., Sangrador-Vegas, A., Salazar, G.A., Tate, J., Bateman, A., 2016. The Pfam protein families database: towards a more sustainable future. *Nucleic acids research* 44, D279-285.

Fisher, D.C., Oppenheimer, M., 1991. Atmospheric nitrogen deposition and the Chesapeake Bay estuary. *Ambio* 20, 102-108.

Fistarol, G.O., Coutinho, F.H., Moreira, A.P.B., Venas, T., Cánovas, A., de Paula, S.E.M., Coutinho, R., de Moura, R.L., Valentin, J.L., Tenenbaum, D.R., Paranhos, R., do Valle, R.d.A.B., Vicente, A.C.P., Amado Filho, G.M., Pereira, R.C., Kruger, R., Rezende, C.E., Thompson, C.C., Salomon, P.S., Thompson, F.L., 2015. Environmental and Sanitary Conditions of Guanabara Bay, Rio de Janeiro. *Frontiers in microbiology* 6, 1-17.

Garrity, G.M., Holt, J.M., Huber, H., Stetter, K.O., Greene, A.C., Patel, B.K.C., Caccavo, F., Allison, M.J., MacGregor, B.J., Stahl, D.A., 2001. Phylum BIX. *Deferribacteres* phy. nov, in: Boone, D.R., Castenholz, R.W., Garrity, G.M. (Eds.), *Bergey's Manual® of Systematic Bacteriology: Volume One : The Archaea and the Deeply Branching and Phototrophic Bacteria*. Springer New York, New York, NY, pp. 465-471.

Gelesh, L., Marshall, K., Boicourt, W., Lapham, L., 2016. Methane concentrations increase in bottom waters during summertime anoxia in the highly eutrophic estuary, Chesapeake Bay, U.S.A. *Limnology and Oceanography* 10, 1002-1027.

Ghoshal, B., Zhou, M., Hernandez-Sanabria, E., Guan, L., 2015. Terrestrial Vertebrate Animal Metagenomics, Domesticated Bovinae, in: Highlander, S.K., Rodriguez-Valera, F., White, B.A.

(Eds.), Encyclopedia of Metagenomics: Environmental Metagenomics. Springer US, Boston, MA, pp. 631-642.

Gilbert, J.A., Steele, J.A., Caporaso, J.G., Steinbrück, L., Reeder, J., Temperton, B., Huse, S., McHardy, A.C., Knight, R., Joint, I., Somerfield, P., Fuhrman, J.A., Field, D., 2012. Defining seasonal marine microbial community dynamics. The ISME journal 6, 298-308.

Glegg, G., Jefferson, R., Fletcher, S., 2015. Marine governance in the English Channel (La Manche): Linking science and management. Marine pollution bulletin 95, 707-718.

Griffin, J., 2014. Ocean Acidification and Methane Hydrates
http://www.climateemergencyinstitute.com/uploads/Ocean_Acidification_Methane.pdf. pp.1-10.

Hammer, Ø., Harper, D., Ryan, P., 2001. Paleontological Statistics Software: Package for Education and Data Analysis. Palaeontologia Electronica 4, 1-9.

Howe, J., Wallace, R., Scott Rikard, F., 1999. Habitat utilization by postlarval and juvenile penaeid shrimps in Mobile Bay, Alabama. Estuaries 22, 971-979.

Huhtanen, P., Bayat, A., Krizsan, S.J., Vanhatalo, A., 2014. Compartmental flux and in situ methods underestimate total feed nitrogen as judged by the omasal sampling method due to ignoring soluble feed nitrogen flow. Br J Nutr 111, 535-546.

Huse, S.M., Huber, J.A., Morrison, H.G., Sogin, M.L., Welch, D.M., 2007. Accuracy and quality of massively parallel DNA pyrosequencing. Genome biology 8, 1-9.

Jickells, T., 2006. The role of air-sea exchange in the marine nitrogen cycle. Biogeosciences Discussions 3, 183-210.

Jung, J., Philippot, L., Park, W., 2016. Metagenomic and functional analyses of the consequences of reduction of bacterial diversity on soil functions and bioremediation in diesel-contaminated microcosms. Scientific reports 6, 23012.

Kanehisa, M., Sato, Y., Morishima, K., 2016. BlastKOALA and GhostKOALA: KEGG Tools for Functional Characterization of Genome and Metagenome Sequences. Journal of Molecular Biology 428, 726-731.

Kim, K.U., Park, S.K., Kang, S.A., Park, M.K., Cho, M.K., Jung, H.J., Kim, K.Y., Yu, H.S., 2013. Comparison of functional gene annotation of *Toxascaris leonina* and *Toxocara canis* using CLC genomics workbench. Korean J Parasitol 51, 525-530.

Knott, N.A., Aulbury, J.P., Brown, T.H., Johnston, E.L., 2009. Contemporary ecological threats from historical pollution sources: impacts of large-scale resuspension of contaminated sediments on sessile invertebrate recruitment. *Journal of Applied Ecology* 46, 770-781.

Ladau, J., Sharpton, T.J., Finucane, M.M., Jospin, G., Kembel, S.W., O'Dwyer, J., Koeppe, A.F., Green, J.L., Pollard, K.S., 2013. Global marine bacterial diversity peaks at high latitudes in winter. *The ISME journal* 7, 1669-1677.

Li, A.D., Li, L.G., Zhang, T., 2015. Exploring antibiotic resistance genes and metal resistance genes in plasmid metagenomes from wastewater treatment plants. *Frontiers in microbiology* 6, 1025.

Li, S., Zhang, X., 2015. Tongue-Coating Microbiome Characterized by the Next-Generation Sequencing and Traditional Tongue Diagnosis, in: Highlander, S.K., Rodriguez-Valera, F., White, B.A. (Eds.), *Encyclopedia of Metagenomics: Environmental Metagenomics*. Springer US, Boston, MA, pp. 732-735.

Lin, C., Markowitz, L.V.M., Mavromatis, K., Ivanova, N.N., Chen, I.M., Chu, K., Kyrpides, N.C., 2009. IMG ER: a system for microbial genome annotation expert review and curation. *Bioinformatics* 25, 2271-2278.

Line, D., White, N., 2007. Effects of development on runoff and pollutant export. *Water Environment Research* 79, 185-190.

Liu, J., Fu, B., Yang, H., Zhao, M., He, B., Zhang, X.H., 2015. Phylogenetic shifts of bacterioplankton community composition along the Pearl Estuary: the potential impact of hypoxia and nutrients. *Frontiers in microbiology* 6, 1-13.

Lozupone, C., Knight, R., 2005. UniFrac: a new phylogenetic method for comparing microbial communities. *Applied and environmental microbiology* 71, 8228-8235.

Lozupone, C.A., Hamady, M., Kelley, S.T., Knight, R., 2007b. Quantitative and qualitative β diversity measures lead to different insights into factors that structure microbial communities. *Applied and environmental microbiology* 73, 1576-1585.

Mayr, L.M., Tenenbaum, D.R., Villac, M.C., Paranhos, R., Nogueira, C.R., Bonecker, S.L., Bonecker, A.C.T., 1989. Hydrobiological characterization of Guanabara bay. *Coastlines of Brazil*, 124-138.

McManus, G.B., Griffin, P.M., Pennock, J.R., 2004. Bacterioplankton abundance and growth in a river-dominated estuary: relationships with temperature and resources. *Aquatic Microbial Ecology* 37, 23-32.

- Meyer, F., Paarmann, D., D'Souza, M., Olson, R., Glass, E.M., Kubal, M., Paczian, T., Rodriguez, A., Stevens, R., Wilke, A., 2008. The metagenomics RAST server—a public resource for the automatic phylogenetic and functional analysis of metagenomes. *Bmc Bioinformatics* 9, 1-8.
- Millward, G.E., Jha, A.N., Minier, C., Pope, N.D., Langston, W.J., 2015. The English Channel and its catchments: Status and responses to contaminants. *Marine pollution bulletin* 95, 523-528.
- Mitra, A., Zaman, S., 2016. *Estuarine Ecosystem: An Overview, Basics of Marine and Estuarine Ecology*. Springer India, New Delhi, pp. 21-52.
- NOAA, 2008. Teacher Guide-Life Science Module Activity 1: Survival in an Estuary. http://estuaries.noaa.gov/Doc/PDF/LS1_SurvivalEstuary.pdf.
- Ortell, N., Ortmann, A.C., 2014. Interactions among members of the microbial loop in an estuary dominated by microzooplankton grazing. *Aquatic Microbial Ecology* 72, 63-71.
- Pennock, J., Boyer, J.N., Herrera-Silveira, J.A., Iverson, R.L., Whitedge, T., Mortazavi, B., Comin, F.A., 1998. Nutrient behavior and phytoplankton production in Gulf of Mexico estuaries. <http://scholars.unh.edu/smsoc/9/>, pp.20-67.
- Pinckney, J., Paerl, H.W., Fitzpatrick, M., 1995. Impacts of seasonality and nutrients on microbial mat community structure and function. *Marine Ecology Progress Series* 123, 207-216.
- Pryor, S.C., Sorensen, L.L., 2002. Dry deposition of reactive nitrogen to marine environments: recent advances and remaining uncertainties. *Mar Pollut Bull* 44, 1336-1340.
- Pucciarelli, S., Devaraj, R.R., Mancini, A., Ballarini, P., Castelli, M., Schrollhammer, M., Petroni, G., Miceli, C., 2015. Microbial Consortium Associated with the Antarctic Marine Ciliate *Euplotes focardii*: An Investigation from Genomic Sequences. *Microbial Ecology* 70, 484-497.
- Rabalais, N.N., 2011. Troubled waters of the Gulf of Mexico. *Oceanography* 24, 200-211.
- Rakowski, C., Magen, C., Bosman, S., Gillies, L., Rogers, K., Chanton, J., Mason, O., 2015. Methane and microbial dynamics in the Gulf of Mexico water column. *Frontiers in Marine Science* 2, 1-10.
- Rashleigh, B., Cyterski, M., Smith, L.M., Nestlerode, J.A., 2009. Relation of fish and shellfish distributions to habitat and water quality in the Mobile Bay estuary, USA. *Environmental monitoring and assessment* 150, 181-192.
- Reed, H.E., Martiny, J.B.H., 2013. Microbial composition affects the functioning of estuarine sediments. *Isme Journal* 7, 868-879.

Rho, M., Tang, H., Ye, Y., 2010. FragGeneScan: predicting genes in short and error-prone reads. *Nucleic acids research* 38, e191-e191.

Roy, P.S., Williams, R.J., Jones, A.R., Yassini, I., Gibbs, P.J., Coates, B., West, R.J., Scanes, P.R., Hudson, J.P., Nichol, S., 2001. Structure and Function of South-east Australian Estuaries. *Estuarine, Coastal and Shelf Science* 53, 351-384.

Scharko, N.K., Berke, A.E., Raff, J.D., 2014. Release of nitrous acid and nitrogen dioxide from nitrate photolysis in acidic aqueous solutions. *Environmental science & technology* 48, 11991-12001.

Shannon, C.E., 2001. A mathematical theory of communication. *ACM SIGMOBILE Mobile Computing and Communications Review* 5, 3-55.

Smith, C.G., Osterman, L.E., Poore, R.Z., 2013. An examination of historical inorganic sedimentation and organic matter accumulation in several marsh types within the Mobile Bay and Mobile-Tensaw River delta region. *Journal of Coastal Research* 63, 68-83.

Smith, L.M., Nestlerode, J.A., Harwell, L.C., Bourgeois, P., 2010. The areal extent of brown shrimp habitat suitability in Mobile Bay, Alabama, USA: targeting vegetated habitat restoration. *Environmental monitoring and assessment* 171, 611-620.

Spooner, D., Maher, W., Otway, N., 2003. Trace metal concentrations in sediments and oysters of Botany Bay, NSW, Australia. *Archives of environmental contamination and toxicology* 45, 0092-0101.

Stamatakis, A., 2014. RAxML version 8: a tool for phylogenetic analysis and post-analysis of large phylogenies. *Bioinformatics* 30, 1312-1313.

Stark, M., Berger, S.A., Stamatakis, A., von Mering, C., 2010. MLTreeMap - accurate Maximum Likelihood placement of environmental DNA sequences into taxonomic and functional reference phylogenies. *BMC genomics* 11, 461-461.

Stout, J.P., Heck, K.L., Valentine, J.F., Dunne, S.J., Sptizer, P.M., 1998. Preliminary characterization of habitat loss: Mobile Bay national estuary program. 301, 1-213.

Sun, Z., Li, G., Wang, C., Jing, Y., Zhu, Y., Zhang, S., Liu, Y., 2014. Community dynamics of prokaryotic and eukaryotic microbes in an estuary reservoir. *Scientific reports* 4, 1-8.

Swann, R., 2014. Coastal Population Growth: The Challenge of Keeping What We've Got.

Tinnon, V.L., 2010. Environmental injustice: health and inequality in mobile county, Alabama. PhD Dissertation. Manhattan. Kansas State University, pp 3-36.

- Trueba, F., Garrabe, E., Hadeif, R., Fabre, R., Cavallo, J.-D., Tsvetkova, K., Chesneau, O., 2006. High Prevalence of Teicoplanin Resistance among *Staphylococcus epidermidis* Strains in a 5-Year Retrospective Study. *Journal of clinical microbiology* 44, 1922-1923.
- Tytgat, B., Verleyen, E., Sweetlove, M., D'Hondt, S., Clercx, P., Van Ranst, E., Peeters, K., Roberts, S., Namsaraev, Z., Wilmotte, A., Vyverman, W., Willems, A., 2016. Bacterial community composition in relation to bedrock type and macrobiota in soils from the Sor Rondane Mountains, East Antarctica. *FEMS microbiology ecology* 92, 1-13.
- Tzortziou, M., Herman, J.R., Cede, A., Loughner, C.P., Abuhassan, N., Naik, S., 2015. Spatial and temporal variability of ozone and nitrogen dioxide over a major urban estuarine ecosystem. *Journal of Atmospheric Chemistry* 72, 287-309.
- Walters, R.A., Cheng, R.T., Conomos, T.J., 1985. Time scales of circulation and mixing processes of San Francisco Bay waters, in: Cloern, J.E., Nichols, F.H. (Eds.), *Temporal Dynamics of an Estuary: San Francisco Bay*. Springer Netherlands, Dordrecht, pp. 13-36.
- Wetz, M.S., Yoskowitz, D.W., 2013. An 'extreme' future for estuaries? Effects of extreme climatic events on estuarine water quality and ecology. *Mar Pollut Bull* 69, 7-18.
- Whitledge, T.E., Malloy, S.C., Patron, C.J., Wirick, C.O., 1981. Automated nutrient analysis in seawater. 51398: 216, National Laboratory. Brookhaven National Lab, Brookhaven, NY. pp.1-29.
- Whittaker, R.H., Likens, G.E., 1975. The Biosphere and Man, in: Lieth, H., Whittaker, R.H. (Eds.), *Primary Productivity of the Biosphere*. Springer Berlin Heidelberg, Berlin, Heidelberg, pp. 305-328.
- Wilke, A., Harrison, T., Wilkening, J., Field, D., Glass, E.M., Kyrpides, N., Mavrommatis, K., Meyer, F., 2012. The M5nr: a novel non-redundant database containing protein sequences and annotations from multiple sources and associated tools. *Bmc Bioinformatics* 13, 1-5.
- Wu, D., Hugenholtz, P., Mavromatis, K., Pukall, R., Dalin, E., Ivanova, N.N., Kunin, V., Goodwin, L., Wu, M., Tindall, B.J., 2009. A phylogeny-driven genomic encyclopaedia of Bacteria and Archaea. *Nature* 462, 1056-1060.
- Xia, Z., Bai, E., Wang, Q., Gao, D., Zhou, J., Jiang, P., Wu, J., 2016. Biogeographic Distribution Patterns of Bacteria in Typical Chinese Forest Soils. *Frontiers in microbiology* 7, 1-17.
- Zhao, H., Chen, Q., 2008. Characteristics of Extreme Meteorological Forcing and Water Levels in Mobile Bay, Alabama. *Estuaries and Coasts* 31, 704-718.

Zhu, R., Shi, Y., Ma, D., Wang, C., Xu, H., Chu, H., 2015. Bacterial diversity is strongly associated with historical penguin activity in an Antarctic lake sediment profile. *Scientific reports* 5, 1-13.

Chapter 3: Taxonomic, phylogenetic and functional insights into bacterial assemblages associated with the stomodeum of *Mnemiopsis leidyi*

Abstract

Mnemiopsis leidyi is a ctenophore of interest to many scientists including studying evolution of metazoans and nervous systems, and the ecology of species invasions and marine systems. Here, we describe the stomodeal ('gut') bacterial assemblages, and predict the metabolic profiles and potential for the gut of *M. leidyi* to harbor antibiotic resistance determinants (ARDs). This study used shotgun metagenomics and downstream bioinformatics analyses of *M. leidyi* gut samples. The bacterial phyla Proteobacteria and Actinobacteria dominated the stomodeum. The metagenomes were dominated by amino acid and carbohydrate metabolism genes. The abundant carbohydrate-active enzymes included GH38 (polysaccharide hydrolysis), GT2 (chitin degradation) and GT48 (1, 3- β -glucan synthase and immunity). Gene ontology annotation revealed genes specifically known to play important roles in interactions with hosts (GO 0051701), in addition to microbial interspecies interactions (GO 0044419). A total of nine (9) types of antibiotic resistance genes (ARGs) (beta-lactamase, aminoglycoside, tetracycline, macrolide, phenicol, quinolone, cationic antimicrobial peptide (CAMP), vancomycin and multidrug resistance) were detected. The abundance and distribution of ARGs were seasonally variant. Our study suggests the possibility of *M. leidyi* harboring microbiota that impart specific functions, such as digestive and immune capability. The bacterial assemblages in the *M. leidyi* stomodeum also revealed the potential to harbor ARDs. This is the first report to functionally characterize *M. leidyi* gut bacterial assemblages.

Introduction

In metazoans, host gut microbiotas are involved in the host stress response, as well as in their general physiological and nutritional status (Lee and Hase, 2014; Malham et al., 2014; Stilling et al., 2014; Wu et al., 2013). Gut microbiota are known to act like a virtual organ, and are important in energy balance as they are involved in nutrient digestion (Tims et al., 2013). Some gut bacteria are mutualistic while others can be pathogenic. Gut bacteria may also harbor antibiotic resistance genes (ARGs) (Santos et al., 2012), whose mobility and acquisition is associated with mobile genetic elements (MGEs) (Beatson and Walker, 2014). The co-selection and cross selection of ARGs and MGEs due to shared regulatory and structural processes lead to proliferation of antibiotic resistance.

Ctenophores are gelatinous zooplankters that belong to the phylum Ctenophora (Harbison and Madin, 1982; Tamm, 2014). Ctenophores are the largest animals known to swim using cilia (Tamm, 2014) and are estimated to comprise nearly 200 species (Harbison and Madin, 1982; Pang and Martindale), with some orders having very short evolutionary distances between them (Podar et al., 2001). Ctenophores are increasingly being recognized as indicators and drivers of ecosystem performance and change (Hao et al., 2015; Hay, 2006; Lucic et al., 2012). They not only alter marine food webs (Lucic et al., 2012; Purcell and Arai, 2001; Shiganova et al., 2003), but are also an indication of environmental perturbation.

The species *Mnemiopsis leidyi* is highly invasive (Ghabooli et al., 2013; Lucic et al., 2012; Reusch et al., 2010). As a predatory planktonic neozootic (introduced accidentally into new habitats outside of native range as larvae in ship's ballast water), it has been found to be extremely damaging to food webs by severely cropping local plankton (Kideys, 2002; Lucic et al., 2012; Reitzel et al., 2007; Shiganova et al., 2003). In the Mediterranean, Baltic, Black and Caspian

Seas, *M. leidy* invasions have been found to be responsible for the severe depletion of fish of economic importance (Bumann and Puls, 1996; Daskalov and Mamedov, 2007; Ghabooli et al., 2013; Hansson, 2006; Jaspers et al., 2012; Reitzel et al., 2007; Reusch et al., 2010; Shiganova et al., 2003).

Mnemiopsis leidy has also been found to act as vector for parasites, bacterial and eukaryotic microorganisms (Hammann et al., 2015; Hao et al., 2015; Moss et al., 2008) and viruses (Breitbart et al., 2015). Although a handful of studies have found *M. leidy* to harbor endobacteria (Daniels and Breitbart, 2012; Hammann et al., 2015; Hao et al., 2015; Moss et al., 2008), none have explored the temporal dynamics and functional potential of their stomodeal ('gut') bacteria. This study used shot-gun sequencing and bioinformatic analyses to characterize *Mnemiopsis leidy* gut bacterial assemblages, and to predict their metabolic profiles and their potential to harbor antibiotic resistance determinants.

Methods

Sample collection

Ctenophore specimens (~5 cm long each) were collected seasonally (February 15th 2014, May 8th 2014, August 25th 2014, and October 10th 2013 between 2013 and 2014) from the Dauphin Island Marina (Alabama, USA) (30 15'47.3"N 88 06'48.5"W) by plankton net. 'Gut' microbe samples for summer (GSU August 25th 2014), fall (GFL October 10th 2013), winter (GWI February 15th 2014) and spring (GSP May 8th 2014) were collected from the stomodeum using round, sharp sterile toothpicks, in less than 5 mins) after removal from sample location. Samples were collected from 7 animals from each sampling date. The toothpicks were gently introduced into the mouth opening and while rotating, pushed back to the aboral-most extent of the

stomodeum. Rotation with the porous wooden pick reliably and reproducibly pulled out a mucus plug from the center/aboral-most regions of the gut. Sample collection did not perforate the gut; nor did it do harm to the animals, which routinely then survived for multiple days after collection. This method allowed us to gently pull out the mucus laden content of the gut and immediately place it on ice in sterile 1.5 mL microcentrifuge tubes, to be further processed upon arrival to the laboratory, 6 hours to 10 hours later.

DNA extraction and library preparation

DNA was extracted using a modified CTAB protocol (Andreou, 2013) and purity checked using a NanoDrop (ND-2000, NanoDrop Technology, Wilmington, DE, USA) to establish the $A_{260}:A_{280}$ ratio. Template DNA with values $> 1.8 A_{260}:A_{280}$ were carried forward for further analysis (this was true for nearly all samples). DNA template concentration was adjusted to $5\text{ng } \mu\text{L}^{-1}$ for use in regular PCR reactions. DNA quantitation prior to creation of libraries for Miseq sequencing was done using Qubit HS reagents (Life Technologies). For shotgun metagenomic sequencing, seasonal samples were pooled and Nextera XT library preparation kits (Illumina, San Diego, CA, USA) used to construct paired-end libraries for sequencing on the MiSeq platform in the Auburn University's Biological Sciences Department.

Sequencing and quality trimming

Nextera XT Libraries were sequenced using Illumina Miseq sequencing platform with Miseq reagent kit v2 (Illumina, USA). FC-402-4001 TruSeq® Rapid SBS Kit (200 cycles) and PE-402-4001 TruSeq® Rapid PE Cluster Kit were used to prepare samples for 100×2 paired end run for HiSeq sequencing at the Genomics & Sequencing Laboratory at Auburn University. FASTQ files from all sequencing runs were imported into CLC Genomics Workbench 9.0 (CLCbio,

Aarhus, Denmark) (Kim et al., 2013). Reads were subjected to quality control using the Sequencing QC Report tool. Both the 100 bp paired-end and 250 bp paired-end Illumina reads were trimmed and filtered using the following parameters: Ambiguous Trim = Yes, Ambiguous Limit = 10, Quality Limit = 0.05, Min distance = 75, Max distance = 350. Adapter sequences were removed from the reads during this process.

Merging and Assembly of metagenomes

To investigate the alpha diversity of the bacterial assemblages, a phylogenetic diversity framework, an effective and sensitive microbial ecology approach was used (Barker, 2002; Faith, 1992; McCoy and Matsen, 2013), in addition to the traditional Operational Taxonomic Unit (OTU)-based Shannon diversity index (H). Trimmed and merged sequences were filtered based on length and number of reads before analysis. OTU clustering and analysis of microbial assemblages for alpha diversity was achieved by using Microbial Genomics Module on CLC Genomics Workbench 9.0 (CLCbio, Aarhus, Denmark) (Kim et al., 2013). Low-abundance OTUs (< 0.005% of the total number of reads) were removed to ensure that low quality reads were not part of the analysis, as previously recommended (Bokulich et al., 2013). Reference based-OTU clustering used the Greengenes database with a species cutoff of 97% with the chimera filter. MUSCLE software (Edgar, 2004) was used for multiple sequence alignment prior to creation of the reference tree used for phylogenetic placement. For beta diversity analysis, the Microbial Genomics Module was used for OTU clustering, using filtered tables.

The trimmed and filtered 100 bp paired-end and 250 bp paired-end reads were *de novo* assembled in CLC Genomics Workbench 9.0 using the following parameters: Mapping Mode = Map reads to contigs (slow), Automatic bubble size = No, Bubble Size = Yes (50), Minimum Contig Length = 75 bp, Automatic Word Size = No, Word Size = 45, Perform Scaffolding =

Yes, Automatically Detect Paired Distances = No, Mismatch Cost = 2, Insertion Cost = 3, Deletion Cost = 3, Length Fraction = 0.5, Similarity Fraction = 0.8. As an alternative to OTU picking approach, determination of the microbial species associated with the stomodeum of *M. leidy* was achieved by first predicting genes in assembled metagenomes using FragGeneScan (Rho et al., 2010), followed by mapping the taxonomy using KEGG Mapper tool for reconstructing KEGG taxonomy (Kanehisa and Goto, 2000).

Phylogenetic inference from *M. leidy* stomodeum metagenomic data

To gain insight into the phylogenetic diversity of the microbial assemblages, the study utilized assembled sequences from each metagenome for phylogenetic analysis. This was achieved by performing a maximum likelihood (ML) of assembled DNA sequences using MLTreeMap (Stark et al., 2010) based on the Genomic Encyclopedia of Bacteria and Archaea (GEBA) as reference (Wu et al., 2009). Results were placed into the RaxML tool following default ML model parameters (Stamatakis, 2014).

Annotation of *M. leidy* assemblies

Functional annotation using assembled reads was achieved by first identifying coding regions (CDS) in the contigs using MetaGeneMark tool (Besemer et al., 2001; Borodovsky and Lomsadze, 2014) on CLC Genomics Workbench 9.0. CDS were then annotated with Pfam domains (Finn et al., 2016) and GO terms (Consortium, 2015). The Metagenomics RAST server (MG-RAST, release 3.3) (Glass et al., 2010) was employed for further taxonomic and functional insights. Annotation using the IMG/ER pipeline (Markowitz et al., 2014) was used to search for all bacterial scaffolds to confirm the diversity of microbial assemblages. In addition, it was used

to investigate the proportion of shared and unique assemblages at species level. It was also used to analyze functional properties of the metagenomes.

Gene prediction and functional annotation

The rRNA prediction was done using by using HMMER 3.0 using the hidden Markov models (HMM) technique of Finn (Finn et al., 2011). Transfer RNA prediction was carried out using program tRNAscan-SE (Lowe and Eddy, 1997) to identify DNA reads containing each type of RNA sequences. Coding sequences (CDS) from the contigs were located using MetageneMark (Zhu et al., 2010) and FragGeneScan (Rho et al., 2010). Predicted gene sequences were then subjected to a search against the KEGG Orthology (KO) database (Kanehisa and Goto, 2000). GhostKOALA (<http://www.kegg.jp/blastkoala/>) (Kanehisa et al., 2016) was used to perform KO (KEGG Orthology) (Kanehisa and Goto, 2000) assignments to characterize individual gene functions as well as reconstruct KEGG pathways. KEGG (Kyoto Encyclopedia of Genes and Genomes) mapper was used to reconstruct BRITE hierarchies and KEGG modules in an effort to infer high-level functions of the microbial assemblages in *M. leidy* stomodeum, including functional prediction for metabolic activity as well as antibiotic resistance in each metagenome. This was achieved with a 50% amino acid identity cutoff on a non-redundant dataset generated using protein-coding genes. Protein domain searches were performed on the predicted gene sequences against the PFAM database (Finn et al., 2010) using HMMER 3.0 (Finn et al., 2014) with an E-value of 0.001.

The Carbohydrate-Active Enzyme database (CAZy), was used for analysis of carbohydrate active enzymes. With this tool, we were able to classify metabolic enzymes into different glycosyl hydrolases (GH) and glycosyl transferase (GT) families, among others. Protein

sequences from the metagenome contigs were predicted by FragGeneScan and normalized to obtain 50,000 amino acid sequences from each metagenome before annotation. Annotation was based on association rules between CAZy families and pfam domains by performing BLASTp with an E-value threshold of 0.001. Comparison between CAZy families was done using the Euclidean Similarity Index and visualized using Non-Metric Multidimensional Scaling (NMDS) and correlation analysis.

Comparisons of *M. leidy* bacterial assemblages and functional potential were carried out with representatives other sister phyla: *Fungia echinata* (Cnidaria) (Badhai et al., 2016) and *Arenosclera brasiliensis* (Porifera) (Trindade-Silva et al., 2012)

Comparative metagenomics was performed in an effort to determine whether *M. leidy* (Ctenophora) taxonomic composition is any different from its closest relatives like corals and sponge. For taxonomic and functional comparison, normalized data on microbial assemblages from *F. echinata*, *A. brasiliensis* and *M. leidy* was annotated with M5NR and KEGG features on an MG-RAST pipeline. This used a maximum e-value of 1e-5, a minimum identity of 80 %, and a minimum alignment length of 15 measured in amino acids for protein and base pairs for RNA databases and compared against *M. leidy* with similar settings as groups (Glass et al., 2010; Wilke et al., 2012).

Statistical analysis

The phylogenetic diversity index was calculated for the metagenomes to determine alpha diversity. Beta-diversity analysis was performed using the Bray-Curtis and Jaccard dissimilarity measures using Principal Coordinate Analysis (PCoA). Box and jitter plots were used to show

the distribution of shared bacterial assemblages based on IMG/ER pipeline using Past3 software (Hammer et al., 2001). STAMP software (Parks et al., 2014) was used to generate and display differences in bacterial assemblage abundance in each MG-RAST annotated metagenome. Storey's FDR correction was utilized for comparative analysis between metagenomes (Storey and Tibshirani, 2003), with the nearest neighbor hierarchical clustering method being used, and graphed as a heatmap to reveal the abundance of taxonomic groups. Additionally, using Past3 software, the Mann-Whitney U test was used to compare whether the medians of taxonomic and functional abundances between the metagenomes was significantly different. Test values were considered significant if p-values were less than 0.05. IMG/ER was used for annotation and used to search for all the shared metagenome scaffolds (with > 230 bp length and 100% lineage percentage) of the bacterial assemblages. The study sought to track the shared scaffolds to determine the nature of the relationship between shared assemblages from each season. To investigate if the association was by chance, a Chi square (χ^2) test was used.

Results

For each of the metagenome (GSU, GFL, GWI and GSP), the reads had an average Phred score above 27 (for each metagenome), meaning that the sequencing was of high quality (Table 3.1). After removal of low quality and universal adapter sequences (CTGTCTCTTATACACATCT), a total number of merged reads 4,602,424 (GSU), 2,338,952 (GWI) 766,040 (GFL) 126,831 (GSP) were obtained for OTU clustering. After quality trimming, we obtained 11,648,797 reads from winter (GWI), 4,429,366 reads from spring (GSP), 19,740,678 reads from summer (GSU) and 7,260,745 reads from fall (GFL) metagenomes. After OTU clustering, we obtained a total of 7,834,247 high-quality reads that were clustered into 1,354,066 OTUs. OTU picking was

performed against the Greengenes database (McDonald et al., 2012) at 97% identity cutoff. The alpha diversity analysis measured using phylogenetic diversity index revealed that GSU and GFL metagenomes had the highest diversity. The alpha diversity analysis further revealed that GSP had the least diversity of the observed OTUs (Fig. 3.1). Based on KEGG organisms, the taxonomic abundance was different only between GSP and GWI (Table 3.2).

Bacterial assemblages from the gut of the *M. leidy*

Based on KEGG taxonomy (using the GhostKOALA annotation), each seasonal metagenome was dominated by the Phylum Proteobacteria (> 37% per metagenome, 12, 624 total K number assignments and Actinobacteria (>15% per metagenome, 2,416 total K number assignments) (Fig. 3.2a-3.2d, Table S3.2 in appendix). Except between GWI and GSP, the Mann-Whitney U test indicated that the total taxonomic abundances were not significantly different among the months of sampling (p-value >0.05; Table 3.3) but followed the order of GWI>GSU>GFL>GSP in terms of magnitude. We inferred differences in the bacterial assemblages between samples using the Bray-Curtis and Jaccard dissimilarity indexes. We found a clear segregation between the samples into different clusters. The distance matrix for between stomodeum metagenomes calculated from Bray-Curtis (Fig. 3.3a) and Jaccard dissimilarity indices (Fig. 3.3b) both showed that metagenomes differed depending on time of collection (Table S3.1 in appendix). The MG-RAST taxonomic data analyzed using STAMP software revealed that GWI and GFL were clustered together, with GSU and GSP also clustering together based on relative abundance (Fig. 3.4). Unlike the previous studies (Daniels and Breitbart, 2012; Hammann et al., 2015; Hao et al., 2015), our study illustrated

that *M. leidy* contains the following previously unreported Phyla in *M. leidy*: Acidobacteria, Chlamydiae, Spirochaetes, Chlorobi and Fusobacteria (Fig. 3.4).

The shared scaffolds included those derived from 11 bacterial lineages. A statistical analysis using χ^2 revealed that there was a significant association ($\chi^2=1023$, $df=30$, $p<0.0001$) between the observed bacterial lineages (Fig. 3.5). The bacterial lineages include those belonging to, *Burkholderia* sp. JC2949, *Enterobacter asburiae*, *Escherichia coli*, *Helicobacter pylori*, *Prochloron didemni*, *Propionibacterium acnes*, *Staphylococcus aureus*, *Staphylococcus epidermidis*, *Streptococcus agalactiae* and *Streptococcus pyogenes* in addition to unclassified bacteria. The study observed seasonally variant species-level bacterial phylogenetic diversity patterns across the metagenomes (Fig. 3.6a-d). GWI had the highest phylogenetic diversity, with GFL having the least.

Functional analysis based on *M. leidy* seasonal metagenomes

GhostKOALA annotation software was used to assign a KEGG identifier (K number) of the predicted protein sequences and revealed that the distinct functional categories for each metagenome were mainly those involved in central cellular metabolism (Fig. 3.7). These GhostKOALA functional categories displayed no considerable differences in functional dynamics correlation ($r>0.92$) between metagenomes, meaning that the predicted functions occurred in all samples, and thus could always be present and perhaps be critical in host-microbe interaction.

Gene prediction using IMG/ER revealed temporal functional differences in metagenome properties (Table 3.1). Most of the Gene Ontologies (GO) biological processes were from those involved in metabolic processes and interspecies interaction (Fig. 3.8). This suggests host-

microbe interaction that maintains essential functionalities, including metabolism of substrates. The CAZy database revealed a diversity of carbohydrate-active enzymes. There were no significant differences ($r > 0.99$) between stomodeum seasonal metagenomes in the diversity and abundance of CAZy enzymes. The most abundant GT classes were GT48 and GT2 genes (Fig. 3.9a, Table S3.3 in appendix). For the glycoside hydrolases (GHs) families, GH38 (involved in polysaccharide hydrolysis) (Verma et al., 2016) was the most abundant. The GT48 CAZy family (EC 2.4.1.34) was distinctly overrepresented compared to other enzymes when analyzed using non-metric multidimensional scaling (nMDS) (Fig. 3.9b) ($p = 0.0001$). CAZy annotation identified 970 GT48 genes. The GT48 family is a family of enzymes also referred to as 1,3- β -D-glucan synthases (called callose synthase) are involved immune response in plants, especially during fungal infections (Voigt, 2014) and are also involved in starch and sucrose metabolism pathway (EC 2.4.1.34). Based on these data, it is possible, similar to the pattern known for other metazoans, that the stomodeum bacterial assemblage's primary role in ctenophores could be to protect its host against fungal pathogens (Ellinger et al., 2013; Fraune et al., 2015).

A total of nine types of antibiotic resistance genes (ARGs) (beta-lactamase, aminoglycoside, tetracycline, macrolide, phenicol, quinolone, cationic antimicrobial peptide (CAMP), vancomycin and multidrug resistance) were detected. The abundance and distribution of ARGs patterns were seasonally variant (Fig. 3.10, Table S3.4 in appendix). The abundant ARGs were those associated with efflux pumps.

Comparative metagenomics with other basal metazoa

Based on the M5NR database with 80% identity cutoff, the predicted relative abundance of the bacterial assemblages (at the phylum level) revealed no significant

differences between *M. leidy*, the coral *F. echinata* and the sponge *A. brasiliensis* ($p > 0.05$, two way-ANOVA). The three metazoans were all dominated by bacteria from Phylum Proteobacteria, Firmicutes, Cyanobacteria and Bacteroidetes (Fig. 3.11). Based on correlation coefficients, *M. leidy* bacterial assemblages appeared to be closely related to both *F. echinata* ($r= 0.9178$, $p<0.05$) and *A. brasiliensis* ($r=0.872$, $p<0.05$). Filtration and processing of metagenomes for functional annotation resulted in different relative abundances for these three basal metazoa (Fig. 3.12a, Table 3.4 and 3.5). Metabolism genes of the *F. echinata* microbiome were significantly over-represented compared to those in *M. leidy* (Mann-Whitney U test, $p< 0.001$) (Table 3.6). This was confirmed using box plots (Fig. 3.12b). Except in the metabolism of cofactors and vitamins, there were significant differences in the abundance of various microbial metabolism genes between *F. echinata* and *M. leidy* ($p< 0.05$, ANOVA). Microbial metabolism genes in the *A. brasiliensis* microbiome were not over-represented compared to *M. leidy* (Mann-Whitney U test, $p= 0.001$) (Table 3.6).

Discussion

There have been four studies that have investigated the bacterial assemblages associated with ctenophores (Daniels and Breitbart, 2012; Hammann et al., 2015; Hao et al., 2015). However, none have indicated whether ctenophores internally harbor microbes; in fact, none indicated that the gut of *M. leidy* contains microbiota. The current study revealed that the *M. leidy* gut harbors at least 10 distinct bacterial lineages, whose distribution is statistically not by chance. It is important to note that it is often hard to find ctenophores in the spring in Mobile Bay. This is most likely a product of seasonal storms and water runoff at that time of the year. It could also be a result of seasonal impacts on the reproductive cycle of ctenophores (Boero et al., 2008). Certainly the low temperatures (which have been shown to limit *M. leidy* distributions in

invaded environments) in addition to the relative lack of copepod as source of food could be the other limiting factors (Boero et al., 2008; Gambill et al., 2015; Lehtiniemi et al., 2012) at that time of year both impact ctenophore productivity in the spring.

The lack of difference in bacterial assemblages among the other seasons at the microbial phylum level (using the Mann-Whitney U test) is indicative of their constant relative abundance, typical of gut microbiota which have a non-linear (are randomly distributed) and dynamic interaction with the host (Mandal et al., 2015). Species-level bacterial phylogenetic diversity was seasonally variant, with GWI having the highest phylogenetic diversity. This could imply that the *M. leidy* stomodeal phylogenetic diversity of bacterial assemblages is neither stable, nor resilient.

This study, using *M. leidy* as model, is the first to reveal the occurrence of previously unnoticed microbial Phyla in ctenophore *M. leidy*: Acidobacteria, Chlamydiae, Spirochaetes, Chlorobi and Fusobacteria. The study also reveals that occurrence of some bacterial lineages is statistically not random. Also, this is the first study predicting the functional potential of stomodeum-associated bacterial assemblages, and indicating the presence of ARGs. Some microbes revealed in our study have been found to produce nutritional and secondary metabolites that are vital to other hosts such as tunicates and insects (Donia et al., 2011; Salem et al., 2013). The uncultivated *Prochloron didemni* for instance has been found to influence the lipid composition of hosts (tunicates) via steroid synthesis, and is involved in the synthesis of cyanobactin and other related secondary metabolites in corals and tunicates (Donia et al., 2011; Lin et al., 2016). Elimination of actinobacteria symbionts in some insects has been attributed to significantly higher mortality and reduced host growth rates, emphasizing the role of gut bacteria in host nutrition (Salem et al., 2013). Host-microbe interactions in *Hydra vulgaris*, a cnidarian,

have been extremely well-studied, and found that these hosts harbor microbes that are critical to host defense against fungal infections (Franzenburg et al., 2012; Franzenburg et al., 2013; Fraune et al., 2015).

Based on the dominant GO functions (Fig.3.8), our study predicted that one of the possible roles of bacterial assemblages in *M. leidy* involves aid in metabolic processes. The lack of shift in functional categories (metabolism genes) based on GhostKOALA could mean that the bacterial assemblages are constant across samples, and thus maybe critical in host-microbe interaction. The study also revealed that *M. leidy* bacterial assemblages harbor ARGs, which emphasizes that the resistome knows no boundaries. Future efforts should include progressive profiling of the bacterial lineages that are strongly associated with *M. leidy* stomodeum and determine their functional capabilities from cydippid to adulthood and to explain the stomodeum, colonization rates (how are the bacterial lineages acquired?) and host and environmental factors involved in the transmission process. To validate this work, the study could have used primers targeting all major bacterial taxa using qPCR, and the use multiplex detection of antibiotic resistance genes (Barisic et al., 2013).

Conclusion

This is the first study to examine functional dynamics of microbial assemblage from the stomodeum of *M. leidy*. The ARGs were most dominant in winter, because the hosts (*M. leidy*) most likely move to the bottom of the water column where temperatures are favorable (Beaulieu et al., 2013), and in the process, come into contact with the sediment, where there are high loads of ARGs, and delayed degradation as antibiotics and heavy metals bind to particulate matter (Berglund et al., 2014; Haraldsson et al., 2014; Tamtam et al., 2008). This study provides a

baseline for understanding the complexity of *M. leidy* stomodeum microbial assemblage and ARD ecology. Future efforts should also aim at determining functional benefits and the maintenance of potential host- microbe homeostasis in *M. leidy* and investigating the role of temporal and spatial changes in *M. leidy* microbial structures on functional capability. This study agrees with previous studies that *M. leidy* harbors low bacterial diversity. This study further determined that overall; *M. leidy* has low bacterial diversity compared to coral *F. echinata* and sponge *A. brasiliensis*.

Data availability

GenBank Biosamples for the Sequence Read Archive (SRA): GSU (SRS1522865) GFL (SRS1522942), GWI (SRS1522753) and GSP (SRS1522598). *M. leidy* stomodeum metagenome samples were also deposited in MG-RAST web server (<http://metagenomics.anl.gov>) under projects 4664006.3 (GSU), 4637717.3 (GFL), 4637719.3 (GWI) and 4637718.3 (GSP). The MG-RAST metadata includes geographical coordinates, sequence counts and country. The metagenome browser for the study includes overviews containing analysis flowcharts, taxonomic and functional category distribution. On IMG Genome portal (<https://img.jgi.doe.gov>), data is deposited under IMG Genome ID 3300006492 (GSU), 3300005727(GFL), 3300005729 (GWI) and 3300005728 (GSP).

Table 3.1: Summary on abundance of features used for functional profiles analysis of microbial assemblages in the ctenophore *M. leidy* from Dauphin Island Marina, Mobile Bay. Gut summer (GSU), fall (GFL) winter (GWI) and spring (GSP) samples were analyzed using CLC Genomics Workbench and IMG/ER pipeline

Summary	GSU	GFL	GW	GSP
Number of reads	18,186,142	6,836,864	11,789,080	4,426,820
Mean PHRED score	32	28	28	27
Number of contigs	65,277	86,231	119,208	23,269
Total length of contigs (bp)	20,633,424	30,134,949	40,546,994	6,593,987
Number of CDS	30,722	33,746	55,844	10,601
CDS with Pfam domains	2,645	2,555	5,336	674
Number of Pfam	1,039	977	2,083	365
Abundance of Pfam features	235,556	53,542	173,069	17,738
Number of GO features	1,288	1,325	1,807	766
Abundance of GO features	2,019,025	279,775	911,285	88,969

Table 3.2: Mann-Whitney test P value summary of taxonomic abundance among seasonal metagenomes at phyla level based on KEGG organisms using MG-RAST server (Glass et al., 2010)

	GSU	GFL	GWI	GSP
GSU	—	8.5823×10^{-1}	5.088×10^{-1}	7.1553×10^{-2}
GFL		—	9.5862×10^{-1}	8.5482×10^{-1}
GWI			—	2.5978×10^{-2}
GSP				—

Table 3.3: Mann-Whitney test P value summary of metabolic genes abundance (KEGG Level 2) between metagenomes representing different seasons using MG-RAST server (Glass et al., 2010)

	GSU	GFL	GWI	GSP
GSU	—	8.5823×10^{-1}	5.088×10^{-1}	7.1553×10^{-2}
GFL		—	9.5862×10^{-1}	8.5482×10^{-1}
GWI			—	2.5978×10^{-2}
GSP				—

Table 3.4: Correlation coefficients in taxonomy (phylum level) and metabolism genes between ctenophore *M. leidy*, coral *Fungia echinata* (Badhai et al., 2016) and sponge *Arenosclera brasiliensis* (Trindade-Silva et al., 2012)

Taxonomic diversity			
	<i>F. echinata</i>	<i>M. leidy</i>	<i>A. brasiliensis</i>
Phyla	11	9	15
Shannon (H')	2.053	1.615	2.145
Correlation coefficients (r) in taxonomy (Phylum level)			
<i>F. echinata</i>	—	0.9177662	0.7776895
<i>M. leidy</i>		—	0.8724452
<i>A. brasiliensis</i>			—
Correlation coefficients (r) in metabolism genes			
<i>F. echinata</i>	—	0.9468656	0.8935404
<i>M. leidy</i>		—	0.8878428
<i>A. brasiliensis</i>			—

Table 3.5: Metagenome properties indicating differences of the assembled *M. leidyi* stomodeum metagenomes based on IMG/ER pipeline annotation(Lin et al., 2009)

Attribute	GSU	GFL	GWI	GSP
IMG Genome ID	3300006492	3300005727	3300005729	3300005728
Number of bases	42,411,657	20,477,574	12,469,141	1,410,814
CRISPR Count	17	8	11	1
rRNA	85	10	250	14
tRNA genes	655	322	380	330
Protein coding genes	141651	65682	41759	4892
with Product Name	8609	3230	2492	328
with COG	7705	2687	2172	152
with Pfam	9363	3621	2794	273
with KO	10965	1710	2055	143
with Enzyme	5371	1246	1542	109
with MetaCyc	1891	365	376	23
with KEGG	6304	635	652	37
COG Clusters	2258	1040	1011	103
Pfam Clusters	2691	1223	1144	106

Table 3.6: Mann-Whitney test P value summary of metabolic genes abundance (KEGG Level 2) between organisms representing sister phyla (Cnidaria and Porifera representatives) based on MG-RAST pipeline

Organisms	<i>F. echinata</i>	<i>M. leidy</i>	<i>A. brasiliensis</i>
<i>F. echinata</i>	—	0.0013	0.0073
<i>M. leidy</i>		—	0.96985
<i>A. brasiliensis</i>			—

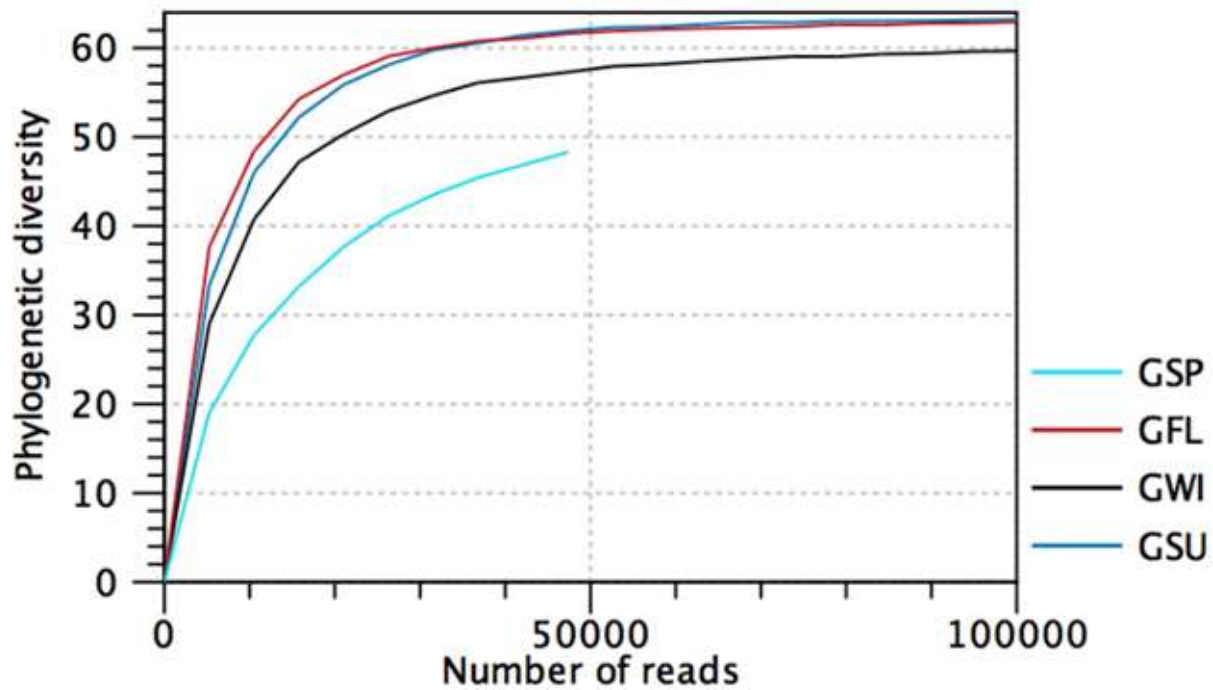
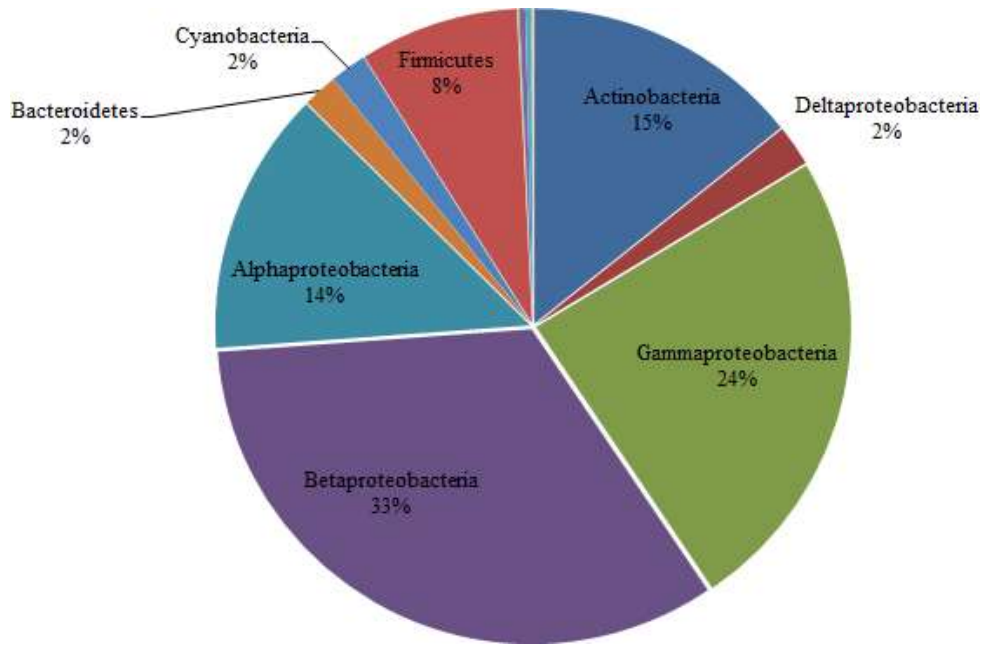
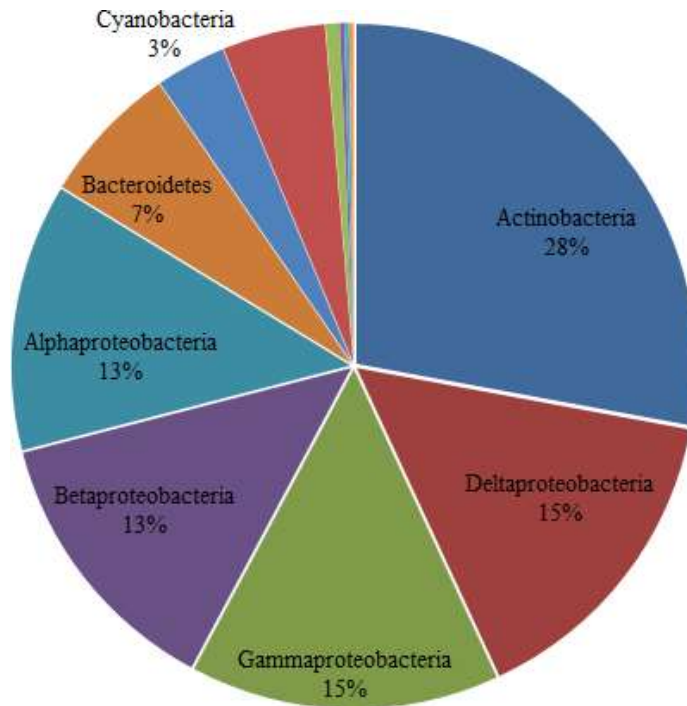


Figure 3.1: Rarefaction curve of phylogenetic diversity in the microbial assemblages in *M. leidy* stomodeum for GSU (Aug. 25th 2014), GFL (Oct. 10th 2013), GWI (Feb, 15th 2014) and GSP (May 8th 2014) metagenomes from Dauphin Island Marina, Mobile Bay. Analysis was performed using CLC Genomics Workbench 9.

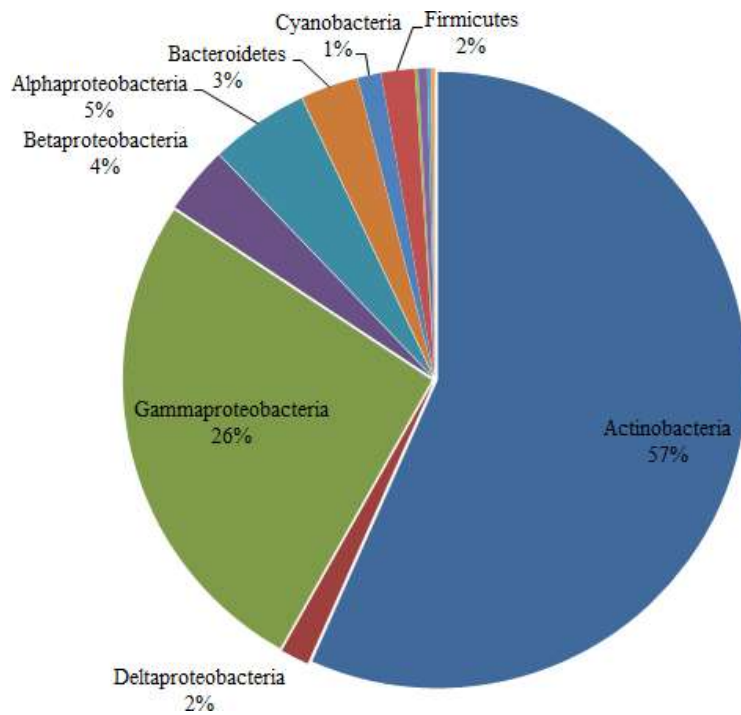
3.2a



3.2b



3.2c



3.2d

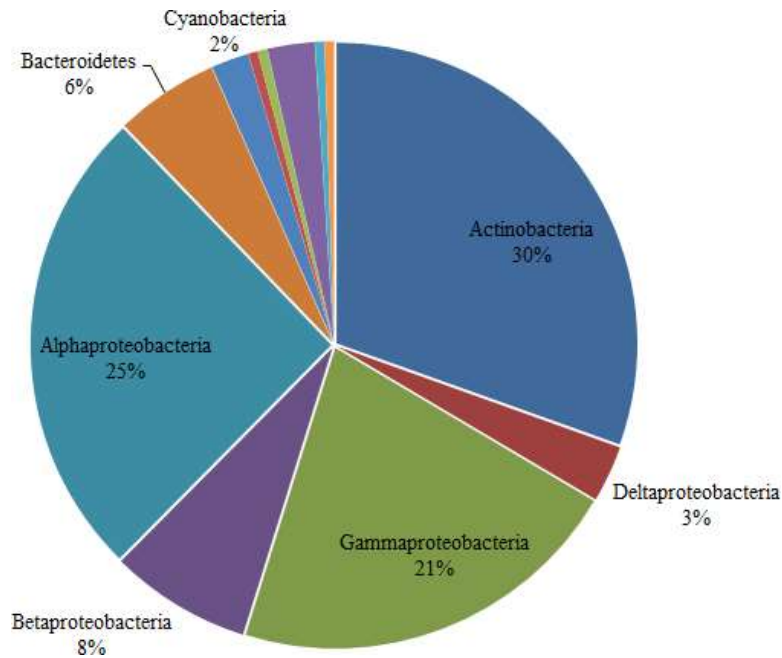
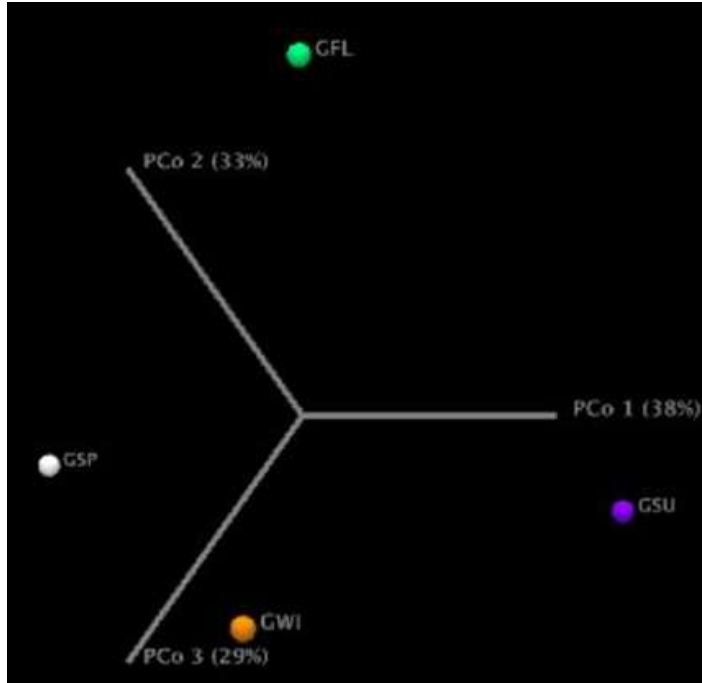


Figure 3.2: Pie charts showing proportion of KEGG organisms (Phylum level, for proteobacteria at class level) based on predicted protein sequences (FragGeneScan) constructed from the prokaryotic database on GhostKOALA annotation server for *M. leidy* host. **Key:** (a) Gut summer (GSU) (b) gut fall (GFL) (c) gut winter (GWI) (d) gut spring (GSP) metagenomes

3.3a



3.3b

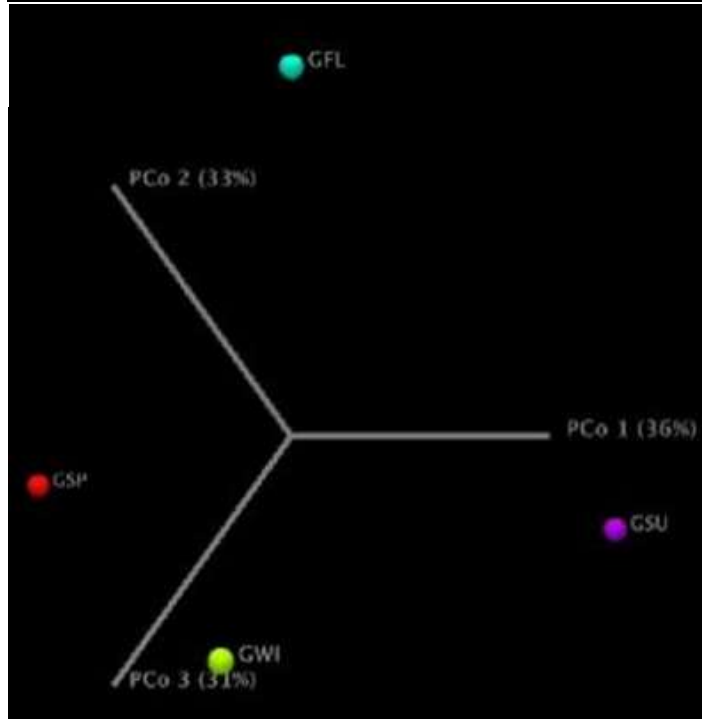


Figure 3.3: Inference of differences in the bacterial assemblages in *M. leidyi* stomodeum using principal coordinates analysis (PCoA) plot of samples based on (a) Bray-Curtis and (b) Jaccard matrices. Parentheses show variance explaining principal coordinates

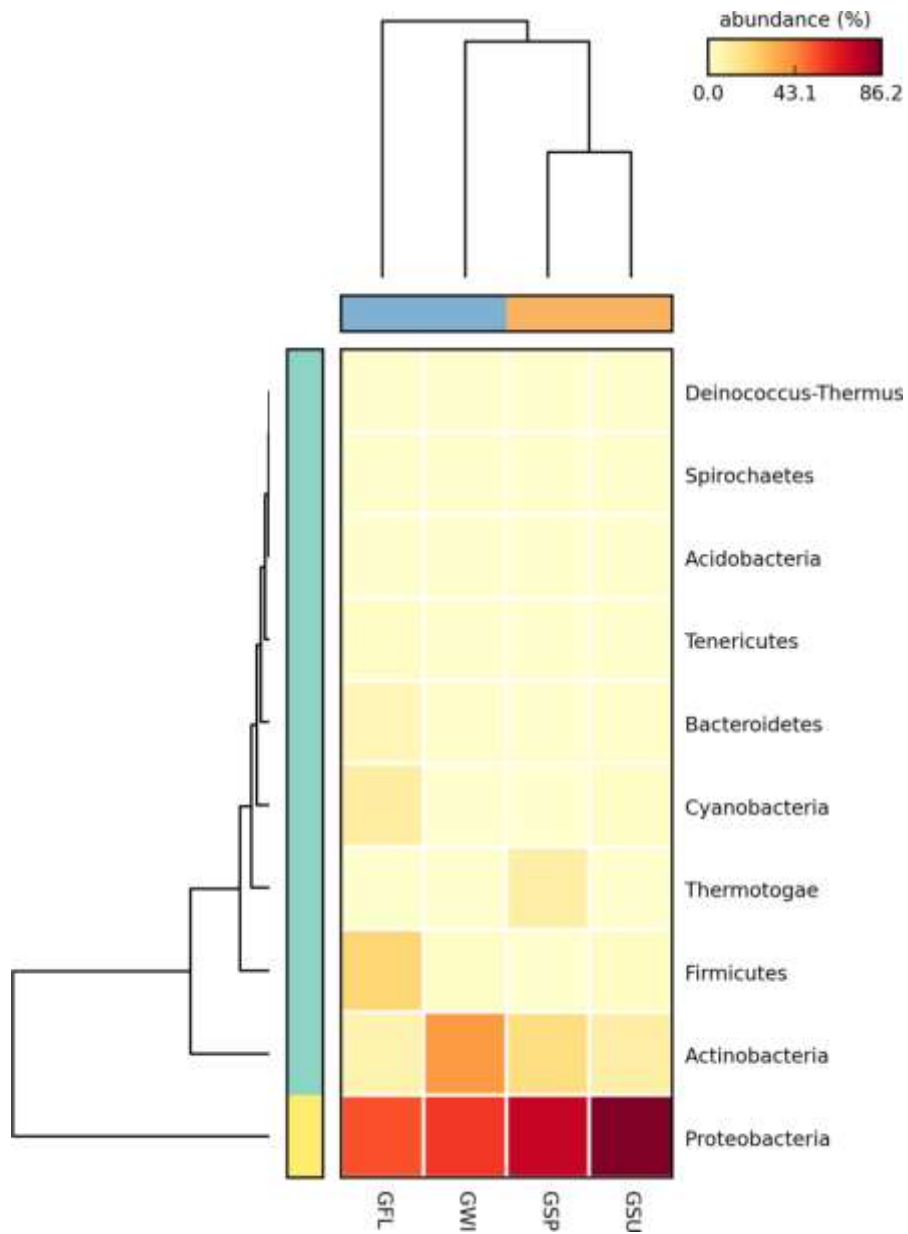


Figure 3.4: Heatmap revealing relative abundance of dominant phyla in *M. leidy* stomodeum, computed by MG-RAST generated using STAMP software. Rows correspond to bacterial taxa, and the columns represent the four seasonal *M. leidy* gut metagenomes used in this study. Dendrograms were created using hierarchical clustering.

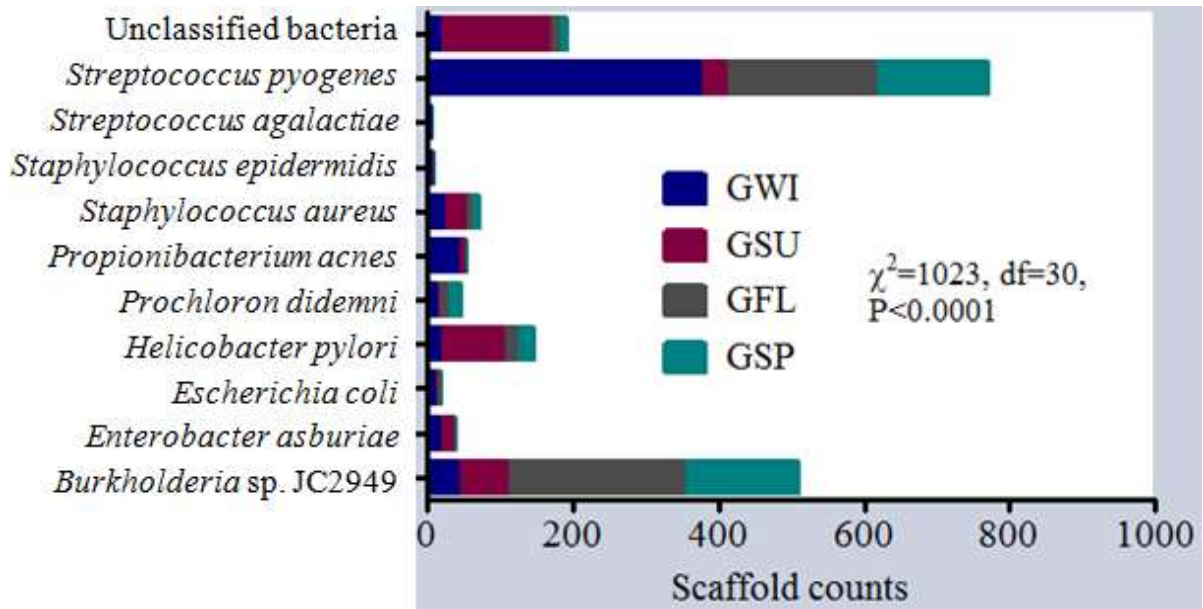


Figure 3.5: Stacked bar graph showing shared scaffolds for bacterial lineages in *M. leidy* stomodeum based on IMG/ER annotation. The χ^2 test revealed possible association (not random observation) of the 10 observed bacterial lineages in the stomodeum of *M. leidy*

Online support for figure 3.6 (a): <https://figshare.com/s/1f05095918a61c59ca99> (DOI 10.6084/m9.figshare.3846837)

Online support for figure 3.6 (b): <https://figshare.com/s/4052a27541112b69334a> (DOI 10.6084/m9.figshare.3846864)

Online support for figure 3.6 (c): <https://figshare.com/s/ae60b04314590cd320a7> (DOI 10.6084/m9.figshare.3846891)

Online support for figure 3.6 (d): <https://figshare.com/s/069a2150d809902bcfe7> (DOI 10.6084/m9.figshare.3846972)

Figure 3.6: MLTreeMap (Stark et al. 2010) analyses of contigs based on the 16S rRNA gene for maximum likelihood (ML) phylogeny using GEBA phylogeny (Wu et al. 2009), **(a)** GSU **(b)** GFL **(c)** GWI **(d)** GSP. The bubble indicates relative weight of placement. Figures above were too large and needed online support for visualization.

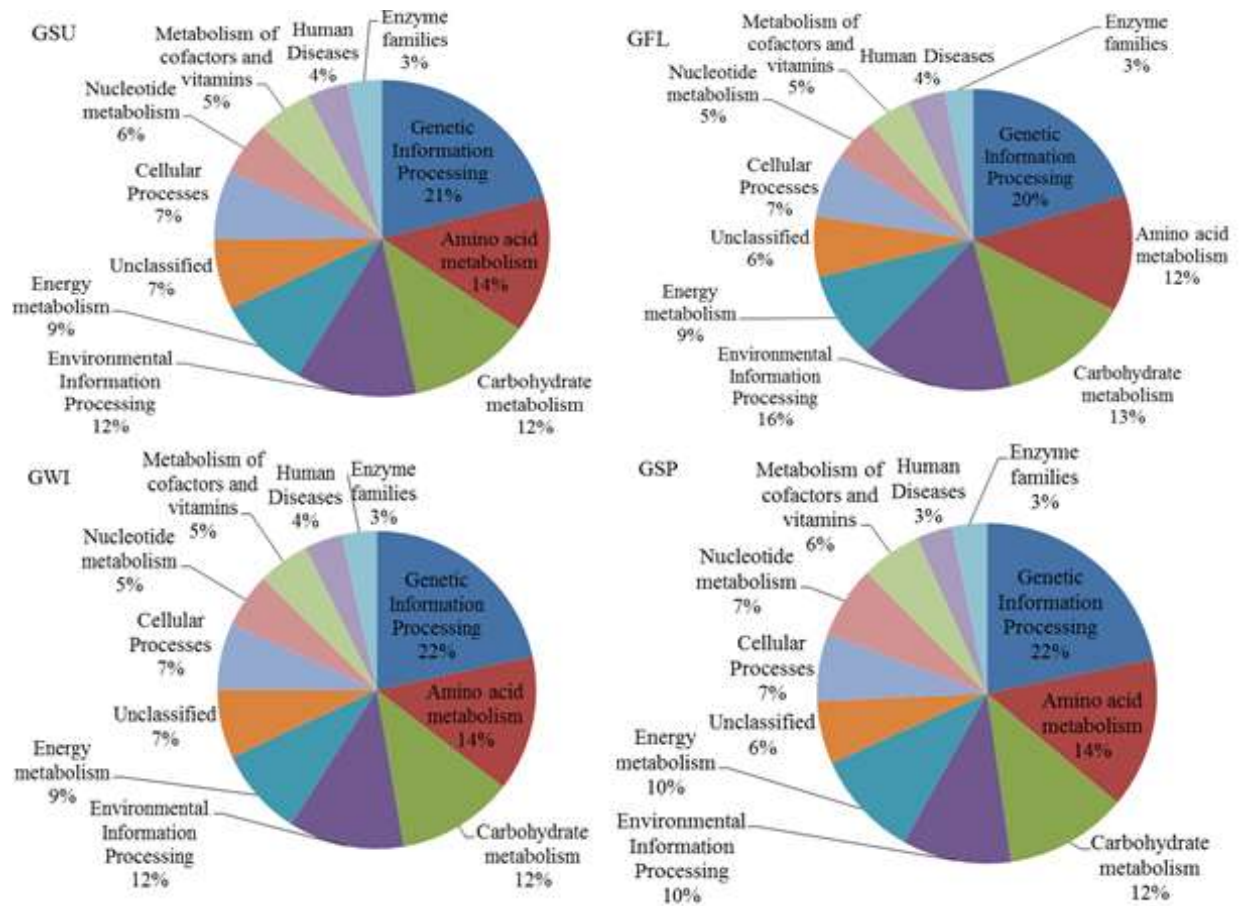


Figure 3.7: Pie charts indicating summary of GhostKOALA (<http://www.kegg.jp/blastkoala/>) annotated functional categories involved in central cellular metabolism in the stomodeum of *M. leidy*. Coding sequences were predicted using FragGeneScan prior to functional analysis.

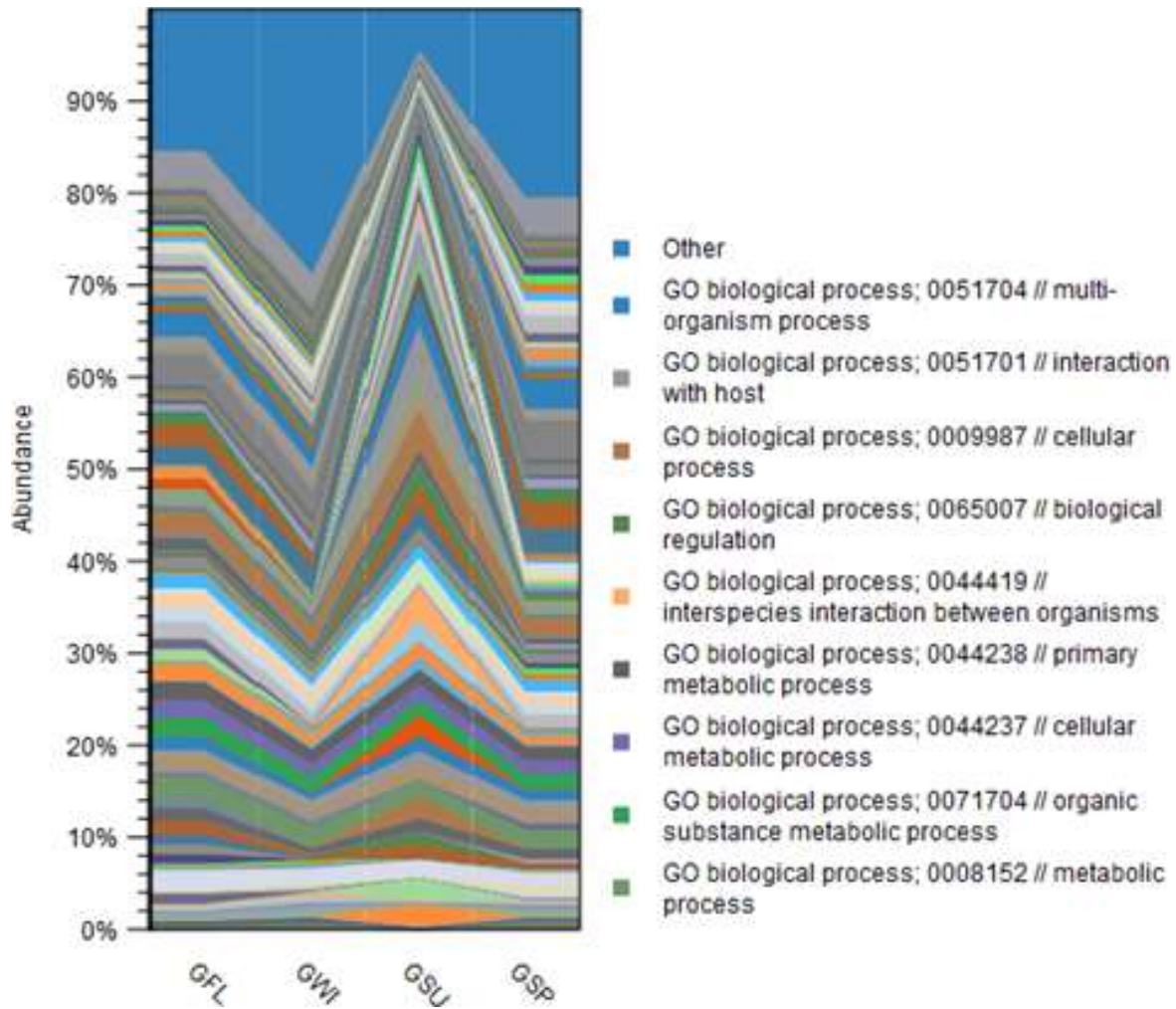


Figure 3.8: Area bar chart on ontology and category assignments for metagenomes for *M. leidy* bacterial assemblages using CLC Microbial Genomics Module. Abbreviations: gut fall (GFL), gut winter (GWI), gut summer (GSU) and gut spring (GSP) sampling dates

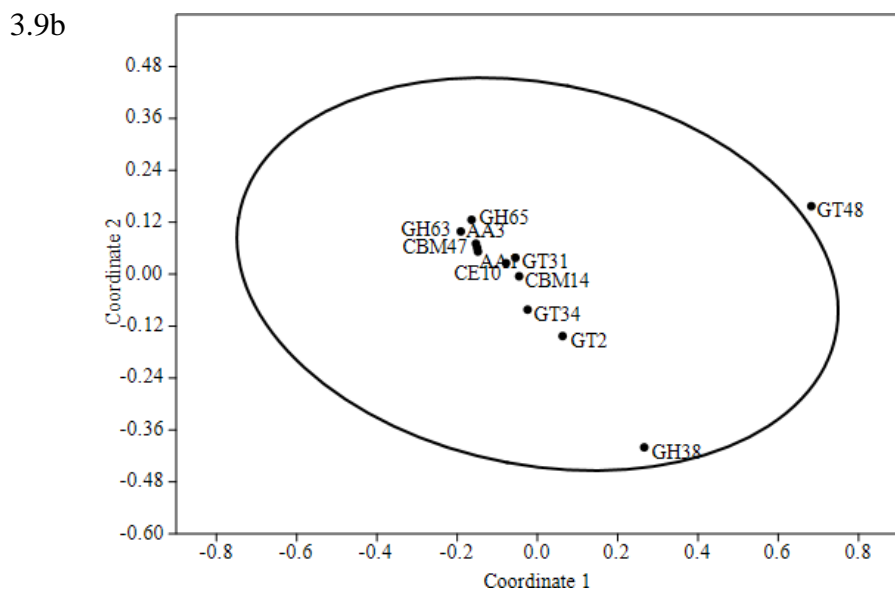
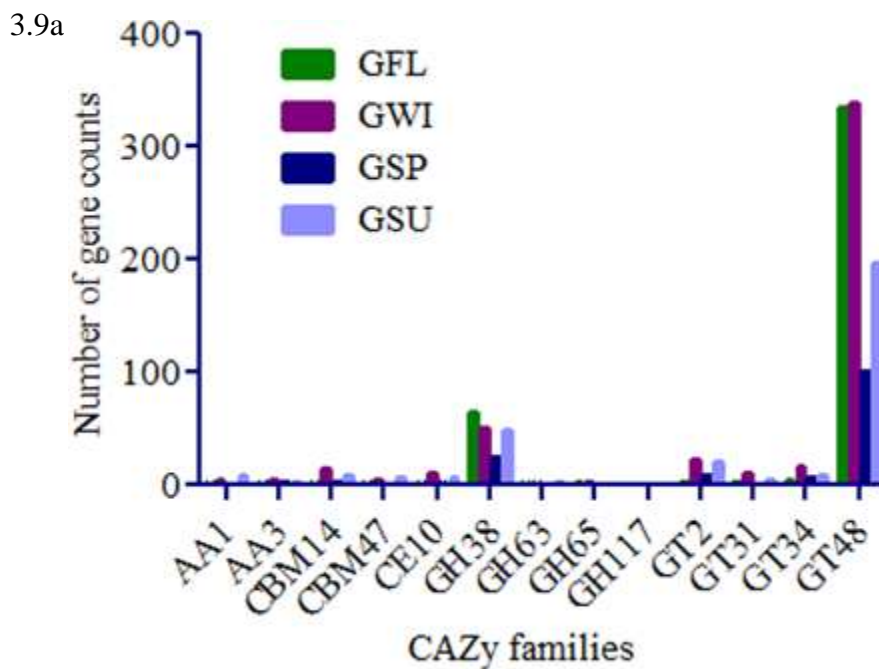


Figure 3.9: Plots representing CAZy families in the stomodeum of *M. leidy* (a) Bar graph of gene counts of different CAZy families (b) Over-representation of GT48 was identified using non-metric multidimensional scaling (NMDS). **Key:** AA (auxiliary activity), CBM (carbohydrate-binding module), CE (carbohydrate esterase) GH (glycosyl hydrolases), GT (glycosyl transferase)

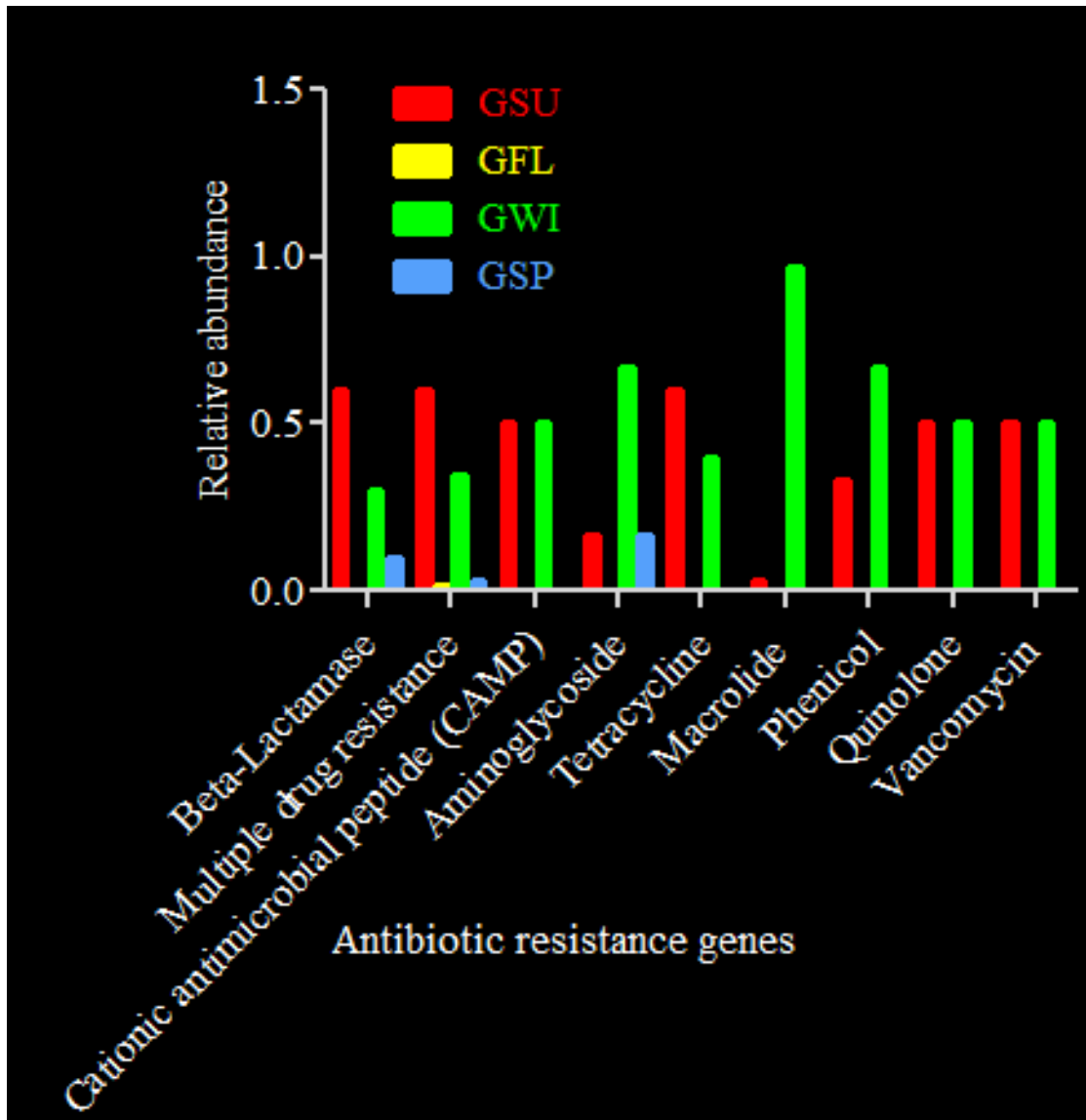


Figure 3.10: Bar graph showing relative abundance of antibiotic resistance genes in *M. leidy* stomodeum using KEGG annotation on GhostKOALA annotation tool (<http://www.kegg.jp/blastkoala/>)

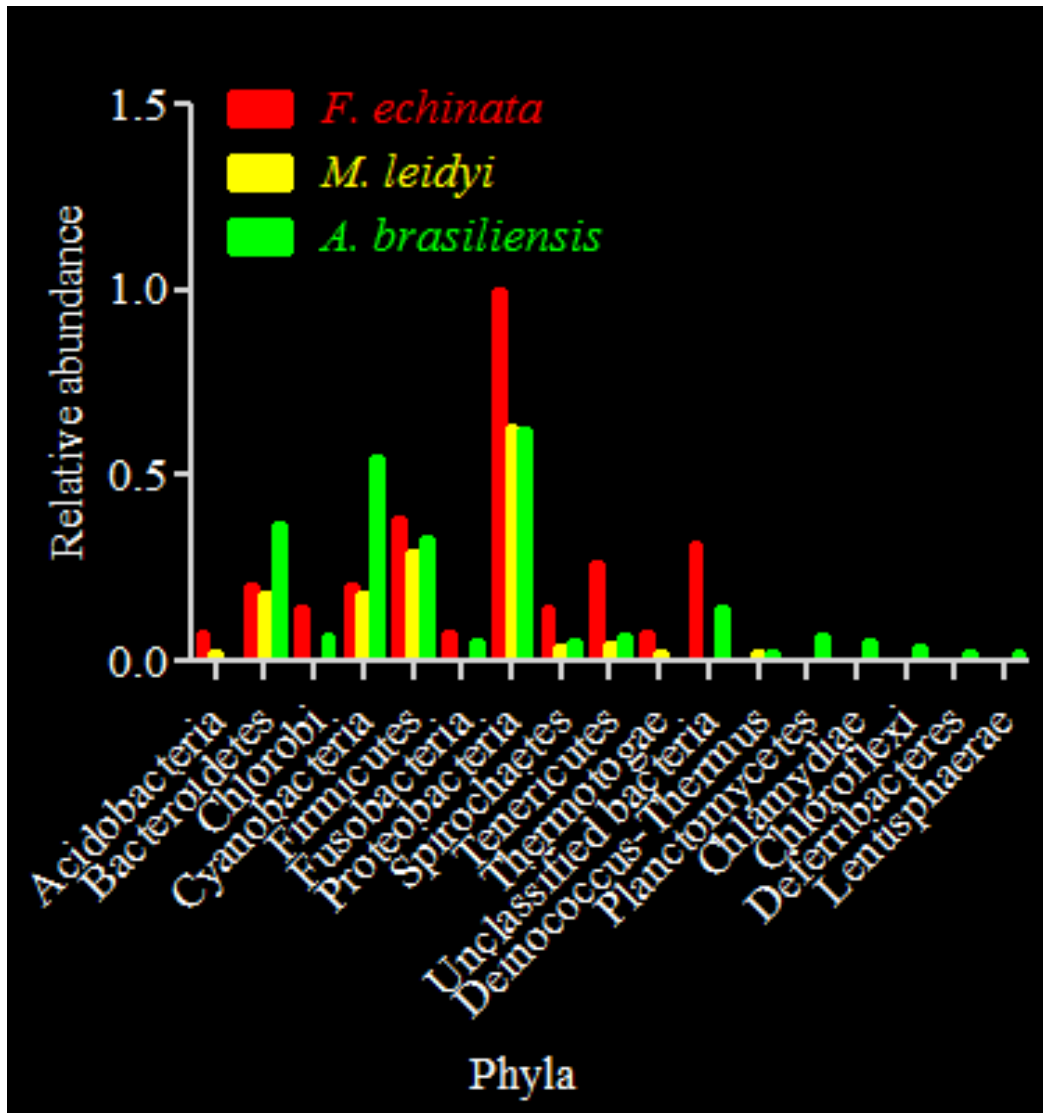
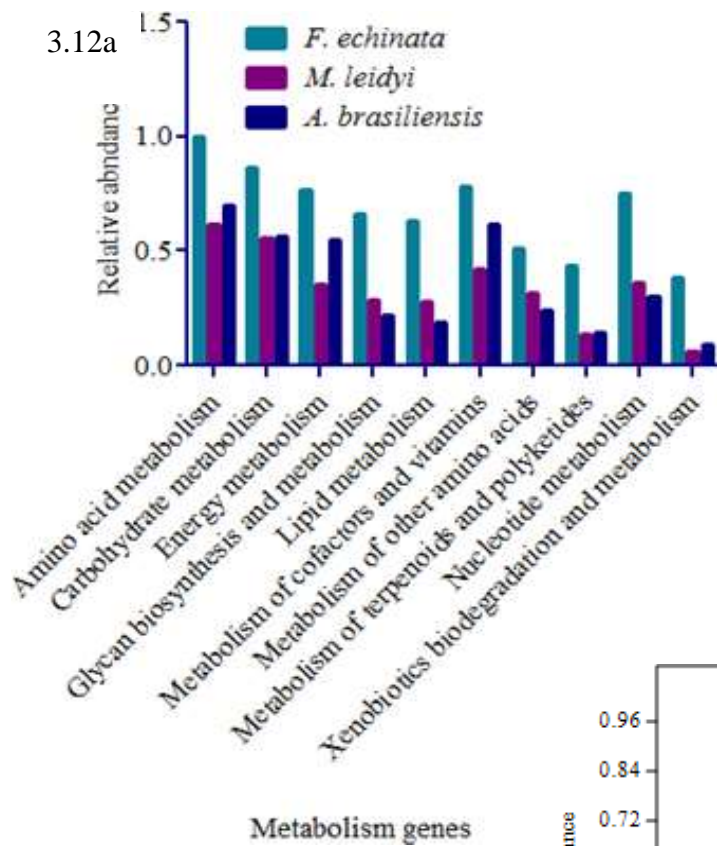


Figure 3.11: Bar graph showing relative abundance of shared bacterial assemblages in *M. leidy*, *F. echinata* and *A. brasiliensis* based on M5NR annotation using MG-RAST pipeline



3.12b

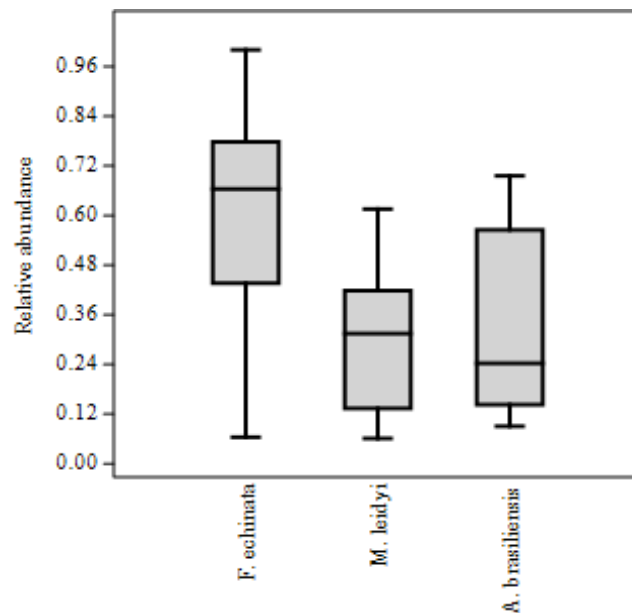


Figure 3.12a: Bar graph indicating the relative abundance of KEGG-level-2 metabolism categories for *M. leidy* and representative of sister phyla, Cnidaria (*Fungia echinata*) and Porifera (*Arenosclera brasiliensis*). **(b)** Box-plot of the KEGG-Level-2 indicating visual variation metabolism genes were generated using Past3

References

- Andreou, L., 2013. Preparation of genomic DNA from bacteria. *Methods Enzymol* 529, 143-151.
- Badhai, J., Ghosh, T.S., Das, S.K., 2016. Composition and Functional Characterization of Microbiome Associated with Mucus of the Coral *Fungia echinata* Collected from Andaman Sea. *Frontiers in microbiology* 7, 1-12.
- Barisic, I., Schoenthaler, S., Ke, R.Q., Nilsson, M., Noehammer, C., Wiesinger-Mayr, H., 2013. Multiplex detection of antibiotic resistance genes using padlock probes. *Diagnostic microbiology and infectious disease* 77, 118-125.
- Barker, G.M., 2002. Phylogenetic diversity: a quantitative framework for measurement of priority and achievement in biodiversity conservation. *Biological Journal of the Linnean Society* 76, 165-194.
- Beatson, S.A., Walker, M.J., 2014. Tracking antibiotic resistance. *Science* 345, 1454-1455.
- Beaulieu, W.T., Costello, J.H., Klein-Macphee, G., Sullivan, B.K., 2013. Seasonality of the ctenophore *Mnemiopsis leidyi* in Narragansett Bay, Rhode Island. *Journal of Plankton Research* 35, 785-791.
- Berglund, B., Khan, G.A., Lindberg, R., Fick, J., Lindgren, P.E., 2014. Abundance and Dynamics of Antibiotic Resistance Genes and Integrons in Lake Sediment Microcosms. *PloS one* 9, 1-8.
- Besemer, J., Lomsadze, A., Borodovsky, M., 2001. GeneMarkS: a self-training method for prediction of gene starts in microbial genomes. Implications for finding sequence motifs in regulatory regions. *Nucleic acids research* 29, 2607-2618.
- Boero, F., Bouillon, J., Gravili, C., Miglietta, M.P., Parsons, T., Piraino, S., 2008. Gelatinous plankton: irregularities rule the world (sometimes). *Marine Ecology Progress Series* 356, 299-310.
- Bokulich, N.A., Subramanian, S., Faith, J.J., Gevers, D., Gordon, J.I., Knight, R., Mills, D.A., Caporaso, J.G., 2013. Quality-filtering vastly improves diversity estimates from Illumina amplicon sequencing. *Nature methods* 10, 57-59.
- Borodovsky, M., Lomsadze, A., 2014. Gene identification in prokaryotic genomes, phages, metagenomes, and EST sequences with GeneMarkS suite. *Current protocols in microbiology* 32, Unit 1E 7. <http://www.currentprotocols.com/protocol/mc01e07>.

Breitbart, M., Benner, B.E., Jernigan, P.E., Rosario, K., Birsa, L.M., Harbeitner, R., Fulford, S., Graham, C., Walters, A., Goldsmith, D.B., Berger, S.A., Nejtgaard, J.C., 2015. Discovery, prevalence, and persistence of novel circular single-stranded DNA viruses in the ctenophores *Mnemiopsis leidyi* and *Beroe ovata*. *Frontiers in microbiology* 6, 1-10.

Bumann, D., Puls, G., 1996. Infestation with larvae of the sea anemone *Edwardsia lineata* affects nutrition and growth of the ctenophore *Mnemiopsis leidyi*. *Parasitology* 113, 123-128.

Consortium, T.G.O., 2015. Gene Ontology Consortium: going forward. *Nucleic acids research* 43, D1049-1056.

Daniels, C., Breitbart, M., 2012. Bacterial communities associated with the ctenophores *Mnemiopsis leidyi* and *Beroe ovata*. *FEMS microbiology ecology* 82, 90-101.

Daskalov, G.M., Mamedov, E.V., 2007. Integrated fisheries assessment and possible causes for the collapse of anchovy kilka in the Caspian Sea. *Ices Journal of Marine Science* 64, 503-511.

Donia, M.S., Fricke, W.F., Partensky, F., Cox, J., Elshahawi, S.I., White, J.R., Phillippy, A.M., Schatz, M.C., Piel, J., Haygood, M.G., Ravel, J., Schmidt, E.W., 2011. Complex microbiome underlying secondary and primary metabolism in the tunicate-*Prochloron* symbiosis. *Proceedings of the National Academy of Sciences of the United States of America* 108, E1423-1432.

Edgar, R.C., 2004. MUSCLE: multiple sequence alignment with high accuracy and high throughput. *Nucleic acids research* 32, 1792-1797.

Ellinger, D., Naumann, M., Falter, C., Zwikowics, C., Jamrow, T., Manisseri, C., Somerville, S.C., Voigt, C.A., 2013. Elevated early callose deposition results in complete penetration resistance to powdery mildew in *Arabidopsis*. *Plant Physiology* 161, 1433-1444.

Faith, D.P., 1992. Conservation evaluation and phylogenetic diversity. *Biological Conservation* 61, 1-10.

Finn, R.D., Bateman, A., Clements, J., Coggill, P., Eberhardt, R.Y., Eddy, S.R., Heger, A., Hetherington, K., Holm, L., Mistry, J., Sonnhammer, E.L.L., Tate, J., Punta, M., 2014. Pfam: the protein families database. *Nucleic acids research* 42, D222-D230.

Finn, R.D., Clements, J., Eddy, S.R., 2011. HMMER web server: interactive sequence similarity searching. *Nucleic acids research* 39, 30-37.

Finn, R.D., Coggill, P., Eberhardt, R.Y., Eddy, S.R., Mistry, J., Mitchell, A.L., Potter, S.C., Punta, M., Qureshi, M., Sangrador-Vegas, A., Salazar, G.A., Tate, J., Bateman, A., 2016. The

Pfam protein families database: towards a more sustainable future. *Nucleic acids research* 44, D279-285.

Finn, R.D., Mistry, J., Tate, J., Coggill, P., Heger, A., Pollington, J.E., Gavin, O.L., Gunasekaran, P., Ceric, G., Forslund, K., Holm, L., Sonnhammer, E.L., Eddy, S.R., Bateman, A., 2010. The Pfam protein families database. *Nucleic acids research* 38, D211-222.

Franzenburg, S., Fraune, S., Künzel, S., Baines, J.F., Domazet-Lošo, T., Bosch, T.C.G., 2012. MyD88-deficient *Hydra* reveal an ancient function of TLR signaling in sensing bacterial colonizers. *Proceedings of the National Academy of Sciences* 109, 19374-19379.

Franzenburg, S., Walter, J., Künzel, S., Wang, J., Baines, J.F., Bosch, T.C., Fraune, S., 2013. Distinct antimicrobial peptide expression determines host species-specific bacterial associations. *Proceedings of the National Academy of Sciences* 110, E3730-E3738.

Fraune, S., Anton-Erxleben, F., Augustin, R., Franzenburg, S., Knop, M., Schroder, K., Willoweit-Ohl, D., Bosch, T.C.G., 2015. Bacteria-bacteria interactions within the microbiota of the ancestral metazoan *Hydra* contribute to fungal resistance. *The ISME journal* 9, 1543-1556.

Gambill, M., Møller, L.F., Peck, M.A., 2015. Effects of temperature on the feeding and growth of the larvae of the invasive ctenophore *Mnemiopsis leidyi*. *Journal of Plankton Research* 37, 1001-1005.

Ghabooli, S., Shiganova, T.A., Briski, E., Piraino, S., Fuentes, V., Thibault-Botha, D., Angel, D.L., Cristescu, M.E., Macisaac, H.J., 2013. Invasion pathway of the Ctenophore *Mnemiopsis leidyi* in the Mediterranean Sea. *PloS one* 8, 1-9.

Glass, E.M., Wilkening, J., Wilke, A., Antonopoulos, D., Meyer, F., 2010. Using the metagenomics RAST server (MG-RAST) for analyzing shotgun metagenomes. *Cold Spring Harbor protocols* 2010, 53-68.

Hammann, S., Moss, A., Zimmer, M., 2015. Sterile Surfaces of *Mnemiopsis leidyi* (Ctenophora) in Bacterial Suspension-A Key to Invasion Success? *Open Journal of Marine Science* 5, 237-246.

Hammer, Ø., Harper, D., Ryan, P., 2001. Paleontological Statistics Software: Package for Education and Data Analysis. *Palaeontologia Electronica* 4, 1-9.

Hansson, H.G., 2006. Ctenophores of the Baltic and adjacent Seas-the invader *Mnemiopsis* is here! *Aquatic Invasions* 1, 295-298

Hao, W., Gerdts, G., Peplies, J., Wichels, A., 2015. Bacterial communities associated with four ctenophore genera from the German Bight (North Sea). *FEMS microbiology ecology* 91, 1-11.

- Haraldsson, M., Bamstedt, U., Tiselius, P., Titelman, J., Aksnes, D.L., 2014. Evidence of Diel Vertical Migration in *Mnemiopsis leidyi*. *PloS one* 9, 1-10.
- Harbison, G., Madin, L., 1982. Ctenophora. Synopsis and classification of living organisms (SP Parker, ed.) 1, 707-715.
- Hay, S., 2006. Marine ecology: Gelatinous bells may ring change in marine ecosystems. *Current Biology* 16, R679-R682.
- Jaspers, C., Haraldsson, M., Bolte, S., Reusch, T.B.H., Thygesen, U.H., Kiorboe, T., 2012. Ctenophore population recruits entirely through larval reproduction in the central Baltic Sea. *Biology letters* 8, 809-812.
- Kanehisa, M., Goto, S., 2000. KEGG: Kyoto encyclopedia of genes and genomes. *Nucleic acids research* 28, 27-30.
- Kanehisa, M., Sato, Y., Morishima, K., 2016. BlastKOALA and GhostKOALA: KEGG Tools for Functional Characterization of Genome and Metagenome Sequences. *Journal of Molecular Biology* 428, 726-731.
- Kideys, A.E., 2002. Ecology. Fall and rise of the Black Sea ecosystem. *Science* 297, 1482-1484.
- Kim, K.U., Park, S.K., Kang, S.A., Park, M.K., Cho, M.K., Jung, H.J., Kim, K.Y., Yu, H.S., 2013. Comparison of functional gene annotation of *Toxascaris leonina* and *Toxocara canis* using CLC genomics workbench. *Korean J Parasitol* 51, 525-530.
- Lee, W.J., Hase, K., 2014. Gut microbiota-generated metabolites in animal health and disease. *Nat Chem Biol* 10, 416-424.
- Lehtiniemi, M., Lehmann, A., Javidpour, J., Myrberg, K., 2012. Spreading and physico-biological reproduction limitations of the invasive American comb jelly *Mnemiopsis leidyi* in the Baltic Sea. *Biological Invasions* 14, 341-354.
- Lin, C., Markowitz, L.V.M., Mavromatis, K., Ivanova, N.N., Chen, I.M., Chu, K., Kyripides, N.C., 2009. IMG ER: a system for microbial genome annotation expert review and curation. *Bioinformatics* 25, 2271-2278.
- Lin, Z., Torres, J.P., Tianero, M.D., Kwan, J.C., Schmidt, E.W., 2016. Origin of Chemical Diversity in *Prochloron*-Tunicate Symbiosis. *Applied and environmental microbiology* 82, 3450-3460.
- Lowe, T.M., Eddy, S.R., 1997. tRNAscan-SE: A Program for Improved Detection of Transfer RNA Genes in Genomic Sequence. *Nucleic acids research* 25, 0955-0964.

- Lucic, D., Pestoric, B., Malej, A., Lopez-Lopez, L., Drakulovic, D., Onofri, V., Miloslavac, M., Gangai, B., Onofri, I., Benovic, A., 2012. Mass occurrence of the ctenophore *Bolinopsis vitrea* (L. Agassiz, 1860) in the nearshore southern Adriatic Sea (Kotor Bay, Montenegro). *Environmental monitoring and assessment* 184, 4777-4785.
- Malham, S.K., Rajko-Nenow, P., Howlett, E., Tuson, K.E., Perkins, T.L., Pallett, D.W., Wang, H., Jago, C.F., Jones, D.L., McDonald, J.E., 2014. The interaction of human microbial pathogens, particulate material and nutrients in estuarine environments and their impacts on recreational and shellfish waters. *Environ Sci Process Impacts* 16, 2145-2155.
- Mandal, R.S., Saha, S., Das, S., 2015. Metagenomic Surveys of Gut Microbiota. *Genomics, Proteomics & Bioinformatics* 13, 148-158.
- Markowitz, V.M., Chen, I.M., Palaniappan, K., Chu, K., Szeto, E., Pillay, M., Ratner, A., Huang, J., Woyke, T., Huntemann, M., Anderson, I., Billis, K., Varghese, N., Mavromatis, K., Pati, A., Ivanova, N.N., Kyrpides, N.C., 2014. IMG 4 version of the integrated microbial genomes comparative analysis system. *Nucleic acids research* 42, D560-567.
- McCoy, C.O., Matsen, F.A.t., 2013. Abundance-weighted phylogenetic diversity measures distinguish microbial community states and are robust to sampling depth. *PeerJ* 1, 1-17.
- McDonald, D., Price, M.N., Goodrich, J., Nawrocki, E.P., DeSantis, T.Z., Probst, A., Andersen, G.L., Knight, R., Hugenholtz, P., 2012. An improved Greengenes taxonomy with explicit ranks for ecological and evolutionary analyses of bacteria and archaea. *The ISME journal* 6, 610-618.
- Moss, A.G., Smith, K., Donovan, E.W., Adams, L.E., 2008. Microbes associated with the coastal ctenophore *Mnemiopsis leidyi*. Orlando: Fla. ASLO Meeting.
<http://www.sgmeet.com/aslo/orlando2008/viewabstract2.asp?AbstractID=1491>.
- Pang, K., Martindale, M.Q., Ctenophores. *Current Biology* 18, R1119-R1120.
- Parks, D.H., Tyson, G.W., Hugenholtz, P., Beiko, R.G., 2014. STAMP: statistical analysis of taxonomic and functional profiles. *Bioinformatics* 30, 3123-3124.
- Podar, M., Haddock, S.H., Sogin, M.L., Harbison, G.R., 2001. A molecular phylogenetic framework for the phylum Ctenophora using 18S rRNA genes. *Molecular phylogenetics and evolution* 21, 218-230.
- Purcell, J., Arai, M., 2001. Interactions of pelagic cnidarians and ctenophores with fish: a review. *Hydrobiologia* 451, 27-44.
- Reitzel, A.M., Sullivan, J.C., Brown, B.K., Chin, D.W., Cira, E.K., Edquist, S.K., Genco, B.M., Joseph, O.C., Kaufman, C.A., Kovitvongsa, K., Munoz, M.M., Negri, T.L., Taffel, J.R., Zuehlke,

- R.T., Finnerty, J.R., 2007. Ecological and developmental dynamics of a host-parasite system involving a sea anemone and two ctenophores. *J Parasitol* 93, 1392-1402.
- Reusch, T.B., Bolte, S., Sparwel, M., Moss, A.G., Javidpour, J., 2010. Microsatellites reveal origin and genetic diversity of Eurasian invasions by one of the world's most notorious marine invader, *Mnemiopsis leidyi* (Ctenophora). *Mol Ecol* 19, 2690-2699.
- Rho, M., Tang, H., Ye, Y., 2010. FragGeneScan: predicting genes in short and error-prone reads. *Nucleic acids research* 38, e191-e191.
- Salem, H., Kreutzer, E., Sudakaran, S., Kaltenpoth, M., 2013. Actinobacteria as essential symbionts in firebugs and cotton stainers (Hemiptera, Pyrrhocoridae). *Environmental microbiology* 15, 1956-1968.
- Santos, S.S., Pardal, S., Proenca, D.N., Lopes, R.J., Ramos, J.A., Mendes, L., Morais, P.V., 2012. Diversity of cloacal microbial community in migratory shorebirds that use the Tagus estuary as stopover habitat and their potential to harbor and disperse pathogenic microorganisms. *FEMS microbiology ecology* 82, 63-74.
- Shiganova, T.A., Musaeva, E.I., Bulgakova Iu, V., Mirzoian, Z.A., MartynIuk, M.L., 2003. New settlers comb jellies *Mnemiopsis leidyi* (A. Agassiz) and *Beroe ovata* Mayer 1912 and their influence on the pelagic ecosystem of the northeastern part of the Black Sea. *Izv Akad Nauk Ser Biol* 2, 225-235.
- Stamatakis, A., 2014. RAxML version 8: a tool for phylogenetic analysis and post-analysis of large phylogenies. *Bioinformatics* 30, 1312-1313.
- Stark, M., Berger, S.A., Stamatakis, A., von Mering, C., 2010. MLTreeMap - accurate Maximum Likelihood placement of environmental DNA sequences into taxonomic and functional reference phylogenies. *BMC genomics* 11, 461-461.
- Stilling, R.M., Bordenstein, S.R., Dinan, T.G., Cryan, J.F., 2014. Friends with social benefits: host-microbe interactions as a driver of brain evolution and development? *Frontiers in cellular and infection microbiology* 4, 1-17.
- Storey, J.D., Tibshirani, R., 2003. Statistical significance for genomewide studies. *Proceedings of the National Academy of Sciences of the United States of America* 100, 9440-9445.
- Tamm, S.L., 2014. Cilia and the life of ctenophores. *Invertebrate Biology* 133, 1-46.
- Tamam, F., Mercier, F., Le Bot, B., Eurin, J., Tuc Dinh, Q., Clement, M., Chevreuil, M., 2008. Occurrence and fate of antibiotics in the Seine River in various hydrological conditions. *The Science of the total environment* 393, 84-95.

Tims, S., Derom, C., Jonkers, D.M., Vlietinck, R., Saris, W.H., Kleerebezem, M., de Vos, W.M., Zoetendal, E.G., 2013. Microbiota conservation and BMI signatures in adult monozygotic twins. *Isme Journal* 7, 707-717.

Trindade-Silva, A.E., Rua, C., Silva, G.G., Dutilh, B.E., Moreira, A.P., Edwards, R.A., Hajdu, E., Lobo-Hajdu, G., Vasconcelos, A.T., Berlinck, R.G., Thompson, F.L., 2012. Taxonomic and functional microbial signatures of the endemic marine sponge *Arenosclera brasiliensis*. *PloS one* 7, 1-10.

Verma, S., Gazara, R.K., Nizam, S., Parween, S., Chattopadhyay, D., Verma, P.K., 2016. Draft genome sequencing and secretome analysis of fungal phytopathogen *Ascochyta rabiei* provides insight into the necrotrophic effector repertoire. *Scientific reports* 6, 1-14.

Voigt, C.A., 2014. Callose-mediated resistance to pathogenic intruders in plant defense-related papillae. *Frontiers in Plant Science* 5, 1-6.

Wilke, A., Harrison, T., Wilkening, J., Field, D., Glass, E.M., Kyrpides, N., Mavrommatis, K., Meyer, F., 2012. The M5nr: a novel non-redundant database containing protein sequences and annotations from multiple sources and associated tools. *Bmc Bioinformatics* 13, 1-5.

Wu, D., Hugenholtz, P., Mavromatis, K., Pukall, R., Dalin, E., Ivanova, N.N., Kunin, V., Goodwin, L., Wu, M., Tindall, B.J., 2009. A phylogeny-driven genomic encyclopaedia of Bacteria and Archaea. *Nature* 462, 1056-1060.

Wu, T., Zhang, Z., Liu, B., Hou, D., Liang, Y., Zhang, J., Shi, P., 2013. Gut microbiota dysbiosis and bacterial community assembly associated with cholesterol gallstones in large-scale study. *BMC genomics* 14, 1-11.

Zhu, W., Lomsadze, A., Borodovsky, M., 2010. *Ab initio* gene identification in metagenomic sequences. *Nucleic acids research* 38, 1-15.

Chapter 4: Isolation and characterization of coagulase-negative, vancomycin, novobiocin and oxacillin susceptible *Staphylococcus mnemiopsis* sp. nov., isolated from the *Mnemiopsis leidy* stomodeum

Abstract

A novel coagulase-negative, vancomycin and oxacillin-susceptible novel isolate of the genus *Staphylococcus*, *Staphylococcus mnemiopsis* sp. nov., was isolated from the stomodeum of *Mnemiopsis leidy* from Mobile Bay, Alabama USA. A polyphasic taxonomic approach comprised of phenotypic, chemotaxonomic and genotypic characteristics was used for analysis. The dominant respiratory quinone detected was MK-7 (100%). Major cellular fatty acids were anteiso-C_{15:0} (40.52%), anteiso-C_{17:0} (13.04 %), C_{-18:0} (11.53%) and C_{-20:0} (10.45%). The polar lipid profile consisted of glycolipid, phospholipid, phosphatidylglycerol and diphosphatidylglycerol. Although *S. mnemiopsis* AOAB had a 16S rRNA gene sequence identity of 99% with *S. warneri* SG1, *S. pasteurii*, *S. devriesei* KS-SP_60, *S. lugdunensis* HKU09-01, *S. epidermidis* RP62A, *S. haemolyticus* JCSC1435 and *S. hominis* DM 122, it could be distinguished from those species based on Multi-Locus Sequence Analysis (MLSA) using 5 marker genes (*hsp60*, *rpoB*, *dnaJ*, *sodA* and *tuf*). MLSA revealed strain AOAB to be closely related to *S. warneri* SG1 and *S. pasteurii* SP1 but distinct from two previously known species. An average nucleotide identity (ANI) analysis indicated that *S. mnemiopsis* has the closest ANI of 84.93% and 84.58% identity to *S. warneri* SG1 and *S. pasteurii* SP1, respectively; similarly, an *in-silico* DNA-DNA hybridization analysis for *S. mnemiopsis* indicated 33.1 % and 32.8% against *S. warneri* SG1 and *S. pasteurii* SP1, respectively. Based on these phenotypic, genotypic and phylogenetic data, we propose to classify the species as *Staphylococcus mnemiopsis* sp. nov., with AOAB as the type strain (= DSM^T102048 =NRRL B-65367^T).

Introduction

Mnemiopsis leidyi (Phylum Ctenophora) is a predatory gelatinous zooplankter endemic to the Western Atlantic that has invaded all of the European enclosed and coastal seas, including the North, Baltic, the Black, Caspian Southern Adriatic, and Mediterranean Seas. *M. leidyi* is also noted for its ability to alter the composition of native plankton communities (Delpy et al., 2012; Jaspers et al., 2012; Lucic et al., 2012). *Mnemiopsis* blooms have been found to coincide with profound environmental perturbation (Purcell, 2012). Much like other zoonotic organisms in exotic habitats (DeLong, 2014), *Mnemiopsis* has been revealed to be a vector of microbial assemblages (Daniels & Breitbart, 2012; Hao, Gerdts, Peplies, & Wichels, 2015; Moss, Estes, Muellner, & Morgan, 2001). Although ctenophores are known to be parasitized by amoebae, dinoflagellates, sea anemones and bacteria (Daniels and Breitbart, 2012; Hammann et al., 2015; Hao et al., 2015; Moss et al., 2001), there is no study that has isolated individual ctenophore gut bacteria for characterization.

This study used phenotypic, genotypic and phylogenetic analysis to characterize a cultured isolate from the *M. leidyi* gut that is proposed as *S. mnemiopsis* AOAB. Previous studies have isolated novel staphylococci species from marine water (Gunn and Colwell, 1983), fresh water, marine crustaceans (Faghri et al., 1984), domesticated animals (Yamashita et al., 2005) and human hosts (Trulzsch et al., 2007), among other sources.

Methods

Sample collection

Ctenophore gut samples were collected from animals obtained from the Dauphin Island Marina, Mobile Bay, Alabama (30 15'47.3"N 88 06'48.5"W), between February 15th 2014, May 8th 2014,

August 25th 2014, and October 10th 2013. Sterile toothpicks were inserted into the gut from the oral end and gently rotated, in order to collect a mucus-rich sample without damage to the stomodeal lining. Tips containing the mucoid gut samples were transferred into 1.5 mL tubes, stored on ice and transported to the laboratory for enrichment. Details of sample collection methods and the study site are presented in Chapter 3.

Enrichment and isolation

The enrichment medium that was used was based on Anacker and Ordal with modifications as previously described (Anacker and Ordal, 1955; Figueiredo et al., 2005; Pilarski et al., 2008). Specifically, an infusion of ctenophore *Mnemiopsis* peptone was prepared using pieces of ctenophore (15 g of dry frozen weight) in 1L of distilled water. Ctenophore tissues were ground (pestle and mortar) and boiled for five minutes. The liquid was allowed to settle for thirty minutes at room temperature (25 °C) and filtered with 0.2 µm filters (Whatman® membrane filters nylon). The infusion was added to broth and solid mannitol growth media after autoclaving at 120°C for 15 minutes.

The enrichment broth was composed of select peptone (Life technologies, Cat. No. 30392-021) 3 gL⁻¹, yeast extract (Sigma, No. Y-4000), 5 gL⁻¹, sodium acetate (Fisher Scientific), 0.02 gL⁻¹, sodium chloride (Fisher Scientific), 0.02 gL⁻¹, ctenophore *M. leidyi* peptone, 100 mL⁻¹ and mannitol salt agar (BD and Sparks co., MD 21152 Ref. 211407-500 g,) 27.75 gL⁻¹. Regular growth and isolation of *Staphylococcus* species was conducted using mannitol salt agar (BD and Sparks co., MD 21152 Ref. 211407-500 g,) and LB agar (Sigma Aldrich). After an initial stage of enrichment, cultures were isolated and maintained using mannitol salt agar (Thavasi et al., 2007) and LB agar (Sigma Aldrich).

Phenotype characterization

Phenotypic tests were carried out following minimum recommended standards to aid in discriminating species (Freney et al., 1999). *S. mnemiopsis* AOAB was tested for its ability to digest carbohydrates using minimal media containing 1% of only one carbon source and basal salts (Table S4.1 in appendix) in twenty-four well microplates. D-glucose was used as control and basal agar and water without carbon source used as negative controls. The microplates were incubated at 30°C for up to 2 weeks to observe growth. Results were compared against published data for the closest related species (Chesneau et al., 1993; Kloos and Schleifer, 1975).

Chemotaxonomy

Chemotaxonomic analyses were also carried out to characterize phenotypes. To assign genus and confirm coagulase test of the isolate, the occurrence of fatty acids ai-C15:0, i-C15:0, i-C17:0, ai-C17:0 and menaquinone (MK) in the cytoplasmic membrane was investigated as recommended (Freney et al., 1999; Heß and Gallert, 2015; Tindall et al., 2010). The analysis for respiratory quinones was carried out by first separating them from other classes using thin layer chromatography on silica gel (Macherey-Nagel Art. No. 805 023), using hexane: tert-butylmethylether (9:1 v/v) as solvent. Menaquinones were then removed from the plate and analyzed using HPLC fitted with a reverse phase column (Macherey-Nagel, 2 mm x 125 mm, 3 µm, RP18) with methanol: heptane 9:1 (v/v) being used as the eluant. Polar lipids were extracted from 100 mg of freeze dried bacterial cells using chloroform: methanol: 0.3% aqueous NaCl mixture 1:2:0.8 (v/v/v), separated using two-dimensional silica gel TLC (Macherey-Nagel Art. No. 818 135) and detected using methods described by Tindall et al. (Tindall et al., 2007) (DSMZ Identification Services, Braunschweig, Germany). Cellular fatty acid composition for *S.*

mnemiopsis AOAB was determined using gas chromatography (chromatograph was fitted with a 5% phenyl-methyl silicone capillary column) using the Sherlock MIS (MIDI Inc, Newark, USA) system. Using the MIDI software package (MIDI Inc, Newark, USA), the fatty acid composition data was also used for clustering using the Euclidean method for differentiation of the species from the closest species.

Antimicrobial susceptibility

Antimicrobial susceptibility was performed using a standard disk diffusion method, following cutoff ranges as outlined by the National Committee for Clinical Laboratory Standards (NCCLS) (Miller et al., 2003). Isolates were inoculated using spread plating, with 100 μ L of inoculum at log phase from LB broth onto LB agar before impregnating with antibiotic discs. Zones of inhibition (ZOI) (in mm) were used to determine the ability of the antibiotics to inhibit the growth. The antibiotics used are shown in Table 4.1. Results were interpreted using commonly accepted zone breakpoints for *Staphylococcus* (Howe and Andrews, 2012). Control discs were sterile 6mm discs without antibiotics (sterile Whatman filter papers).

DNA extraction and touchdown PCR

Genomic DNA was isolated using the CTAB protocol (Andreou, 2013) with minor modifications that included the use of 0.5 mm silica beads (Biospec Products, Inc. Cat. No. 110791052z), shaken using a specialized MO BIO Vortex-Genie^R 2 (MO BIO Laboratories). DNA purity was checked using a NanoDrop reader (ND-2000, NanoDrop Technologies, Wilmington, DE, USA) and precision-quantified using Qubit HS reagents (Life Technologies). The DNA template concentration was adjusted to 5 ng prior for use in touchdown PCR reactions.

Amplification for most of the 16S rRNA gene was achieved using the universal primers 63f (5'-CAG GCC TAA CAC ATG CAA GTC-3') and 1387r (5'-GGG CGG WGT GTA CAA GGC-3') as described by Suriyachadkun *et al.* (Suriyachadkun et al., 2009).

Contents of a 25 μ L PCR mixture included 12.5 μ L of EconoTaq Plus Green 2X Master Mix (Lucigen), 0.5 μ L of 20 μ M of forward and reverse primers, 10.5 μ L water and 1 μ L of 5 ng μ L⁻¹ genomic template DNA. PCR was carried out using 'touchdown' conditions: initial denaturation was at 95 °C for 5 min, followed by 20 cycles at 95 °C for 1min 61°C for 45 sec, and extension at 72 °C for 90 sec. The touchdown method was followed by another 30 cycles at 95 °C (1min) 51 °C (45 sec) 72 °C (90 sec). The final extension was done for 7 min at 72 °C.

The study also targeted a 370 bp *tuf* gene that is well established for *Staphylococcus* taxonomy (Martineau et al., 2001). Primer selection and melting temperature determination was done using an *in silico* PCR simulator (<http://insilico.ehu.es/PCR>); (San Millan et al., 2013). The PCR mixture included 0.4 μ M of each *Staphylococcus*-specific primers (*tuf*-F (TStaG422) 5'-GGC CGT GTT GAA CGT GGT CAA ATC A-3 and *tuf*-R (TStag76) 5'-TIA CCA TTT CAG TAC CTT CTG GTA A-3') (Tm 59.3°C). The PCR reagent ratios were similar to those used in the 16S rRNA gene amplification. Touchdown PCR conditions were as previously described (Martineau et al., 2001) with modifications that included 5 min at 95°C, 30 cycles of 30 s at 95°C, 30 s at 55°C and 45 s at 72°C, and final extension for 7 min at 72°C. Amplified PCR products were purified using QIAquick (Qiagen, Maryland, USA) purification kit following manufacturer's instructions prior to sequencing using ABI 3100 DNA Genetic Analyzer at Auburn University's Genomics and Sequencing Laboratory (GSL).

Library preparation and sequencing

Genomic DNA of the isolate was used for library construction. We used the Agilent 2100 BioAnalyzer (Agilent Technologies, USA) to perform size fractionation and quantification of DNA. DNA was then fragmented and libraries prepared using Nextera XT (Illumina) according to manufacturer's protocol before being run on an Illumina MiSeq with a 2 × 250 sequencing kit. Quantification of the fragment library before loading on MiSeq sequencer was performed using the Kapa quantification kit (RT-PCR) Kapa Biosystems, Wilmington, MA USA). Sequence reads were filtered for quality and assembled using CLC Genomics Workbench 8.0.1 (CLCbio, Aarhus, Denmark) (Kim et al., 2013), SPAdes 3.6 (Bankevich et al., 2012) and Velvet 1.2 (Zerbino and Birney, 2008). QUAST β (<http://quast.bioinf.spbau.ru/>) (Gurevich et al., 2013) was used for quality check of the assemblies and for the determination of % G+C content of genomes.

Gene prediction and functional analysis

FASTA-formatted genomic sequences of closely related *Staphylococcus* spp. genomes were obtained from the RefSeq database on GenBank and uploaded to PATRIC for annotation. Protein coding genes in genomes were identified using GeneMarkS (Borodovsky and Lomsadze, 2014). Non-coding RNA prediction was achieved using RNAMMER 1.2 online server (Lagesen et al., 2007). Predictions for tRNA and tmRNA genes were done with the ARAG ORN tRNA and tmRNA prediction program (Laslett and Canback, 2004). Functional annotation of the protein gene models was achieved using multiple bioinformatic softwares including the RAST server (Overbeek et al., 2014), PATRIC (Wattam et al., 2014) and IMG/M (Markowitz et al., 2012). Annotation for antibiotic resistance genes was achieved using PATRIC via BLASTp

sequence homology search from the Antibiotic Resistance Genes Database (ARDB) (Liu and Pop, 2009) and the Comprehensive Antibiotic Resistance Database (CARD) (McArthur et al., 2013) databases. To remove database-based redundancy, replicates were removed. Analysis for occurrence of metal resistance genes (MRGs) was performed using BLASTx against the Antibacterial Biocide and Metal Resistance Genes Database (MRDB) database with an e-value cutoff of 0.01 (Altschul et al., 1997). To achieve this, the BaCMet experimentally confirmed database of MRDB was used (Pal et al., 2014).

Phylogenetic analysis

The 16S rRNA gene sequences of *S. mnemiopsis* AOAB and closely related *Staphylococcus* spp. representatives were structurally aligned using SSU-ALIGN v0.1.1 (Nawrocki, 2009), and used for reconstruction of a neighbor-joining tree. Separate sequence alignments was done using ClustalW algorithm in MEGA7 (Kumar et al., 2016) for unrooted neighbor-joining tree (Figure 4.3). FASTA sequences of housekeeping genes from the closest species were obtained from GenBank. Concatenated DNA sequences from five housekeeping genes (*tuf*, *sodA*, *dnaJ*, *hsp60* and *rpoB*) were used for MLSA. Sequences were aligned using MUSCLE (Edgar, 2004). The evolutionary history of *S. mnemiopsis* AOAB was inferred by using the Maximum Likelihood method based on the Jukes-Cantor model (Jukes and Cantor, 1969). Evolutionary analyses were conducted in MEGA7 (Kumar et al., 2016).

To infer genomic distance between *S. mnemiopsis* AOAB and the closest species, pairwise average nucleotide identity (ANI) was computed using IMG/M system (Varghese et al., 2015). With a species cut off set at 96%, this method has been found to be robust in delineating bacteria based on genome sequence data (Kim et al., 2014). *In silico* DNA-DNA hybridization

(DDH) was achieved using GBDP (Genome Blast Distance Phylogeny), which reliably infers genome-to-genome distances by utilizing Genome Blast Distance Phylogeny using logistic regression (Meier-Kolthoff et al., 2013).

Results

Phenotypic characterization

S. mnemiopsis grown on LB and mannitol agar at 30 °C produced yellow, medium (2-3 mm), round, smooth colonies after 3 days of growth (Figure 4.1). The isolate is catalase-positive and coagulase-negative. The polar lipid profile consisted of glycolipid, phospholipid, phosphatidylglycerol and diphosphatidylglycerol (Figure 4.7), typical of *Staphylococcus* species (Nahae et al., 1984). But unlike *S. warneri* and other *Staphylococcus* spp. (Nahae et al., 1984), *S. mnemiopsis* AOAB did not have detectable β -gentiobiosyl diacylglycerol (Figure 4.7) as part of its polar lipid profile. The presence of fatty acids ai-C_{15:0}, i-C_{15:0}, i-C_{17:0}, and ai-C_{17:0}, confirmed the isolate as being affiliated with the genus *Staphylococcus* (Figure 4.5). Cluster analysis of the fatty composition of our isolate based on Euclidean distance revealed that our isolate does not affiliate with any known *Staphylococcus* species (Figure 4.6) as MIDI dendrogram software places the same species cutoff at about 10 Euclidian Distance (<http://www.midilabs.com/fatty-acid-analysis>). The presence of menaquinone (MK-7) in the cytoplasmic membrane helped confirm *S. mnemiopsis* AOAB as coagulase negative (Heß and Gallert, 2015).

Disk diffusion confirmed that *S. mnemiopsis* AOAB has resistance against the penicillins (Penicillin and Ampicillin), fluoroquinolones (Ciprofloxacin, Nalidixic acid), a polypeptide (Bacitracin) and an aminoglycoside (Kanamycin). *S. pasteurii* strains have mixed results (+/-)

against penicillin. Unlike *S. mnemiopsis* AOAB, *S. pasteurii* strains are susceptible to kanamycin (Chesneau et al., 1993), which helped in further discrimination of the two species (Table 4.2). Also, *S. mnemiopsis* AOAB was revealed to be susceptible to vancomycin, oxacillin, tetracycline, Amoxicillin/clavulanic acid and chloramphenicol (Table 4.1). *S. pasteurii* strains generally have mixed results against tetracycline (Chesneau et al., 1993).

Phylogenetics

Phylogenetic analysis using the 16S rRNA gene using neighbor-joining method indicated that the isolate was closely related to *S. pasteurii* and *S. warneri* (Figure 4.4.2). Further phylogenetic analysis using MLSA (Figure 4.4) clustered the isolate as novel bacteria. Both ANI and DDH using genome sequence data confirmed delineation of the isolate as a novel species. None of the closest species met the ANI cut off of 96% or the DDH cut off of 70% (Table 4.3).

Genome mining

Whole genome sequencing yielded a total of 905,410 paired reads for *S. mnemiopsis* AOAB. The PATRIC annotated genome size was 2,617,061 bp. A number of genomic features differentiated it from the two closest relatives (Table 4.4). Genomic characterization of *S. mnemiopsis* AOAB using the Comprehensive Antibiotic Resistance Database (CARD), Antibiotic Resistance Genes Database (ARDB) and RAST annotation server revealed that the isolate harbors antibiotic resistance determinants (virulence factors, antibiotic resistance and drug targets and heavy metal resistance genes) (Table 4.5, Figure 4.8). In addition to antibiotic resistance genes, MRG-like sequences were detected in the genome of *S. mnemiopsis* AOAB. The most dominant ones were copper (22), arsenic (11) and zinc (4) metal resistance genes. *S. warneri* had copper (12), zinc (7) cadmium (7) and arsenic (5) as the dominant metal resistance

genes and for *S. pasteurii* SP1, it was copper (12), zinc (7), cadmium (6) and arsenic (5), thus aiding in further discrimination. To the best of our knowledge, this study is the first report of *Staphylococcus* isolation from the gut (stomodeum) of *M. leidyi*. The results clearly show that *M. leidyi*, an invasive zooplankton, harbors culturable but previously uncharacterized *Staphylococcus* species that can harbor and potentially disseminate genes that confer antibiotic resistance. Future research efforts will involve investigation of the *M. leidyi* host-*S. mnemiopsis* microbial interactions.

Discussion

Description of *S. mnemiopsis* sp. nov. (mne.mi.op'sis. N.L. gen. n. *mnemiopsis* of the sea walnut *Mnemiopsis*) was isolated from the gut (stomodeum) of *M. leidyi*. Cells are Gram positive, coagulase negative, catalase positive, pigmented and susceptible to novobiocin. *S. mnemiopsis* is kanamycin resistant, unlike *S. pasteurii* SP1. In contrast to *S. warneri* SG1 and *S. pasteurii* SP1, *S. mnemiopsis* AOAB was xylose and mannose-positive. It was distinguished from closely related species based on MLSA using 5 marker genes (*hsp60*, *rpoB*, *dnaJ*, *sodA* and *tuf*). The *in-silico* DNA-DNA hybridization revealed that *S. mnemiopsis* showed 27.8 % relatedness with *S. warneri* SG1 and 27.60 % with *S. pasteurii* SP1. Unlike *S. warneri*, *S. mnemiopsis* AOAB has no detectable β -gentiobiosyl diacylglycerol. *S. mnemiopsis* AOAB has an average nucleotide identity of 84.93 % and 84.58 % against *S. warneri* SG1 and *S. pasteurii* SP1 respectively. Phenotypic, genotypic and phylogenetic characterization of the isolate AOAB are in agreement with the species description that is proposed to be classified as *Staphylococcus mnemiopsis* sp. nov., with AOAB as the type strain (= DSM^T102048 = NRRL B-65367^T). Future efforts should include isolation and phenotype characterization of mobile genetic elements such as plasmids. It

is important to determine what antibiotic resistance genes are harbored mobile genetic elements, as that will point towards potential transmission through horizontal gene transfer.

Conclusion

The study reveals that *M. leidyi* stomodeum harbors potentially novel *Staphylococcus* spp., which potentially harbors antibiotic resistance determinants (antibiotic resistance and heavy metal resistance). This is the first report on the isolation and characterization of *Staphylococcus* spp. from *M. leidyi*.

Data availability

The Whole Genome Shotgun project has been deposited at DDBJ/ENA/GenBank under the accession LZFL00000000. The version described in this paper is version LZFL01000000.

The SRA accession number is SRP076995. The DDBJ/ENA/GenBank accession numbers for marker genes is; 16S rRNA gene (KU497670.1), *tuf* (LC158075.1), *sodA* (LC158854.1), *rpoB* (LC158855.1), *hsp60* (LC158856.1) and *dnaJ* (LC158857.1).

RAST server IDs are: *S. mnemiopsis* (6666666.127652), *S. pasteurii* SP1 (6666666.123700), *S. warneri* SG1 (6666666.123634). PATRIC Genome IDs: *S. mnemiopsis* AOAB (1279.166), *S. pasteurii* SP1 (1276282.3), *S. warneri* SG1 (1194526.3).

Table 4.1: Antibiotic susceptibility: ZOI (Zone of inhibition) of *Staphylococcus mnemiopsis* AOAB collected and cultured from the stomodeum of *M. leidy*, as measured (in mm) from the edge of disc to edge of inhibition zone (Kaushik et al., 2015). Resistant (R) and susceptible (S) assigned based on previously defined breakpoints (Howe and Andrews, 2012). Below the breakpoints, a given isolate is resistant. Antibiotics with unrevised break points are indicated as dash (-). Experiments were performed in triplicates.

Antibiotic	Avg. ZOI	R/S	Breakpoint (mm)
Bacitracin 0.04 iu (A)	6	R	>14
Nalidixic acid (30 µg) NA30)	7	R	>19
Ciprofloxacin 5 µg	14	R	>21
Kanamycin 30 µg (K30)	14.3	R	>18
Penicillin(P10 iu)	15	R	>25
Ampicillin 10 µg (AM10)	16.3	R	>26
Vancomycin (VA 30 ug)	18.3	S	>12
Tetracycline 30 µg (TE30)	23.4	S	>20
Amoxicillin/Clavulanic acid 20/10 µg (AMC 30)	25	S	>25
Chloramphenicol 30 µg (C30)	28.3	S	>15
Novobiocin (30 µg NB30)	35	S	>16
Oxacillin 1µg (OX1)	19	S	>15
Control: Polymyxin B (PB 300 iu)	6	R	NA

R=resistant; S=susceptible

Table 4.2: Phenotypic characterization of *Staphylococcus mnemiopsis* AOAB and comparison with two closely related species, *S. warneri* and *S. pasteuri*

Characteristic	<i>S. mnemiopsis</i> AOAB	<i>S. warneri</i>	<i>S. pasteuri</i>
Sucrose	+	+	+
D-xylose	++	-	-
Lactose	++	+,-	+,-
D-ribose	+	+, -	-
D-(+) mannose	+	-	-
D-mannitol	+	+, -	+, -
D-(+) Trehalose	+	+	+
B-D(+) glucose	+	+	+
Fructose	+	+	+
Xylan	+	ND	ND
Chitin	+	ND	ND
Starch	+	ND	ND
D Sorbital	+	ND	ND
Rhamnose	-	ND	ND
D (+) Galactose	+	-	ND
I-inositol	-	ND	ND
L- arabinose	-	-	-
Catalase	+	+	+
Coagulase	-	-	-

Urease	+	+	+
Novobiocin	susceptible	susceptible	susceptible
Kanamycin	resistant	ND	susceptible

Comparative data for *S. warneri* were obtained from Kloos and Schleifer 1975 (Kloos and Schleifer, 1975) in addition to for *S. pasteurii* from Chesneau et al. 1993 (Chesneau et al., 1993). ND, not determined. Genome mining using RAST server confirmed that *S. mnemiopsis* AOAB has enzymes to degrade xylose, mannose, and chitin as part of its subsystems (Figure 4.8). Growth not better than negative control (-), Growth like positive control (glucose) (+), Growth better than positive control (++)

Table 4.3: Pairwise average nucleotide identity (ANI) analysis and DNA-DNA hybridization (DDH) between *S. mnemiopsis* AOAB (ANI2) and closely related *Staphylococcus* species

Species	ANI1>2	ANI2>1	DDH
<i>S. warneri</i> SG1	85.02	84.93	27.80
<i>S. pasteurii</i> SP1	84.79	84.58	27.60
<i>S. hominis</i> C80	79.62	79.59	22.40
<i>S. haemolyticus</i> JCSC1435	79.52	79.31	22.60
<i>S. saprophyticus</i> ATCC 15305	78.03	77.66	21.90
<i>S. aureus</i> MRSA252	78.85	78.73	22.70
<i>S. epidermidis</i> ATCC 12228	79.4	79.36	19.00
<i>S. lugdunensis</i> HKU09-01	78.21	78.04	22.0
<i>S. hominis</i> VCU122	79.62	79.59	22.40

Table 4.4: Genome characteristics of *S. mnemiopsis* AOAB and close relatives within Genus *Staphylococcus* based on IMG/ER annotation pipeline

Feature	<i>S. mnemiopsis</i>	<i>S. pasteurii</i> SP1	<i>S. warneri</i> SG1
Size (bp)	2,617,061	2,559,946	2,560,716
% G+C	32.13	32.71	32.73
CDS	2,695	2,457	2,435
rRNA	9	16	16
tRNA	59	48	60
tmRNA	1	1	1
Hypothetical proteins	595	559	539
Proteins functional assignments	2,100	1,898	1,896
Proteins with EC number assignments	770	719	739
Proteins with GO assignments	695	728	737
Proteins with Pathway assignments	630	559	579
Proteins with FIGfam assignments	2,294	2,194	2,214

Table 4.5: Antibiotic resistance genes from *S. mnemiopsis* AOAB (PATRIC Genome ID: 1279.166)

Gene	Source	GO assignments	Highest sequence similarity	Organism
Multi antimicrobial extrusion protein, MATE family of MDR efflux pumps	ARDB	GO:0015559	93	<i>S. warneri</i> L37603
Quinolone resistance protein norA	ARDB / CARD	-	94	<i>S. warneri</i> L37603
Undecaprenyl-diphosphatase	ARDB	GO:0050380	96	<i>S. warneri</i> L37603
Beta-lactamase	ARDB / CARD	GO:0008800	100	<i>S. aureus</i>
Topoisomerase IV subunit A	CARD	GO:0003916	84	<i>S. aureus</i> USA300_TCH1516
Topoisomerase IV subunit B	CARD	GO:0003916	91	<i>S. aureus</i> USA300_FPR3757
Lipid A export ATP-binding / permease protein MsbA	CARD	-	90	<i>S. aureus</i> Mu50
Two component system histidine kinase ArlS	CARD	GO:0000155	82	<i>S. epidermidis</i> ATCC 12228
Transcriptional regulator,	CARD	-	92	<i>S. aureus</i> JH1

MarR family				
Translation elongation factor	CARD	-	97	<i>S. aureus</i> ED98
Tu				
DNA gyrase subunit A	CARD	GO:0003918	89	<i>S. epidermidis</i> ATCC 12228
Alkaline phosphatase	CARD	-	86	<i>S. aureus</i> MW2
synthesis transcriptional regulatory protein PhoP				
Putative response regulator	CARD	-	82	<i>S. aureus</i> ED98
ArlR				
Transcriptional regulator	CARD	-	93	<i>S. aureus</i> Mu3
MgrA (Regulator of autolytic activity)				
DNA-directed RNA	CARD	GO:0003899	97	<i>S. aureus</i> USA300_TCH1516
polymerase beta subunit				
Mn-dependent	CARD	-	83	<i>S. aureus</i> MRSA252
transcriptional regulator MntR				
Beta-lactamase regulatory	CARD	-	99	<i>S. aureus</i>
sensor-transducer BlaR1				
Beta-lactamase repressor	CARD	-	100	<i>S. aureus</i> USA300_TCH959
BlaI				

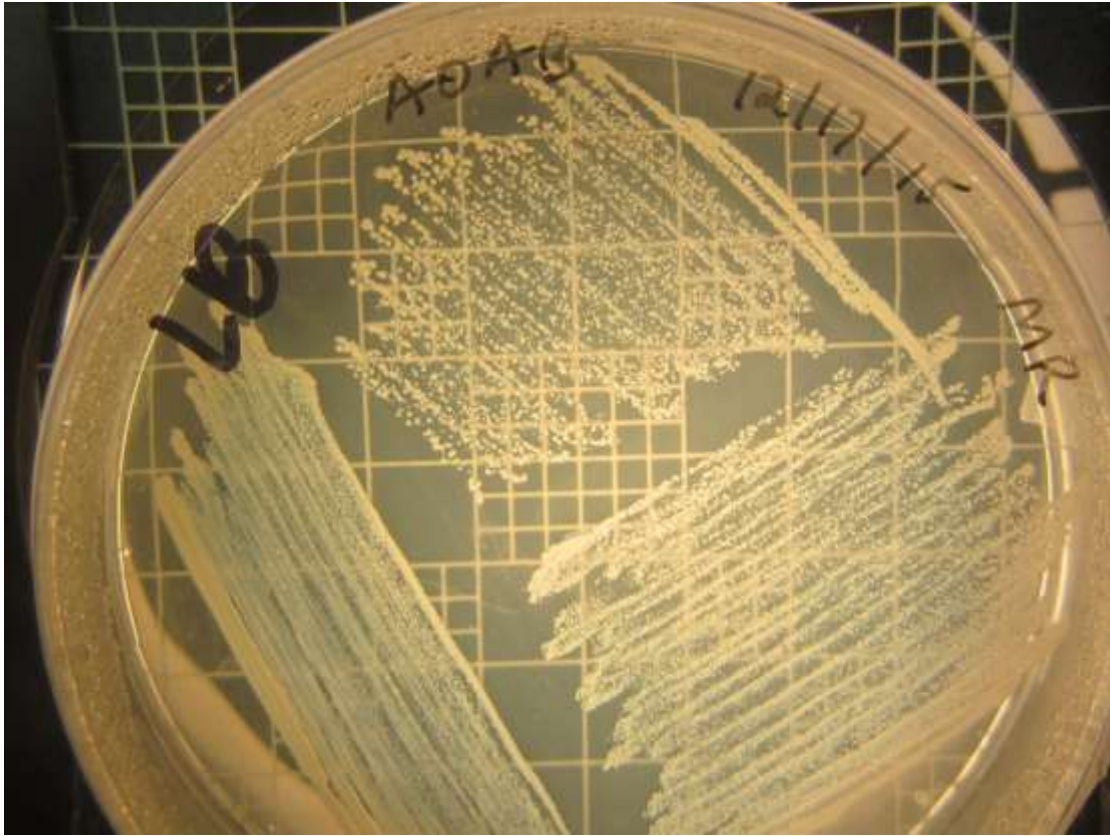


Figure 4.1: Growth of yellow pigmented *Staphylococcus mnemiopsis* AOAB on LB agar after 3 days at 30°C

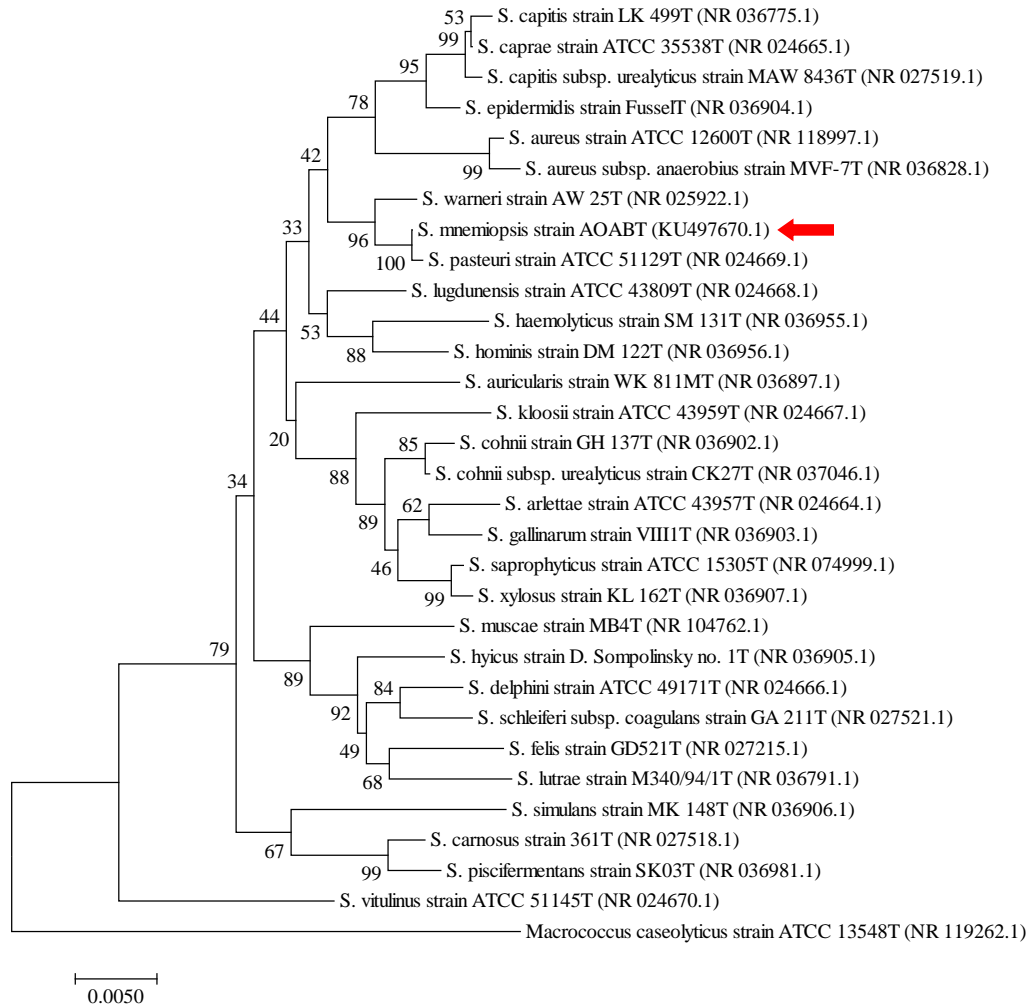


Figure 4.2: Neighbor-joining tree based on SSU-ALIGN for 16S rRNA gene sequences of *S. mnemiopsis* AOAB with closely related *Staphylococcus* species. Numbers at nodes indicate the percentage of bootstrap support based on 1000 replications. Rooting was done using *Macrocooccus caseolyticus* for discriminatory purposes

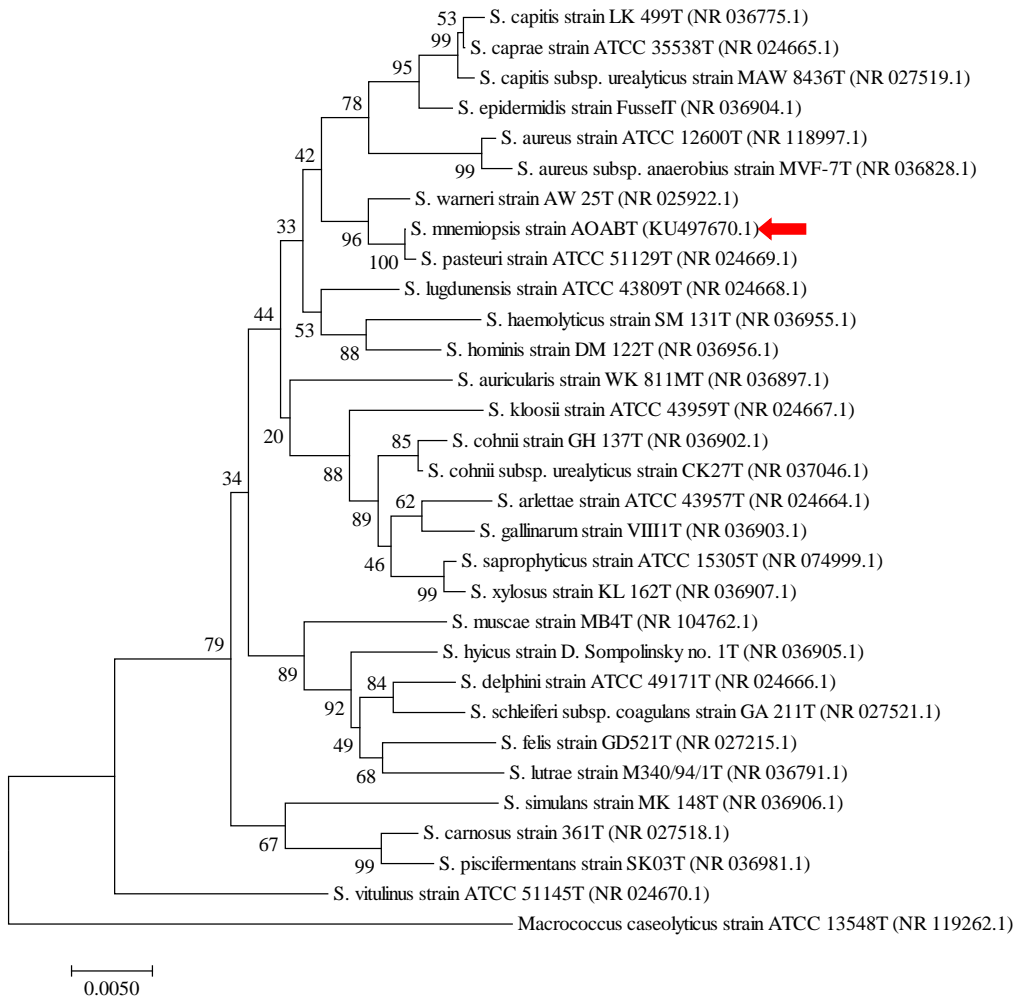


Figure 4.3: Unrooted neighbor-joining tree based on ClustalW alignments for 16S rRNA gene sequences of *S. mnemiopsis* AOAB with closely related *Staphylococcus* species. Numbers at nodes indicate the percentage of bootstrap support based on 1000 replications.

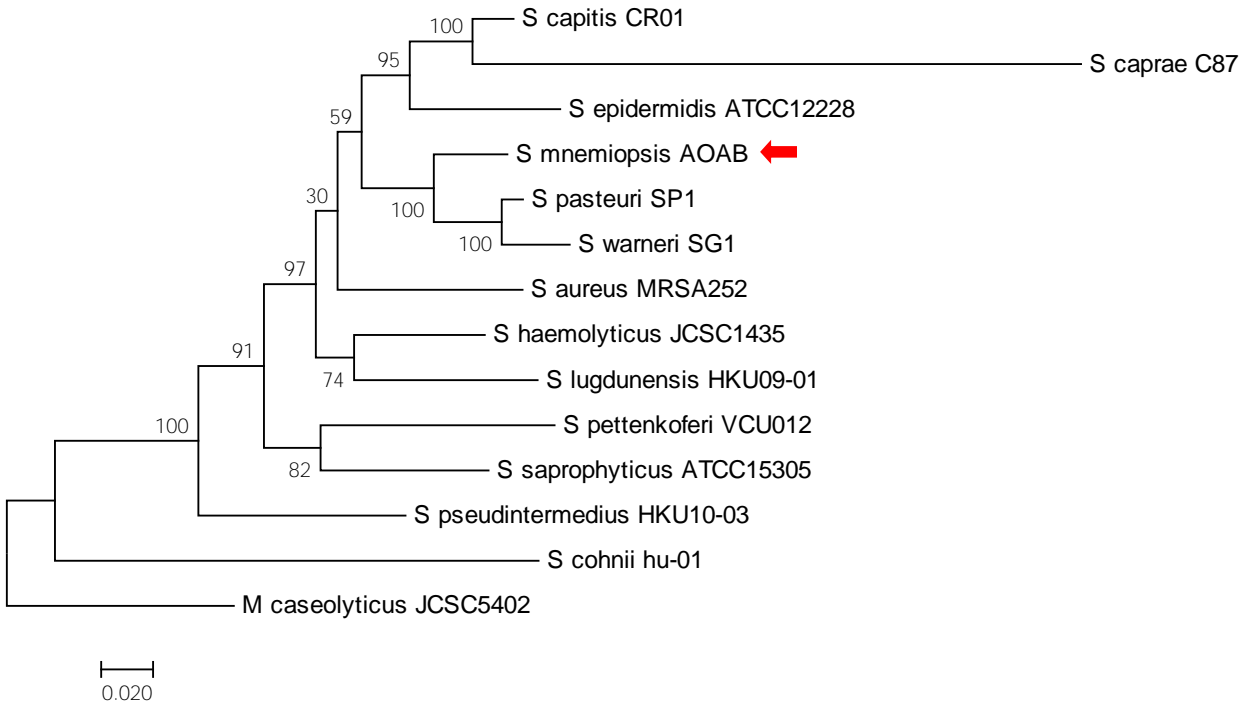
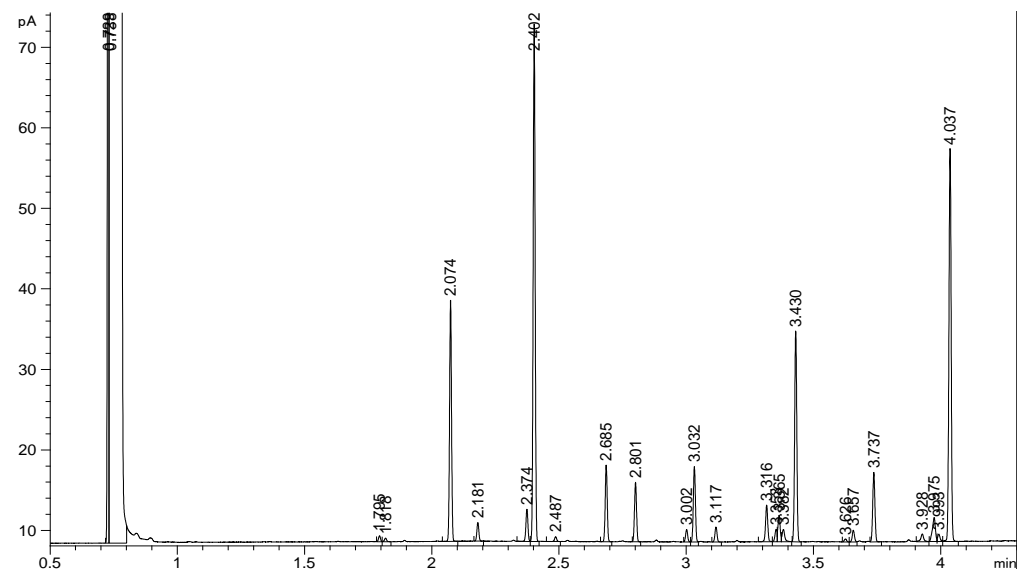


Figure 4.4: Evolutionary history of *S. mnemiopsis* AOAB inferred by using Maximum Likelihood method based on Jukes-Cantor model. Evolutionary tree was constructed using MEGA7. The tree is drawn to scale. Numbers on the nodes indicate bootstrap values as a percentage based on 1000 replications with branch lengths measured in the number of substitutions per site. The tree was based on concatenated MLSA of, *tuf*, *sodA*, *dnaJ*, *hsp60* and *rpoB* gene sequences.

4.5a.



4.5b.

RT	Response	Ar/Ht	RFact	ECL	Peak Name	Percent
0.7291	200492	0.005	----	6.6227		----
0.7376	1.191E+9	0.018	----	6.6813	SOLVENT PEAK	----
1.7949	543	0.008	1.027	12.6233	13:0 iso	0.17
2.0741	5888	0.008	0.994	13.6277	14:0 iso	1.83
2.1813	841	0.009	0.984	13.9997	14:0	0.26
2.3740	21254	0.009	0.969	14.6311	15:0 iso	6.43
2.4030	134286	0.009	0.967	14.7261	15:0 anteiso	40.52
2.6859	5319	0.009	0.949	15.6335	16:0 iso	1.58
2.8010	10225	0.009	0.944	15.9991	16:0	3.01
3.0018	16624	0.009	0.936	16.6358	17:0 iso	4.86
3.0329	44699	0.009	0.935	16.7343	17:0 anteiso	13.04
3.1173	318	0.009	0.932	17.0019	17:0	0.09
3.3162	3574	0.009	0.927	17.6353	18:0 iso	1.03
3.4304	39929	0.009	0.925	17.9987	18:0	11.53
3.6260	6156	0.009	0.923	18.6371	19:0 iso	1.77
3.6571	10734	0.009	0.923	18.7384	19:0 anteiso	3.09
3.7375	588	0.009	0.922	19.0010	19:0	0.17
3.9284	580	0.010	0.923	19.6368	20:0 iso	0.17
4.0372	36243	0.010	0.923	19.9992	20:0	10.45
4.2534	525	0.009	----	20.7193		----

ECL Deviation: 0.001
 Total Response: 337800
 Percent Named: 100.00%

Reference ECL Shift
 Total Named: 337800
 Total Amount: 320321

Figure 4.5: Cellular fatty acid composition for *Staphylococcus mnemiopsis* AOAB using gas chromatography (chromatograph was fitted with a 5% phenyl-methyl silicone capillary column).

Peak areas (a) and standard deviation (b) on percentage composition identified 17 fatty acids.

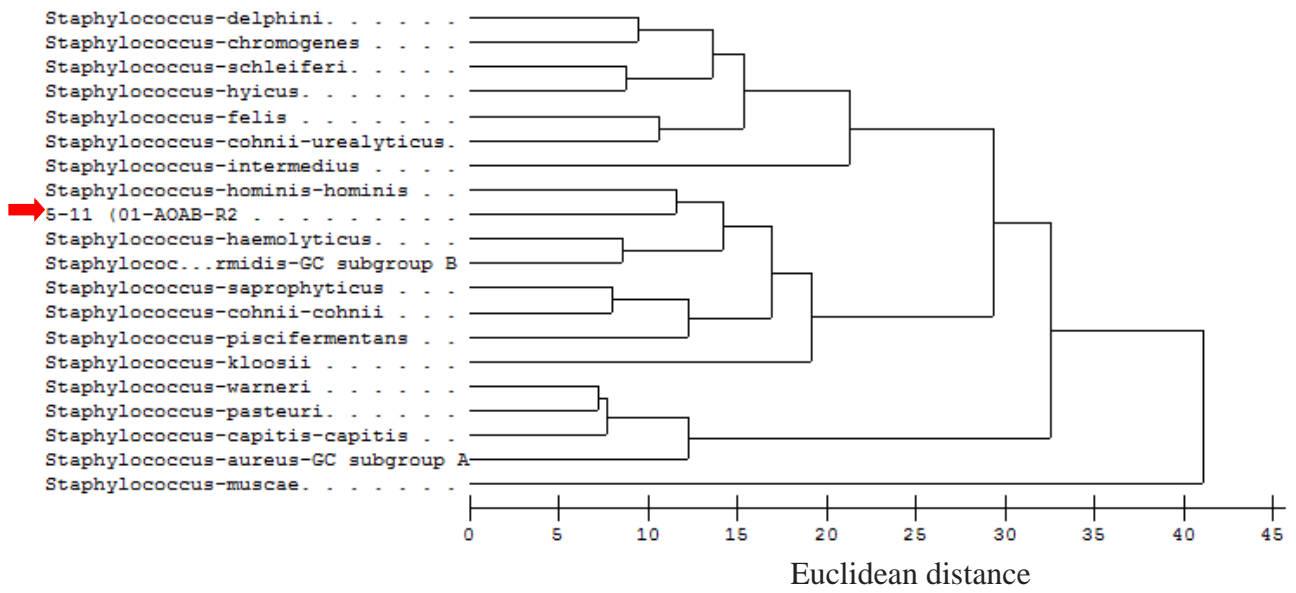
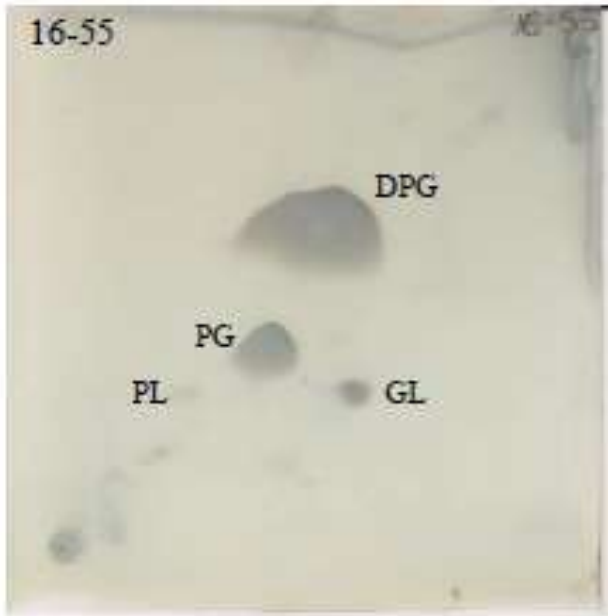


Figure 4.6: A dendrogram showing GC fatty acid profile similarities with 19 other *Staphylococcus* species.



GL = Glycolipid

PL= Phospholipid

PG = Phosphatidylglycerol

DPG = Diphosphatidylglycerol

Figure 4.7: Polar lipids analysis of *Staphylococcus mnemiopsis* AOAB (= DSMT102048 =NRRL B-65367T) using two-dimensional silica gel TLC (Macherey-Nagel Art. No. 818 135)

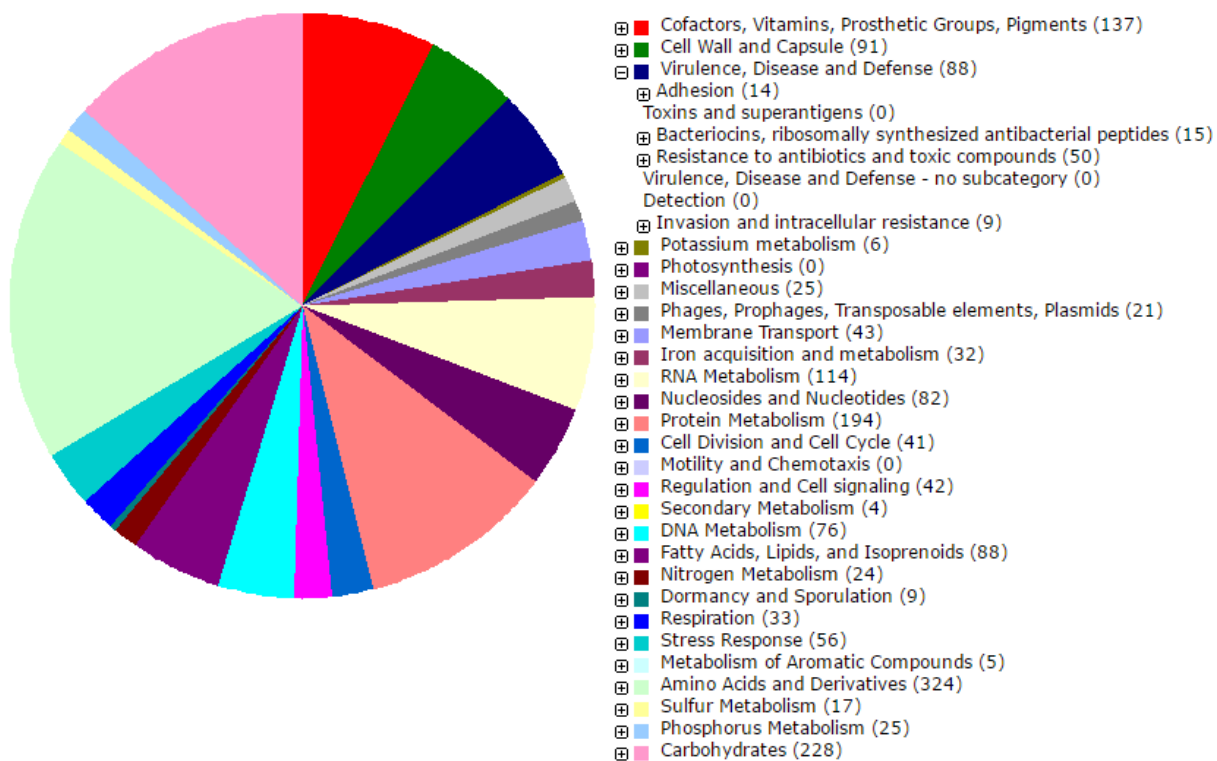


Figure 4.8: Subsystem category distribution of *S. mnemiopsis* AOAB (Based on RAST annotation server)

References

- Altschul, S.F., Madden, T.L., Schaffer, A.A., Zhang, J., Zhang, Z., Miller, W., Lipman, D.J., 1997. Gapped BLAST and PSI-BLAST: a new generation of protein database search programs. *Nucleic acids research* 25, 3389-3402.
- Anacker, R.L., Ordal, E.J., 1955. Study of a bacteriophage infecting the myxobacterium *Chondrococcus columnaris*. *J Bacteriol* 70, 738-741.
- Andreou, L., 2013. Preparation of genomic DNA from bacteria. *Methods Enzymol* 529, 143-151.
- Bankevich, A., Nurk, S., Antipov, D., Gurevich, A.A., Dvorkin, M., Kulikov, A.S., Lesin, V.M., Nikolenko, S.I., Pham, S., Prjibelski, A.D., Pyshkin, A.V., Sirotkin, A.V., Vyahhi, N., Tesler, G., Alekseyev, M.A., Pevzner, P.A., 2012. SPAdes: A New Genome Assembly Algorithm and Its Applications to Single-Cell Sequencing. *Journal of Computational Biology* 19, 455-477.
- Borodovsky, M., Lomsadze, A., 2014. Gene identification in prokaryotic genomes, phages, metagenomes, and EST sequences with GeneMarkS suite. *Current protocols in microbiology* 32, Unit 1E 7. <http://www.currentprotocols.com/protocol/mc01e07>.
- Chesneau, O., Morvan, A., Grimont, F., Labischinski, H., El Solh, N., 1993. *Staphylococcus pasteurii* sp. nov., Isolated from Human, Animal, and Food Specimens. *International Journal of Systematic and Evolutionary Microbiology* 43, 237-244.
- Daniels, C., Breitbart, M., 2012. Bacterial communities associated with the ctenophores *Mnemiopsis leidyi* and *Beroe ovata*. *FEMS microbiology ecology* 82, 90-101.
- DeLong, E.F., 2014. Alien invasions and gut "island biogeography". *Cell* 159, 233-235.
- Delpy, F., Pagano, M., Blanchot, J., Carlotti, F., Thibault-Botha, D., 2012. Man-induced hydrological changes, metazooplankton communities and invasive species in the Berre Lagoon (Mediterranean Sea, France). *Mar Pollut Bull* 64, 1921-1932.
- Edgar, R.C., 2004. MUSCLE: multiple sequence alignment with high accuracy and high throughput. *Nucleic acids research* 32, 1792-1797.
- Faghri, M.A., Pennington, C.L., Cronholm, L.S., Atlas, R.M., 1984. Bacteria associated with crabs from cold waters with emphasis on the occurrence of potential human pathogens. *Applied and environmental microbiology* 47, 1054-1061.
- Figueiredo, H.C., Klesius, P.H., Arias, C.R., Evans, J., Shoemaker, C.A., Pereira, D.J., Jr., Peixoto, M.T., 2005. Isolation and characterization of strains of *Flavobacterium columnare* from Brazil. *J Fish Dis* 28, 199-204.

Freney, J., Kloos, W.E., Hajek, V., Webster, J.A., Bes, M., Brun, Y., Vernozy-Rozand, C., 1999. Recommended minimal standards for description of new staphylococcal species. *International Journal of Systematic and Evolutionary Microbiology* 49, 489-502.

Gunn, B.A., Colwell, R.R., 1983. Numerical Taxonomy of Staphylococci Isolated from the Marine-Environment. *International journal of systematic bacteriology* 33, 751-759.

Gurevich, A., Saveliev, V., Vyahhi, N., Tesler, G., 2013. QUASt: quality assessment tool for genome assemblies. *Bioinformatics* 29, 1072-1075.

Hammann, S., Moss, A., Zimmer, M., 2015. Sterile Surfaces of *Mnemiopsis leidyi* (Ctenophora) in Bacterial Suspension-A Key to Invasion Success? *Open Journal of Marine Science* 5, 237-246.

Hao, W., Gerdt, G., Peplies, J., Wichels, A., 2015. Bacterial communities associated with four ctenophore genera from the German Bight (North Sea). *FEMS microbiology ecology* 91, 1-11.

Heß, S., Gallert, C., 2015. *Staphylococcus argensis* sp. nov., a novel staphylococcal species isolated from an aquatic environment. *International Journal of Systematic and Evolutionary Microbiology* 65, 2661-2665.

Howe, R.A., Andrews, J.M., 2012. BSAC standardized disc susceptibility testing method (version 11). *The Journal of antimicrobial chemotherapy* 67, 2783-2784.

Jaspers, C., Haraldsson, M., Bolte, S., Reusch, T.B., Thygesen, U.H., Kiorboe, T., 2012. Ctenophore population recruits entirely through larval reproduction in the central Baltic Sea. *Biology letters* 8, 809-812.

Jukes, T.H., Cantor, C.R., 1969. *Evolution of Protein Molecules*. New York: Academic Press, pp. 21-132.

Kaushik, K.S., Kessel, A., Ratnayeke, N., Gordon, V.D., 2015. A low-cost, hands-on module to characterize antimicrobial compounds using an interdisciplinary, biophysical approach. *PLoS Biol* 13, 1-11.

Kim, K.U., Park, S.K., Kang, S.A., Park, M.K., Cho, M.K., Jung, H.J., Kim, K.Y., Yu, H.S., 2013. Comparison of functional gene annotation of *Toxascaris leonina* and *Toxocara canis* using CLC genomics workbench. *Korean J Parasitol* 51, 525-530.

Kim, M., Oh, H.-S., Park, S.-C., Chun, J., 2014. Towards a taxonomic coherence between average nucleotide identity and 16S rRNA gene sequence similarity for species demarcation of prokaryotes. *International Journal of Systematic and Evolutionary Microbiology* 64, 346-351.

Kloos, W.E., Schleifer, K.H., 1975. Isolation and Characterization of Staphylococci from Human Skin II. Descriptions of Four New Species: *Staphylococcus warneri*, *Staphylococcus capitis*, *Staphylococcus hominis*, and *Staphylococcus simulans*. International Journal of Systematic and Evolutionary Microbiology 25, 62-79.

Kumar, S., Stecher, G., Tamura, K., 2016. MEGA7: Molecular Evolutionary Genetics Analysis Version 7.0 for Bigger Datasets. Molecular biology and evolution, 1-11.

Lagesen, K., Hallin, P., Rodland, E.A., Staerfeldt, H.H., Rognes, T., Ussery, D.W., 2007. RNAmmer: consistent and rapid annotation of ribosomal RNA genes. Nucleic acids research 35, 3100-3108.

Laslett, D., Canback, B., 2004. ARAGORN, a program to detect tRNA genes and tmRNA genes in nucleotide sequences. Nucleic acids research 32, 11-16.

Liu, B., Pop, M., 2009. ARDB-Antibiotic Resistance Genes Database. Nucleic acids research 37, D443-447.

Lucic, D., Pestoric, B., Malej, A., Lopez-Lopez, L., Drakulovic, D., Onofri, V., Miloslavac, M., Gangai, B., Onofri, I., Benovic, A., 2012. Mass occurrence of the ctenophore *Bolinopsis vitrea* (L. Agassiz, 1860) in the nearshore southern Adriatic Sea (Kotor Bay, Montenegro). Environmental monitoring and assessment 184, 4777-4785.

Markowitz, V.M., Chen, I.M.A., Chu, K., Szeto, E., Palaniappan, K., Grechkin, Y., Ratner, A., Jacob, B., Pati, A., Huntemann, M., Liolios, K., Pagani, I., Anderson, I., Mavromatis, K., Ivanova, N.N., Kyrpides, N.C., 2012. IMG/M: the integrated metagenome data management and comparative analysis system. Nucleic acids research 40, D123-D129.

Martineau, F., Picard, F.J., Ke, D., Paradis, S., Roy, P.H., Ouellette, M., Bergeron, M.G., 2001. Development of a PCR assay for identification of staphylococci at genus and species levels. Journal of clinical microbiology 39, 2541-2547.

McArthur, A.G., Wagglechner, N., Nizam, F., Yan, A., Azad, M.A., Baylay, A.J., Bhullar, K., Canova, M.J., De Pascale, G., Ejim, L., Kalan, L., King, A.M., Koteva, K., Morar, M., Mulvey, M.R., O'Brien, J.S., Pawlowski, A.C., Piddock, L.J., Spanogiannopoulos, P., Sutherland, A.D., Tang, I., Taylor, P.L., Thaker, M., Wang, W., Yan, M., Yu, T., Wright, G.D., 2013. The comprehensive antibiotic resistance database. Antimicrobial agents and chemotherapy 57, 3348-3357.

Meier-Kolthoff, J.P., Auch, A.F., Klenk, H.P., Goker, M., 2013. Genome sequence-based species delimitation with confidence intervals and improved distance functions. BMC Bioinformatics 14, 1-14.

- Miller, R.A., Walker, R.D., Baya, A., Clemens, K., Coles, M., Hawke, J.P., Henricson, B.E., Hsu, H.M., Mathers, J.J., Oaks, J.L., Papapetropoulou, M., Reimschuessel, R., 2003. Antimicrobial susceptibility testing of aquatic bacteria: quality control disk diffusion ranges for *Escherichia coli* ATCC 25922 and *Aeromonas salmonicida* subsp. *salmonicida* ATCC 33658 at 22 and 28 degrees C. *Journal of clinical microbiology* 41, 4318-4323.
- Moss, A.G., Estes, A.M., Muellner, L.A., Morgan, D.D., 2001. Protistan epibionts of the ctenophore *Mnemiopsis mccradyi* Mayer. *Hydrobiologia* 451, 295-304.
- Nahae, M.R., Goodfellow, M., Minnikin, D.E., Hajek, V., 1984. Polar Lipid and Isoprenoid Quinone Composition in the Classification of *Staphylococcus*. *Microbiology* 130, 2427-2437.
- Nawrocki, E., 2009. Structural RNA homology search and alignment using covariance models. PhD Dissertation. Washington University in St. Louis, pp. 36-79.
- Overbeek, R., Olson, R., Pusch, G.D., Olsen, G.J., Davis, J.J., Disz, T., Edwards, R.A., Gerdes, S., Parrello, B., Shukla, M., Vonstein, V., Wattam, A.R., Xia, F., Stevens, R., 2014. The SEED and the Rapid Annotation of microbial genomes using Subsystems Technology (RAST). *Nucleic acids research* 42, D206-214.
- Pal, C., Bengtsson-Palme, J., Rensing, C., Kristiansson, E., Larsson, D.G., 2014. BacMet: antibacterial biocide and metal resistance genes database. *Nucleic acids research* 42, D737-743.
- Pilarski, F., Rossini, A.J., Ceccarelli, P.S., 2008. Isolation and characterization of *Flavobacterium columnare* (Bernardet et al. 2002) from four tropical fish species in Brazil. *Braz J Biol* 68, 409-414.
- Purcell, J.E., 2012. Jellyfish and ctenophore blooms coincide with human proliferations and environmental perturbations. *Annual review of marine science* 4, 209-235.
- San Millan, R.M., Martinez-Ballesteros, I., Rementeria, A., Garaizar, J., Bikandi, J., 2013. Online exercise for the design and simulation of PCR and PCR-RFLP experiments. *BMC Res Notes* 6, 513.
- Suriyachadkun, C., Chunhametha, S., Thawai, C., Tamura, T., Potacharoen, W., Kirtikara, K., Sanglier, J.J., 2009. *Planotetrastpora thailandica* sp nov., isolated from soil in Thailand. *Int J Syst Evol Microbiol* 59, 992-997.
- Thavasi, R., Aparnadevi, K., Jayalakshmi, S., Balasubramanian, T., 2007. Plasmid mediated antibiotic resistance in marine bacteria. *Journal of environmental biology / Academy of Environmental Biology, India* 28, 617-621.

- Tindall, B.J., Rosselló-Móra, R., Busse, H.-J., Ludwig, W., Kämpfer, P., 2010. Notes on the characterization of prokaryote strains for taxonomic purposes. *International Journal of Systematic and Evolutionary Microbiology* 60, 249-266.
- Tindall, B.J., Sikorski, J., Smibert, R.A., Krieg, N.R., 2007. Phenotypic Characterization and the Principles of Comparative Systematics, Methods for General and Molecular Microbiology, Third Edition. American Society of Microbiology, pp. 335-344.
- Trulzsch, K., Grabein, B., Schumann, P., Mellmann, A., Antonenka, U., Heesemann, J., Becker, K., 2007. *Staphylococcus pettenkoferi* sp. nov., a novel coagulase-negative staphylococcal species isolated from human clinical specimens. *Int J Syst Evol Microbiol* 57, 1543-1548.
- Varghese, N.J., Mukherjee, S., Ivanova, N., Konstantinidis, K.T., Mavrommatis, K., Kyrpides, N.C., Pati, A., 2015. Microbial species delineation using whole genome sequences. *Nucleic acids research* 43, 6761-6771.
- Wattam, A.R., Abraham, D., Dalay, O., Disz, T.L., Driscoll, T., Gabbard, J.L., Gillespie, J.J., Gough, R., Hix, D., Kenyon, R., Machi, D., Mao, C.H., Nordberg, E.K., Olson, R., Overbeek, R., Pusch, G.D., Shukla, M., Schulman, J., Stevens, R.L., Sullivan, D.E., Vonstein, V., Warren, A., Will, R., Wilson, M.J.C., Yoo, H.S., Zhang, C.D., Zhang, Y., Sobral, B.W., 2014. PATRIC, the bacterial bioinformatics database and analysis resource. *Nucleic acids research* 42, D581-D591.
- Yamashita, K., Shimizu, A., Kawano, J., Uchida, E., Haruna, A., Igimi, S., 2005. Isolation and characterization of staphylococci from external auditory meatus of dogs with or without otitis externa with special reference to *Staphylococcus schleiferi* subsp. *coagulans* isolates. *J Vet Med Sci* 67, 263-268.
- Zerbino, D.R., Birney, E., 2008. Velvet: Algorithms for de novo short read assembly using de Bruijn graphs. *Genome research* 18, 821-829.

Appendix

Table S2.1: Data from historical nutrient measurements in Mobile Bay, which were used to analyze variation in microbial assemblage samples collected between January, March, July and September in 2010 and 2011

Avg. 2010 & 2011	DIN (μM) \pm SE	PO ₄ ³⁻ (μM) \pm SE	DSi (μM) \pm SE	DON (μM) \pm SE
September	3.790 \pm 1.836	0.6082 \pm 0.2991	29.41 \pm 8.562	19.28 \pm 2.864
July	0.6003 \pm 0.09531	0.2795 \pm 0.06901	40.82 \pm 10.20	16.10 \pm 2.067
March	8.573 \pm 1.594	0.2158 \pm 0.05147	69.97 \pm 8.396	28.58 \pm 2.286
January	7.311 \pm 3.996	0.1966 \pm 0.04843	54.08 \pm 23.72	25.49 \pm 6.901

Sampling was done from Mid Bay (MB) [30°27'45.0"N 88°00'59.7"W] (n=12) and Dauphin Island (DI) [30°15'09.2"N 88°03'14.7"W] (n=12) in 2010 and 2011. For our study, data from the corresponding months from 2010 and 2011 were averaged (as seen in table) and used for analysis.

Table S2.2: Relationship between historical nutrient measurements (DIN, PO₄³⁻, DSi and DON) and the physicochemical parameters from the 11 day sampling period. The physicochemical parameters (without historical nutrient measurements) from the 11 day sampling period are shown in Chapter 2.

	Salinity	DO	Cond	CH ₄	NO ₂	NH ₄ ⁺	pH	DIN	PO ₄ ³⁻	DSi	DON
Temp.	0.849	-0.972*	0.860	0.998*	-0.837	-0.971*	-0.117	-0.943	0.676	-0.887	-0.965*
Salinity		-0.925	0.995*	0.841	-0.592	-0.766	-0.257	-0.872	0.330	-0.508	-0.813
DO			-0.917	-0.960*	0.703	0.895	0.040	0.984*	-0.491	0.776	0.972*
Cond				0.859	-0.656	-0.800	-0.342	-0.849	0.406	-0.530	-0.800
CH ₄					-0.868	-0.983*	-0.171	-0.921	0.714	-0.889	-0.948
NO ₂							0.504	0.607	-0.956*	0.841	0.682
NH ₄ ⁺							0.281	0.837	-0.829	0.910	0.884
pH								-0.137	-0.487	-0.043	-0.137
DIN									-0.400	0.776	0.988*
PO ₄ ³⁻										-0.806	-0.509
DSi											0.865

*Significant correlation (r) (2-tailed) at 95% CI

Table S2.3: Correlation between microbial assemblage of dominant phyla from all sampling periods against historical nutrient measurements (January, March, July and September 2010 & 2011)

Phyla	DIN (μM)	PO_4^{3-} (μM)	DSi (μM)	DON (μM)
Acidobacteria	-0.183	0.954	-0.729	-0.320
Actinobacteria	0.642	-0.808	0.670	0.664
Bacteroidetes	0.998*	-0.375	0.778	0.988*
Chlamydiae	-0.775	-0.268	-0.263	-0.688
Chlorobi	-0.827	-0.157	-0.296	-0.734
Chloroflexi	-0.138	-0.787	0.272	-0.057
Cyanobacteria	-0.926	0.704	-0.883	-0.951*
Deffribacteria	-0.237	0.983*	-0.731	-0.361
Deinococcus-Thermus	-0.827	-0.157	-0.296	-0.734
Firmicutes	0.239	0.0817	-0.228	0.121
Fusobacteria	0.148	0.070	-0.278	0.035
Gemmatimonadetes	-0.921	0.715	-0.889	-0.948
Nitrospirae	0.649	-0.380	0.817	0.728
Plancomycetes	-0.499	0.364	-0.759	-0.596
Proteobacteria	0.945	-0.632	0.826	0.951*
Spirochaetes	-0.595	0.895	-0.967*	-0.711
Tenericutes	0.890	-0.0256	0.405	0.808
Verrumicrobia	-0.883	0.781	-0.918	-0.924
"unclassified bacteria"	0.996*	-0.376	0.732	0.973*

*Significant correlation (r) (2-tailed) at 95% CI

Table S3.1: Distance matrix for gut metagenomes based on 97% similarity cut-off using Greengenes reference database

Sample	GSU	GWI	GFL	GSP
GSU	0.00 ^a 0.00 ^b	0.91 ^a 0.95 ^b	0.96 ^a 0.98 ^b	1.00 ^a 1.00 ^b
GWI		0.00 ^a 0.00 ^b	0.91 ^a 0.95 ^b	0.99 ^a 1.00 ^b
GFL			0.00 ^a 0.00 ^b	0.98 ^a 0.99 ^b
GSP				0.00 ^a 0.00 ^b

*Bray-Curtis (a), Jaccard (b)

Table S3.2: Taxonomic categories of bacterial assemblages associated with *M. leidyi* gut using KEGG Mapper for reconstructing KEGG taxonomy

Class	GFL	GSU	GWI	GSP
Actinobacteria	125	184	2047	60
Deltaproteobacteria	68	27	54	6
Gammaproteobacteria	66	310	944	42
Betaproteobacteria	59	428	128	15
Alphaproteobacteria	57	174	186	50
Bacteroidetes	30	23	109	11
Cyanobacteria	15	24	44	4
Firmicutes	22	105	63	1
Chlorobi	3	1	6	1
Fusobacteria	2	1	0	1
Chlamydiae	2	1	8	0
Nitrospirae	2	1	3	0
Deinococcus-Thermus	2	3	5	0
Tenericutes	1	0	3	0
Verrucomicrobia	1	4	17	5
Acidobacteria	1	4	7	1
Epsilonproteobacteria	1	1	7	1
Synergistetes	0	1	0	0
Elusimicrobia	0	1	1	0
Thermodesulfobacteria	0	1	0	0
Deferribacteres	0	1	3	0
Armatimonadetes	0	1	0	0
Unclassified Bacteria	0	2	5	1
Thermotogae	0	2	0	0
Aquificae	0	2	0	0
Chloroflexi	0	0	18	2
Spirochaetes	0	0	4	0

Table S3.3: The most abundant CAZy families in the stomodeum of *M. leidy*

CAZy family with Pfam domain	GFL	GWI	GSP	GSU	Mean	Pfam domains	Subject GenBank-Accession
AA1	1	5	0	9	3.750	Cu-oxidase_3 Cu-oxidase Cu-oxidase_2	AFR93734.1
AA3	1	4	2	3	2.500	GMC_oxred_N GMC_oxred_C	ABS64212.1
CBM14	1	14	2	8	6.250	SRCR SRCR Trypsin	ACY95481.1
CBM47	1	5	0	6	3.000	Pentaxin	AAI58266.1
CE10	1	10	1	6	4.500	DPPIV_N Peptidase_S9	AAL82802.1
GH38	64	50	25	48	46.750	Glyco_hydro_38 Alpha-mann_mid Glyco_hydro_38C	CAN65410.1
GH63	1	1	0	3	1.250	Glyco_hydro_63	AEO34443.1
GH65	2	2	0	0	1.000	Glyco_hydro_65m	AFK10199.1
GT31	3	11	0	4	4.500	Galactosyl_T	BAA94500.1
GT34	5	16	6	9	9.000	Cytochrome P450 (degradation of environmental toxins)	EAA66095.1
GT48	334	338	101	197	242.500	Glucan synthase	CAN82685.1

Table S3.4: Different types of antimicrobial resistance genes based on Brite reconstruction of KEGG Mapper

Antimicrobial resistance genes	KO	ARG subtype	Contig location
GSU			
Beta-lactamase	K18698; K07644; K07665	blaTEM; beta-lactamase class A TEM; cusS, copS, silS; two-component system, OmpR family, heavy metal sensor histidine kinase CusS; silR; two-component system, OmpR family, copper resistance phosphate regulon response regulator CusR	281249.1; 919925.1; 162136.1;189556.1; 561089.1;807721.1
Aminoglycoside	K00984	aadA; streptomycin 3"-adenylyltransferase	438226.1
Tetracycline	K08151	tetA; MFS transporter, DHA1 family, tetracycline resistance protein	198010.1;428321.1; 509897.1
Macrolide	K18230	tylC, oleB, carA, srmB; macrolide transport system ATP-binding/permease protein	959041.1
Phenicol	K18552; K07552	cmlA, cmlB, floR; MFS transporter, DHA1 family, florfenicol/chloramphenicol resistance protein; bcr; MFS transporter, DHA1 family, bicyclomycin/chloramphenicol resistance protein	642527.1;214818.1; 802095.1
Quinolone	K08167	smvA, qacA, lfrA; MFS transporter, DHA2 family, multidrug resistance protein	256108.1
Vancomycin	K07260	vanY; D-alanyl-D-alanine carboxypeptidase	556140.1
Cationic antimicrobial peptide (CAMP)	K07637	phoQ; two-component system, OmpR family, sensor histidine kinase PhoQ	1049322.1

Multidrug efflux	K03585; K18138; K18139; K18143; K12340; K18902; K08167	acrA, mexA, adeI, smeD, mtrC, cmeA; membrane fusion protein, multidrug efflux system; acrB, mexB, adeJ, smeE, mtrD, cmeB; multidrug efflux pump; oprM, emhC, ttgC, cusC, adeK, smeF, mtrE, cmeC, gesC; outer membrane protein, multidrug efflux system; adeS; two-component system, OmpR family, sensor histidine kinase AdeS; tolC; outer membrane protein; bpeF; multidrug efflux pump; smvA, qacA, lfrA; MFS transporter, DHA2 family, multidrug resistance protein	118229.1;138774.1;164914.1;344836.1950159. 1;81301.1;127238.1;129742.1;141146.1;203739 .1;215622.1;244160.1;334364.1;375517.1;3832 57.1;405262.1;410422.1;471788.1;519415.1;55 5489.1;604150.1;631356.1;652873.1;740855.1; 815844.1;890841.1;914163.1;973050.1; 698172.1;126464.1;566285.1;838897.1;430390. 1;476852.1;588952.1;605714.1;992020.1;25610 8.1
GFL			
Multidrug efflux	K18138	acrB, mexB, adeJ, smeE, mtrD, cmeB; multidrug efflux pump	73919.1
GWI			
Beta-Lactam	K18698; K17836; K07665	blaTEM; beta-lactamase class A TEM; penP; beta-lactamase class A; cusR, copR, silR; two-component system, OmpR family, copper resistance phosphate regulon response regulator CusR	92576.1;117657.1; 310409.1
Aminoglycoside	K00984; K19300	aadA; streptomycin 3"-adenylyltransferase; aph3-II; aminoglycoside 3'-phosphotransferase II;	660289.1; 5.4;5.8; 397855.1;603984.1
Tetracycline	K08151	tetA; MFS transporter, DHA1 family, tetracycline resistance protein	132916.1;740508.1
Macrolide	K19350	lsa; lincosamide and streptogramin A transport system ATP-binding/permease protein	372824.1; 378956.1; 379041.1;379064.1; 379085.1; 379106.1; 379127.1;379148.1 379168.1;379190.1; 379211.1;379233.1; 379255.1;379277.1; 379300.1;379324.1;

			379346.1;379368.1; 379391.1;379413.1; 379435.1; 379457.1; 379482.1;379507.1; 379532.1;379557.1; 379582.1;379607.1; 379632.1;379657.1; 379682.1;379707.1; 379732.1; 379757.1; 379782.1
Phenicol	K07552; K19271; K00638	bcr; MFS transporter, DHA1 family, bicyclomycin/chloramphenicol resistance protein; catA; chloramphenicol O-acetyltransferase type A; catB; chloramphenicol O-acetyltransferase type B	117811.1;209292.1; 356273.1;728610.1; 25638.1;61006.1
Quinolone	K08167	smvA, qacA, lfrA; MFS transporter, DHA2 family, multidrug resistance protein	585243.1
Vancomycin	K08641	vanX; D-alanyl-D-alanine dipeptidase	560068.1
Cationic antimicrobial peptide (CAMP)	K14205	mprF, fmtC; phosphatidylglycerol lysyltransferase	140591.1
Multidrug resistance	K03585; K18138; K12340; K18902; K08170; K08167; K09476	acrA, mexA, adeI, smeD, mtrC, cmeA; membrane fusion protein, multidrug efflux system; acrB, mexB, adeJ, smeE, mtrD, cmeB; multidrug efflux pump; tolC; outer membrane protein; bpeF; multidrug efflux pump; norB, norC; MFS transporter, DHA2 family, multidrug resistance protein; smvA, qacA, lfrA; MFS transporter, DHA2 family, multidrug resistance protein; ompF; outer membrane pore protein F	66775.1;73271.1; 85235.1;273365.1; 669972.1;59134.1; 59553.1;64548.1; 273118.1;416003.1; 423048.1;498697.1; 558967.1;582063.1; 585040.1;613771.1; 662107.1;123033.1; 592735.1;182772.1; 585243.1;283624.1
GSP			
beta-Lactamase	K18698	blaTEM; beta-lactamase class A TEM	103235.1;
Aminoglycoside	K19300	aph3-II; aminoglycoside 3'-phosphotransferase II	8950.1

Multidrug resistance	K18138	acrB, mexB, adeJ, smeE, mtrD, cmeB; multidrug efflux pump	104081.1; 111336.1

Table S4.1: Basal salts mixture

Basal salts		gL ⁻¹
1	(NH ₄) ₂ SO ₄	2.64
2	KH ₂ PO ₄	2.38
3	K ₂ HPO ₄	4.31
4	MgSO ₄ 7H ₂ O	1.0
Trace element solution		
1	CuSO ₄ .5H ₂ O	0.64
2	FeSO ₄ .7H ₂ O	0.11
3	ZnSO ₄ .7H ₂ O	0.15
4	MnCl ₂ .4H ₂ O	0.79

*Trace elements filter sterilized using 0.2 μM filters (Whatman® membrane filters nylon)

before adding them to the autoclaved analytical grade basal salts